



**MARMARA UNIVERSITY
INSTITUTE FOR GRADUATE STUDIES
IN PURE AND APPLIED SCIENCES**



**ONE DIMENSIONAL MODELING OF SI
ENGINES FUELLED WITH GASOLINE-
ALCOHOL BLENDS**

RAMIN SAADAT POUR

MASTER THESIS

Department of Mechanical Engineering

Thesis Supervisor

Assistant Prof. Mustafa. YILMAZ

Thesis CO- Supervisor

Assistant Prof. Hasan KÖTEN

ISTANBUL, 2017



MARMARA UNIVERSITY
INSTITUTE FOR GRADUATE STUDIES
IN PURE AND APPLIED SCIENCES



**ONE DIMENSIONAL MODELING OF SI
ENGINES FUELLED WITH GASOLINE-
ALCOHOL BLENDS**

RAMIN SAADAT POUR

(524613901)

MASTER THESIS

Department of Mechanical Engineering

Thesis Supervisor

Assistant Prof. Mustafa. YILMAZ

Thesis CO- Supervisor

Assistant Prof. Hasan KÖTEN

ISTANBUL, 2017

ACKNOWLEDGEMENT

I would like to thank my supervisor, Assistant Prof Mustafa Yılmaz and co- supervisor, Assistant Prof Hasan köten for their support, guidance and encouragement during the study. Finally I want to thank to my Family for their help ,encouregement and patience during the study.



CONTENTS

| | |
|---|-------------|
| ACKNOWLEDGEMENT | i |
| CONTENTS | ii |
| ÖZET | vi |
| ABSTRACT | vii |
| LIST OF SYMBOLS..... | viii |
| ABBREVIATIONS..... | ix |
| LIST OF FIGURES..... | xi |
| LIST OF TABLES..... | xiii |
| CHAPTER 1. INTRODUCTION AND AIM..... | 1 |
| 1.1. INTRODUCTION..... | 1 |
| 1.2. AIM: | 5 |
| 1.3. METHODOLOGY: | 5 |
| CHAPTER 2. MATERIAL AND METHOD: | 7 |
| 2.1. Historical Background: | 7 |
| 2.2. Classification of Internal Combustion Engines: | 9 |
| 2.3. Self-Ignition and Octane Number: | 10 |
| 2.4. Burning velocities of alcohols and hydrocarbons: | 12 |
| 2.5. Injection times:..... | 13 |
| 2.6. Effects of heated ethanol on injector performance:..... | 14 |
| 2.6.1. Effects of pressure drop on fuel flow rate:..... | 15 |
| 2.6.2. Effects of temperature on fuel flow rate..... | 16 |
| 2.6.3. Discharge coefficient | 17 |

| | |
|---|-----------|
| 2.7. Effect of ethanol–gasoline blends on cold start emissions in SI engines:..... | 18 |
| 2.8. Effect of ethanol–gasoline blend on NOx emission:..... | 19 |
| 2.8.1. Formation of NOx: | 19 |
| 2.8.2. Effect of blend concentration | 20 |
| 2.8.3. Effect of hydrous ethanol: | 24 |
| 2.8.4. Effect of compression ratio..... | 25 |
| 2.8.5. Effect of engine load..... | 26 |
| 2.8.6. Effect of equivalence ratio | 27 |
| 2.8.7. Effect of speed: | 28 |
| 2.8.8. Application of thermal barrier coating:..... | 29 |
| 2.8.9. Effect of separate aqueous ethanol injection: | 29 |
| 2.8.10. Effect of different vehicles:..... | 31 |
| 2.9. Combustion in SI engines: | 34 |
| 2.10. Spray and evaporation characteristics of ethanol and gasoline:..... | 36 |
| 2.11. Spark knock or knock:..... | 37 |
| 2.11.1. The Effect of Alcohols–gasoline Dual-Fuel on knock suppression:..... | 37 |
| 2.12. Regulations to prevent vapor lock: | 39 |
| 2.12.1. The effect of ethanol on vapor lock: | 39 |
| 2.12. Biofuels: | 40 |
| 2.12.1. First generation biofuels:..... | 40 |
| 2.12.2. Second generation of biofuels: | 41 |
| 2.12.3. Third generation biofuels:..... | 41 |
| 2.13. Ethanol:..... | 41 |
| 2.13.1. Dry Milling: | 41 |

| | |
|--|----|
| 2.13.1.1 Milling: | 41 |
| 2.13.1.2 Liquefaction: | 42 |
| 2.13.1.3. Saccharification: | 42 |
| 2.13.1.4 Fermentation:..... | 42 |
| 2.13.1.5 Distillation: | 42 |
| 2.13.1.6. Dehydration: | 42 |
| 2.13.1.7. Denaturing: | 43 |
| 2.13.2.Net Energy: | 43 |
| 2.13.3. Fuel properties: | 43 |
| 2.14. Fuel Quality:..... | 45 |
| 2.14.1. Volatility and Vapor Pressure: | 45 |
| 2.15. Previous studies:..... | 46 |
| CHAPTER 3. RESULTS and DISCUSSIONS: | 59 |
| 3.1. 1D Engine Modeling with Detailed Reaction Kinetics: | 59 |
| 3.2. MODEL: | 60 |
| 3.2.1. The stochastic reactor model for engine in-cylinder simulation: | 60 |
| 3.2.2. The PDF and the MDF: | 60 |
| 3.2.3. The SRM for DICI: | 61 |
| 3.2.4. The Homogeneous Reactor Model (HRM): | 61 |
| 3.2.5. The catalyst model: | 62 |
| 3.2.6. Diesel particulate filter model: | 63 |
| 3.3. Chemkin-Pro vs SRM-Suite: | 64 |
| 3.4.Wiebe Function: | 66 |
| 3.4.1.Fuel burning and heat release rate correlations:..... | 67 |
| 3.4.2. Combustion Chemistry:..... | 69 |
| 3.4.2.1. Thermal NOx formation | 71 |

| | |
|---|-----------|
| 3.4. The Burning Reactions: | 71 |
| 3.5.1-D Combustion modeling: | 73 |
| 3.6. Result: | 74 |
| CHAPTER 4 CONCLUSIONS | 86 |
| REFERENCES | 88 |
| CURRICULUM VITAE: | 94 |



ÖZET

TEK BOYUTLU MODELLEME KULLANILARAK ÇİFT YAKITLI BİR MOTORUN PERFORMANSINI FARKLI PROGRAMLARDA İNCELEYİP KARŞILAŞTIRILMASI:

Bu çalışmanın amacı benzin ve benzin –alkol karışımıyla beslenen ateşlemeli motorların performansını incelemektir. Motorun performansı basınç ve emisyonlar bakımından incelenmiştir. Bunun için Chemkin-Pro,SRM suite ve GT-POWER programları kullanılmıştır.

Çalışmanın ilk kısmında motorun performansı Chemkin-Pro ve SRM suite programını kullanılarak incelenmiştir.Bu bölümde detaylı ve kısaltılmış mekanizmalar kullanılmıştır ve kullanılan yakıt E100 dür.

Araştırmanın sonunda detaylı mekanizmaların deneysel sonuçlarla daha yakın olduğu gözlemlenmiştir bunun nedeniyle detaylı mekanizmaların ara reaksiyonları hesaba katmasıdır.

SRM Suite'in avantajı deneysel sonuçlara yakın olmasıdır. Chemkin-Pro'nun avantajı hızlı olmasıdır özellikle detaylı mekanizmalarda Chemkin-Pro çok daha hızlıdır.Çalışmanın ikinci kısmında motorun performansı E0,E5,E10,E15,E20 ve E100 yakıtları kullanarak incelenmiştir.

Bunun için GT-POWER programından yararlanılmıştır. Sonuçlar, alkolün yüzdesi arttırıldıkça motorun emisyonlarının düşüşü gözlenmektedir, nedeniyle alkol yapısında olan oksijenin daha etkili yanmaya yol açmasıdır.

Tüm değişkenleri hesaba katarak bu motor için en uygun alkol yüzdesinin 8% olduğuna karar verilmiştir fakat daha net bir cevap için bir optimizasyon programı kullanılmalıdır.

ABSTRACT

ONE DIMENSIONAL MODELING OF GASOLINE ALCHOL COMBUSTION ENGINE

The aim of this study is to investigate the performance of an SI engine fuelled with ethanol and ethanol-gasoline blends under various conditions.

The performance of engine was investigated form in-cylinder pressure point, which affects engine power also from engine emissions point. For this aim, the following software package were used Chemkin-Pro,SRM Suite and GT-POWER.

At the first part of the study the performance of engine was investigated employing Chemkin-Pro and SRM-Suite software packages under detailed and reduced chemical mechanism the used fuel was E100 due to factoring in intermediate reactions detailed mechanisms are in much better agreement with experimental results.

The main advantage of SRM-Suite is that its results is near to experimental results and the main advantage of Chemkin-pro is that its faster compared with similar software's especially in detailed mechanism evaluations.

At the second part of study the following fuels were employed: E0, E5, E10, E15, E20 and E100. The evaluation were done employing GT-POWER software package and the results were compared to each other and experimental data, outcomes showed that due to oxygen content of the ethanol, by increasing ethanol concentration in the blend the total amount of emissions decreased and engine showed better performance because the higher content of ethanol results in complete combustion. At the last part of the study the optimal concentration of ethanol in the blend was determined and it was clear that by factoring in all the parameters E8 was the best blend that could be employed and for the much precise results it was offered to optimization software be employed.

LIST OF SYMBOLS

Symbols

a, b, c

C_{11} , C_{12} , C_2

Nu

P

P_m

Pr

P_r , V_r , T_r

Re

SEA

SIP

S_p

V_d

w

S_p

B

λ

μ

G

A_p

T_w

V_p ,

constants for Nusselt equation

constants of Woschni correlation

Nusselt number

instantaneous cylinder pressure (bar)

instantaneous motored cylinder pressure (bar)

Prandtl number

volume, temperature and pressure evaluated at any reference condition

Reynolds number

Statistical Energy Boundry

Self-Ignition Temperature

mean piston speed

displaced volume

average cylinder gas velocity

mean piston speed

cylinder bore

gas thermal conductivity

dynamic viscosity

gas mass rate of flow

piston area

chamber surface temperature

$h_{r,c}$ coefficient of heat transfer by radiation.

ABBREVIATIONS

| | |
|-------|--|
| 1-D | One Dimensional |
| 3-D | Three Dimensional |
| ANN | Artificial Neural Network |
| ANOVA | Analysis Of Variance |
| BEP | Brake Engine Power |
| BP | Brake Power |
| BEA | Boundary Element Analysis. |
| BOV | Blow Off Valve |
| BSNO | Brake Specific Nitrogen Oxides |
| CAD | crank angle degree |
| CFD | computational fluid dynamics |
| DARS | Digital Analysis of Reaction Systems |
| DPF | Diesel Particulate Filter |
| DOE | Department of Energy |
| EFI | Electronic Fuel Injector |
| EGR | Exhaust Gas Recirculation |
| FEM | Finite Element Method |
| FFV | Flexible fuel vehicle |
| EMS | Engine Manage System |
| EPA | Energy Protection Agency |
| EVR | Exhaust Gas Recirculation Vacuum Regulator |
| EGR | Exhaust Gas Recirculation |
| EVC | Exhaust Valve Closing Time |
| EVO | Exhaust Valve Opening Time |
| HCCI | Homogenous.Charge Compression Ignition |
| HRR | Heat Release Rate |
| ICE | Internal Combustion Engine |
| ID | Ignition delay |
| IP | Indication Power |
| IVC | Intake Valve Closing time |
| IVO | Intake Valve Opening time |
| LMM | Localness Mixing Model |
| LHV | lower heating value |
| MBT | Maximum Brake Torque |
| OEM | Original Equipment Manufacturer |
| OBD | On-board diagnostic |
| PDF | Probability Density Function |
| PEMS | Portable Emissions Measurement System |

RPM
PRF
RON
SRM
VSP

Revolution Per Minute
Primary Reference Fuel
Research Octane Number,
Stochastic Reactor Model
Vehicle Specific Power



LIST OF FIGURES

| | |
|--|----|
| Figure 1.1 World Energy Consumption apportioned according to energy sources..... | 1 |
| Figure 1.2 Historical gasoline, ethanol, and MTBE consumption for US road..... | 3 |
| Figure 2.1 Otto-Langen engine..... | 8 |
| Figure 2. 2 Rudolf Diesel compression ignition engine..... | 9 |
| Figure 2.3 Estimated RON and RON + cooling ON of ethanol–gasoline blends for two blend stock RON values (88 or 92 RON)..... | 11 |
| Figure 2.4 Injection times for all tested fuels during 120 km/h steady-state test..... | 13 |
| Figure 2.5. Fuel injector test cell..... | 15 |
| Figure 2.6 Fuel mass flow rate dependency on pressure drop across injector nozzle at40°C fuel temperature..... | 15 |
| Figure 2.7 Fuel mass flow rate dependency on fuel injection temperature | 16 |
| Figure 2.8 (a) Discharge coefficient variation with fuel injection temperature | 17 |
| Figure 2.9 Correlation of NO _x and HC emission with ethanol percentage at 2000 rpm.... | 22 |
| Figure 2.10 Correlation of NO _x and HC with the percentage of ethanol at 3500 rpm | 23 |
| Figure 2.11 NO _x emission changes for ethanol / water fuel with respect to gasoline | 31 |
| Figure 2.12 Necessary modification to the engine to increase ethanol–gasoline blend..... | 32 |
| Figure 2.13 Increase of NO _x emission than gasoline fuel versus different engines for ethanol–gasoline blend..... | 34 |
| Figure 2.14 Overhead view of combustion chamber with the deactivated exhaust valve shown missing..... | 34 |
| Figure 2.15. Schematic of Alcohols–Gasoline Dual-Fuel Spark Ignition Combustion..... | 38 |
| Figure 2.16: Effect of ethanol blending on vapor pressure of gasoline..... | 40 |
| Figure 2.17. Engine test set-up and test instruments..... | 47 |
| Figure 2.18. The Schematic diagram of experimental setup..... | 49 |
| Figure 2.19. Influence of the blended fuels on the increase of engine torque output (relative to pure gasoline) at 3000 rpm. | 53 |
| Figure.2.20. The test procedure followed in the study..... | 57 |

| | |
|---|----|
| Figure 3.1 Illustration of the cell discretization in the catalytic channels..... | 63 |
| Figure 3.2 Illustration of the DPF model..... | 64 |
| Figure 3.3. Wiebe functions with different m values..... | 68 |
| Figure 3.4. Wiebe functions of different duration..... | 69 |
| Figure 3.5. Combustion Process..... | 70 |
| Figure 3.6. (a) Pressure curves from experimental and modeling with detailed mechanism. (b) Experimental and modeling with detailed mechanism heat release rate curves..... | 75 |
| Figure 3.7. (a) Pressure curves from experimental and modeling with reduced mechanism. (b) Experimental and modeling with reduced mechanism heat release rate curves..... | 76 |
| Figure 3.8 Temperature curves..... | 77 |
| Figure 3.9 Fuel consumption curves for E100 for different solvers and chemical mechanisms depending on CAD..... | 78 |
| Figure 3.10 (a) CO and CO ₂ (b) curves for different solvers and chemical mechanisms depending on CAD..... | 79 |
| Figure 3.11. (a) OH and H ₂ O ₂ (b) for different solvers and chemical mechanisms depending on CAD..... | 80 |
| Figure 3.12 Experimental and computational values of CO, CO ₂ , and O ₂ | 81 |
| Figure 3.13 Variation of maximum cylinder pressure with ethanol concentration in the blend..... | 82 |
| Figure 3.14 Variation of maximum cylinder temperature with ethanol concentration in the blend..... | 83 |
| Figure 3.15 Variation of specific fuel consumption with ethanol concentration in the blend..... | 84 |
| Figure 3.16 Variation of CO ₂ mole fraction with ethanol concentration in the blend..... | 84 |
| Figure 3.17 Variation of NO mole fraction with ethanol concentration in the blend..... | 85 |

LIST OF TABLES

| | |
|---|----|
| Table 2.1. Properties of different gasoline-ethanol blended fuels..... | 20 |
| Table 2.2 Properties of Ethanol and Gasoline..... | 44 |
| Table 3.1. Engine parameters in details..... | 65 |



CHAPTER 1. INTRODUCTION AND AIM

1.1. INTRODUCTION

Energy is one of the fundamental components that directly influence economy, since every manufacturing facility and service demand on its supplies. It is a well-known fact that there is a global growth in economies, which yields an increase in overall energy demand, thus an increase in overall supply and use of energy sources. In a closer look, coal, natural gas, oil, hydroelectricity and nuclear energy are the major energy sources for the world. Further categorizing, coal, natural gas and oil are defined as fossil fuels and these three types are limited in reserves. [1] As it's obvious in Figure 1.1 conventional sources of energy provide approximately 80% of world energy demand it's clear that this sources of energy are limited [2]. Some rare areas of middle east are almost the only parts on the earth which the low coast oil is still available beside that undergoing circumstance its predictable that the global energy demand will increase by 37% by 2040 the increasing use for oil derives in transportation system will result in higher consumption of oil which is 90 million barrels per day (mb/d) in 2014 to 104(mb/d) in 2040 this poses a great risk for oil shocks like what happened in 1970s in ahead decades on the other hand the investments that has done in renewable energy technologies and low carbon fuels the share of biofuels in transportation will be three times of what is today and it will be almost 4.6 (mb/d) by 2040.[3]

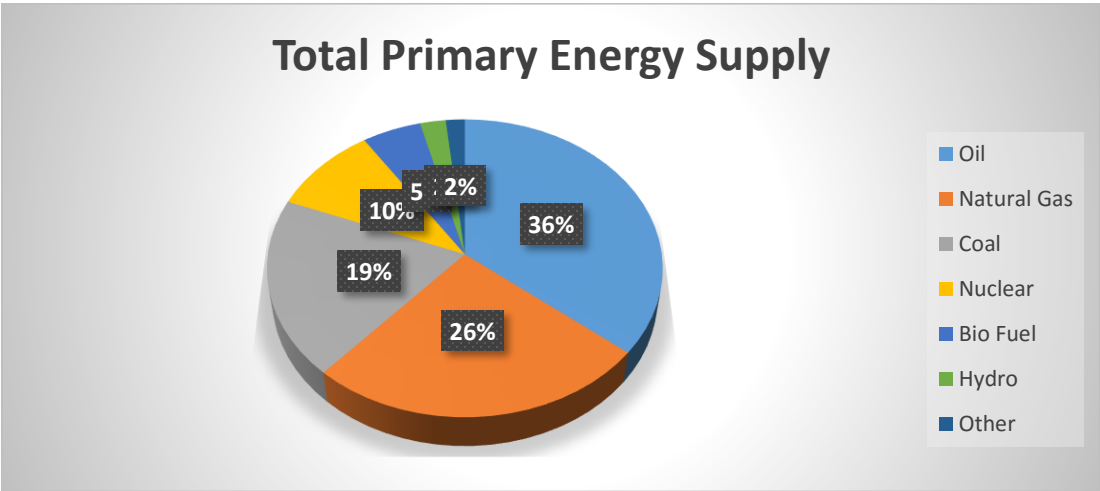


Figure 1.1 World Energy Consumption apportioned according to energy sources [1]

We are now at time of great change and opportunity in the transportation industry, including the availability of large volumes of ethanol (with higher octane ratings than gasoline-derived refinery streams) more efficient engine technology options requiring higher octane ratings, and the goals of reducing greenhouse gas (GHG) emissions and petroleum consumption. The magnitude of the GHG impact of ethanol varies depending on the feedstock with the overall net impact being the subject of debate [4]. In the coming years sustainable energy sources will be evaluated by several parameters like cost effectiveness and technical constraints. To resolve the issues a mix of various technical and managerial solutions will be needed. Energy crops based biofuels should have main role in the transportation system. In developed countries like United States for supporting and modifying the biofuel market government has set forcibly targets for using biofuels as component of fuel in road transportation [5].

The EU Renewable Energy Directive (RED) has sets at least 10% target for the share of renewable fuels in transportation, which should be achieved by 2020 [4]

Ethanol was added to US gasoline in the 1980s and 1990s at similar concentrations as today (10% v, E10), but total ethanol volumes were considerably less (Figure.2). In the early 2000s, ethanol use increased due to its use as an alternative oxygenate in reformulated gasoline when methyl t-butyl ether (MTBE) was phased out.

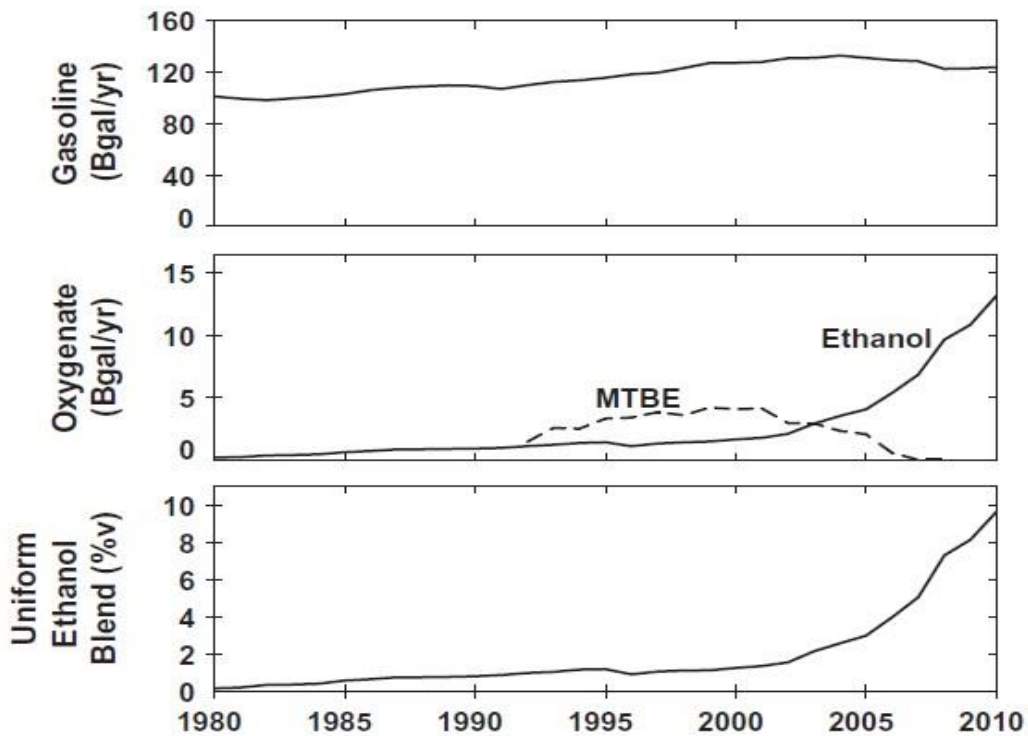


Figure 1.2. Historical gasoline, ethanol, and MTBE consumption for US road transportation, and hypothetical nationwide uniform ethanol–gasoline blend level.[6]

The physical properties of ethanol provide important benefits when added to gasoline. Ethanol has both a higher octane rating and a higher heat of vaporization than typical gasoline.

The octane rating of a fuel is a measure of the fuel's ability to resist auto-ignition and knock in a spark-ignited engine. Higher octane-rated fuel is desirable as it enables improved engine efficiency.

Coordination of increases in engine CRs and gasoline octane ratings would represent a resumption of earlier historical trends.

With the exception of the World War II years, the octane ratings of regular-grade gasoline in the US increased steadily from 1930 (60 RON, 60 AKI) until the early 1970s (94 RON, 90 AKI) [6].

Fuel industry practices have adapted to the increased availability of ethanol, allowing final fuel blends to meet minimum octane ratings by producing and blending with blend stocks having lower octane ratings.

Fossil fuel combustion generates two kinds of emissions:

i. GHGs: That includes carbon dioxide (CO_2), methane (CH_4) and nitrous oxide (N_2O)_which fossil fuel related (CO_2) emission from global transportation almost generates 23% of total CO_2 emissions.

ii. Non GHG: Emissions that includes Hydrocarbons (HC), Oxides of nitrogen (NO_x) total particular matter (PM) and sulfur dioxide SO_2 .

Climate scientists have observed that the amount of Carbon Dioxide (CO_2) concentration in the atmosphere have been increasing noticeably during the past century compared to pre-industrial era.

At 2015 concentration of (CO_2) was about 40% higher than in the mid-1800s with an average increase of 2 ppmv/year parts per million by volume in the last decade. Remarkable increasing has also occurred in levels of (CH_4) and nitrous oxide (N_2O) [7]. NO_x causes various health and environmental issues because of wide compounds and derivative's in the family of nitrogen oxide, which includes nitrogen oxides like nitrogen dioxide nitric acid and nitrous oxide [6].

1.2. AIM:

The aim of this study is to analyze performance of gasoline-alcohol combustion engine and finding out how blending a gasoline with ethanol affects the performance of the engine. For this purpose, we used Chemkin-Pro and SRM-Suite and also GT-POWER software's and compared the results with experimental results and analyzed the outcomes and found out under this condition its logical to blend the gasoline with ethanol or not.

1.3. METHODOLOGY:

The methodology employed in this project was designed to accomplish the objectives described in section 1.2.

i. Literature review: The first task was to carry out a comprehensive and critical survey of available literature in the area under study. This review was done to fully understand the progress made so far made in this particular field of research; this aided with the identification of issues/areas of further research.

The survey took into account are published books, journals, papers. It was broadened to take into account information published on the Marmara University internet website and on the World Wide Web.

ii. Pre-simulation: After the study of the SRM and Chemkin-Pro and also GT-POWER soft wares documentation, some tutorials were carried out to aid with the simulations.

iv. Simulation: Simulation results were compared to experimental data in terms of pressure; heat release rate, emission and engine performance Variation of the temperature, the parameters that could not be obtained experimentally were evaluated for comparisons between the two codes.

v. Analysis: Analysis showed that both codes have advantages over each other. Crevice and blow-by, ring gap and probability density function (PDF) e based stochastic reactor modeling are main advantages of SRM Suite software and these capabilities helped with better convergence of the results. But, Chemkin-Pro results were acceptable and solution time was fairly shorter than SRM Suite. It was also seen that detailed and reduced kinetic mechanisms affected the analysis. About GT-Power

vi. Conclusion: Conclusions were drawn based on the analysis of the results.



CHAPTER 2. MATERIAL AND METHOD:

2.1. Historical Background:

During the second half of the 19th century, many different styles of internal combustion engines were built and tested.

These engines operated with variable success and dependability using many different mechanical systems and engine cycles. The first fairly practical engine was invented by J.J.E. Lenoir (1822-1900) and appeared on the scene about 1860. During the next decade, several hundreds of these engines were built with power up to about 4.5 kW (6 hp) and mechanical efficiency up to 5%.

In 1867 the Otto-Langen engine, with efficiency improved to about 11%, was first introduced, and several thousands of these were produced during the next decade.



Figure 2.1 Otto-Langen engine[8]

This was a type of atmospheric engine with the power stroke propelled by atmospheric pressure acting against a vacuum. Nicolaus A. Otto (1832-1891) and Eugen Langen (1833-1895) were two of many engine inventors of this period. During this time, engines operating on the same basic four-stroke cycle as the modern automobile engine began to evolve as the best design. Although many people were working on four-stroke cycle design, Otto was given credit when his prototype engine was built in 1876.

In the 1880s the internal combustion engine first appeared in automobiles. Also in this decade the two-stroke cycle engine became practical and was manufactured in large numbers. By

1892, Rudolf Diesel (1858-1913) had perfected his compression ignition engine into basically the same diesel engine known today. [8]

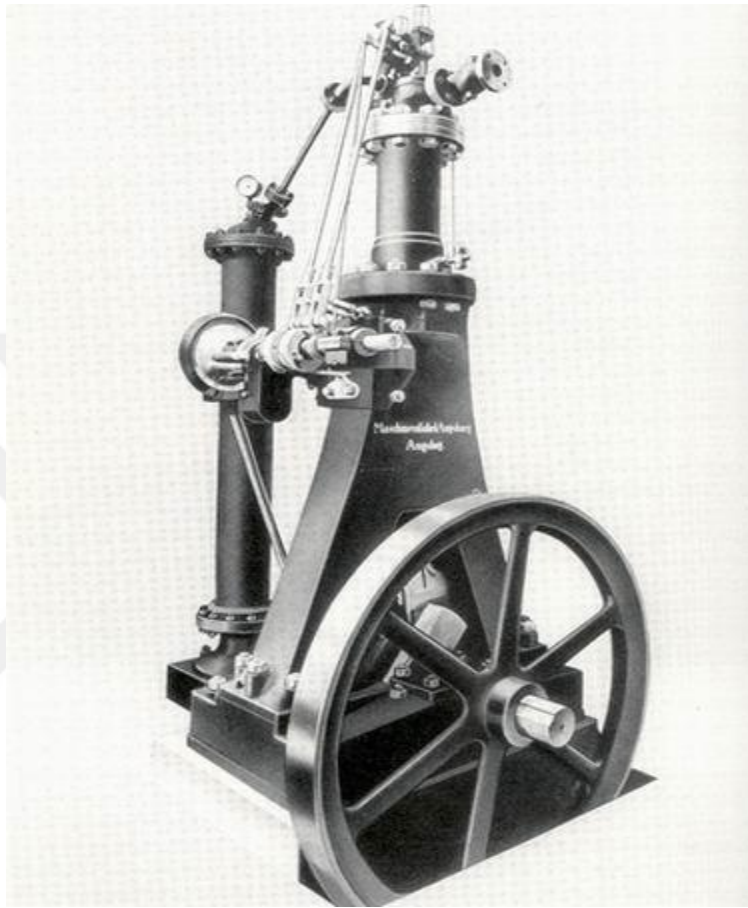


Figure2.2 Rudolf Diesel compression ignition engine [8]

2.2. Classification of Internal Combustion Engines:

There are different types of IC engines that can be classified on the following basis:

According to thermodynamic cycle:

- i.** Otto cycle engine or Constant volume heat supplied cycle.
- ii.** Diesel cycle engine or Constant pressure heat supplied cycle.
- iv.** Dual-combustion cycle engine.

According to the fuel used:

- i.** Gasoline engine
- ii.** Diesel engine
- iv.** Gas engine

According to the number of cylinders:

- i. Single cylinder engine
- ii. Multi cylinder engine

According to the arrangement of cylinder:

- i. Horizontal engine
- ii. Vertical engine
- iv. V-engine
- v. In-line engine
- vi. Radial engine, etc.

According to the method of cooling the cylinder:

- i. Air cooled engine
- ii. Water cooled engine

According to their applications:

- i. Stationary engine
- ii. Automobile engine
- iv. Aero engine.
- v. Locomotive engine
- vi. Marine engine, etc. [engine book]

2.3. Self-Ignition and Octane Number:

Anderson et al evaluated the effect of ethanol in ethanol- gasoline blends on octane number of fuel [6]. As high octane rating of ethanol could be used in a mid-level ethanol blend to increase the minimum octane number (Research Octane Number, RON) of regular-grade gasoline. Higher RON would enable greater thermal efficiency in future engines through higher compression ratio (CR) and/or more aggressive turbocharging and downsizing, and in current engines on the road today through more aggressive spark timing.

Developing scenarios of future ethanol availability, it's possible to estimate that large increases (4–7 points) in the RON of US gasoline are possible by blending in an additional 10–20% v ethanol above the 10% already present.

Estimates of RON of ethanol–gasoline blends were calculated using the methodology introduced by authors in which the RON of an ethanol–gasoline blend (RON_{blend}) is a linear function of the molar ethanol concentration (x_{alc}),

$$RON_{blend} = (1 - X_{alc}) RON_{gasoline} + (X_{alc}) bRON_{mol,alc} \quad (2-1)$$

Molar ethanol concentrations were calculated using Eqs. (2) and (3), where C_{alc} = volumetric concentration (%) of ethanol, and r_{mv} = ratio of liquid molar volumes of ethanol and gasoline blend stock (v_{alc} and $v_{gasoline}$, cm^3/mol).

$$X_{alc} = C_{alc} / [C_{alc} + (1 - C_{alc}) r_{mv}] \quad (2-2)$$

The liquid molar volume ratio, r_{mv} , was estimated using molecular weights (M_{alc} and $M_{gasoline}$, g/mol) and densities (ρ_{alc} and $\rho_{gasoline}$, kg/m³) of the alcohol and blend stock.

$$r_{mv} = V_{alc}/V_{gasoline} = (M_{alc}/\rho_{alc})(M_{gasoline}/\rho_{gasoline}) \quad (2-3)$$

Equations. (1) – (3) are summarized in Figure. 2-3 showing estimated RON values of ethanol–gasoline blends following contour lines of constant blend stock RON

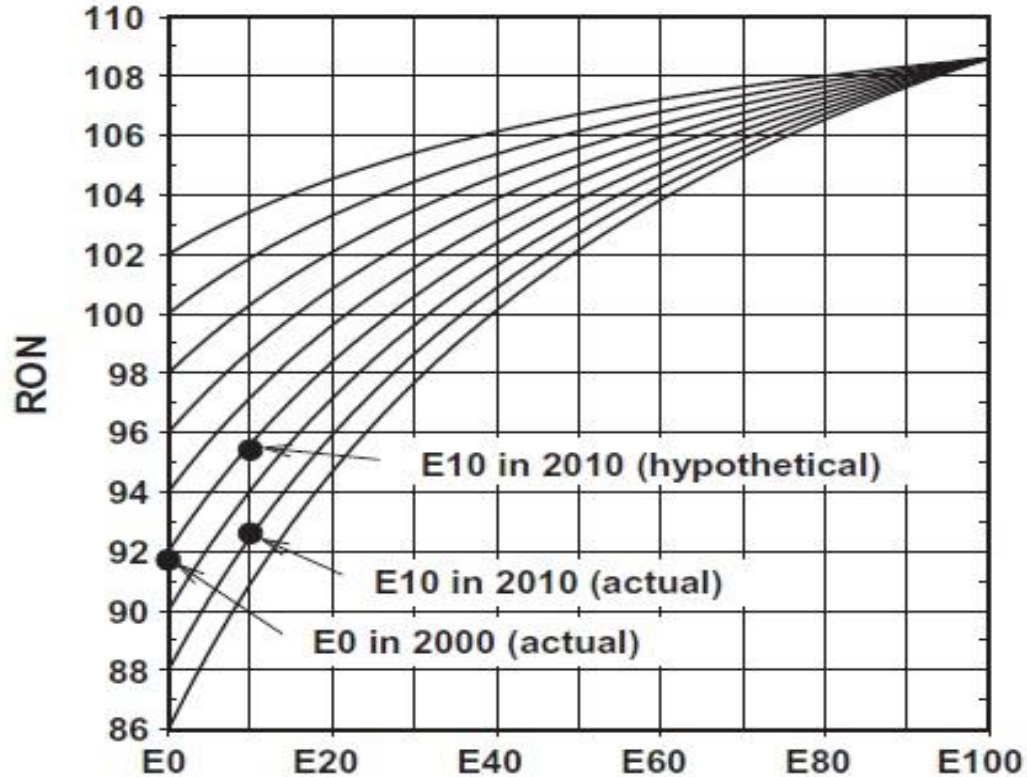


Figure.2.3. Estimated RON and RON + cooling ON of ethanol–gasoline blends for two blend stock RON values (88 or 92 RON). [6]

Which the solid lines show estimated RON values for ethanol–gasoline blends for two blend stocks, either 88 or 92 RON, with 88 RON being the estimated RON of the average blend stock used for regular-grade E10, and 92 RON being the average of regular-grade E0 gasoline in the US. So incorporating ethanol with its inherent high octane rating is one opportunity to enable an increase in the minimum octane rating for regular-grade fuel. This would differ from the current approach in which the octane rating of the blend stock is reduced such that the resulting E10 blend just meets the current minimum specification.

Using scenarios of future ethanol availability, large increases (4–7 points) in the RON of US fuel are possible by blending in an additional 10–20%v ethanol above the 10%v already present. Greater RON increases may be possible through improvements to the blend stock RON and/or hydrocarbon composition. Potential compression ratio increases were estimated to be on the order of 1–3 CR above respective baselines for DI engines in which the greater evaporative cooling of ethanol can be fully utilized.

2.4. Burning velocities of alcohols and hydrocarbons:

Major aspect of understanding combustion of fuels in engines is their

Laminar flame speed is a property of a combustible mixture. It is the speed at which an unstretched laminar flame will propagate through a quiescent mixture of unburned reactants.

and turbulent burning velocities in controlled environments and at engine relevant conditions.

Furthermore, in most of the published databases, the effect of burned gas on laminar burning velocity has not been quantified in detail and hence very few data exist that are directly relevant to realistic in-cylinder conditions.

The overall effect of burned gas residuals on burning velocities has been quantified to be much stronger than that of excess air, temperature or pressure; with residual fractions of 0.15–0.2, the laminar burning velocity of iso-octane has been found to decrease by 35–45%. Such levels of residuals are commonly found in DISI engines at part-load operation or when Exhaust Gas Recirculation (EGR) systems are employed to control NO_x formation over arrange of loads.

Furthermore, despite effort that have quantified turbulent flame speed in DISI engines by direct flame visualization (chememiluminescence) with a variety of fuels, including iso-octane, gasoline ethanol, butanol and some of their blends very little information exists on flame speeds obtained by planer imaging by x ray techniques in modern geometry SI engines, but no detailed planer data have been derived specifically with ethanol and butanol fuels in direct comparison to iso-octane and gasoline. [9]

2.5. Injection times:

Costagliola et al[10] investigated the effect of bioethanol–gasoline blends on the exhaust emissions and engine combustion of a four-stroke motorcycle at experimental part of study they employed a Euro 3 large-size motorcycle fueled with commercial gasoline and bioethanol/gasoline blends which the ethanol contents of fuels are like: G5 (ethanol/G0 5/95% v), G10 (ethanol/G0 10/90% v), G20 (ethanol/G0 20/80% v) and G30 (ethanol/G0 30/70% v).

The engine characteristics are:

Displacement is 999.6 cm³ (bore/stroke 78/52.3 mm and compression ratio 13:1) with a maximum power of 132.4 kW at 12,500 rpm and a maximum torque of 115 Nm at 10,000 rpm. The motorcycle was tested on a two-wheeler chassis dynamometer (AVL Zollner 20" - single roller), which simulated vehicle inertia and road load resistance.

In one part of study the authors diagnosed the influence of gasoline –ethanol blend in injection time of engine

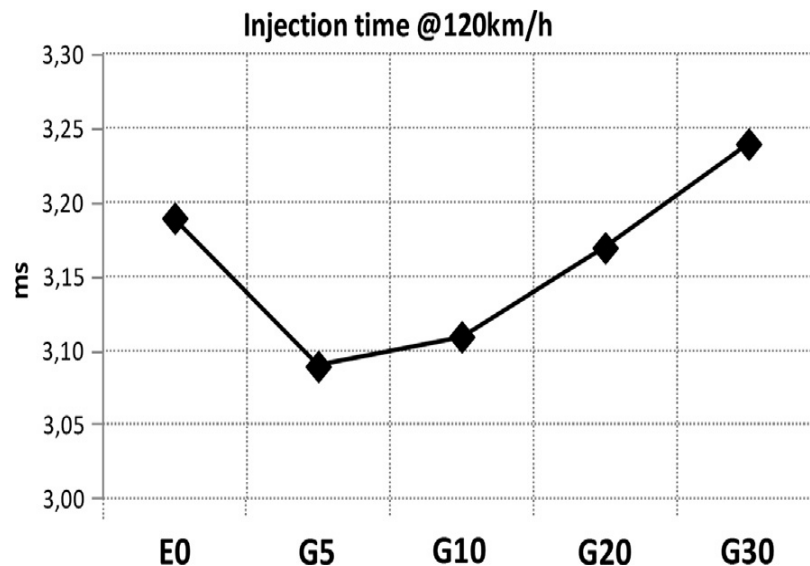


Figure. 2.4 Injection times for all tested fuels during 120 km/h steady-state test. [10]

From the analysis of some on-board diagnostic (OBD) parameters, it was observed that the use of bioethanol in the fuel strongly influenced the injection time. It rises as the ethanol percentage increases (figure 2.4). The increases in the injection time with the ethanol

percentage of the blends is due to the reduced specific heat. The specific heat capacity of a material is the amount of energy (Q) needed to raise 1 kg of a material through a temperature change of 1 kelvin., which is also responsible of an increment of fuel consumption.

Regarding spark advance, no trend could be found, reflecting the fact that the engine ECU did not modify this parameter when the fuel changed. In other words, the ethanol could be used in a high percentage (<30%) blend with gasoline without any engine and ECU parameter modifications.

2.6. Effects of heated ethanol on injector performance:

For gasoline direct injection engines, Chen and Nishida [11] studied the spray evaporation and combustion of ethanol- gasoline blends (E0, E85, and E100) injected by hole-type nozzle. The tests in a high-temperature and high-pressure quiescent constant volume vessel equipped with a dual-wavelength laser absorption scattering technique were investigated. Ethanol evaporates faster than gasoline while the combustion becomes more vigorous due to the oxygen content in ethanol. Furthermore, the ethanol-gasoline blends improved combustion stability particularly when advancing the ignition timing.

Chuepeng diagnosed Effects of heated ethanol on retrofit single-hole gasoline injector performance [11]. The main aim of this work is to explore the injector performance in terms of fuel mass flow rate and discharge coefficient when ethanol is in use with gasoline injectors at elevated temperatures. The operating fuel injection was at the pressures between 0.2 and 0.4 MPa and the temperatures in a range of 40–80 °C.

A fuel injector test cell with electronic control for injection pulse, timing and pressure was set to 120 Hz and 60 min injection duration to drive three single-hole 0.34 mm nozzle diameter injectors. The fuels were injected into a known volume flask at quiescence atmospheric pressure and weighed to attain the fuel mass flow rates.

The injector test cell is schematically depicted in Figure. 2.5

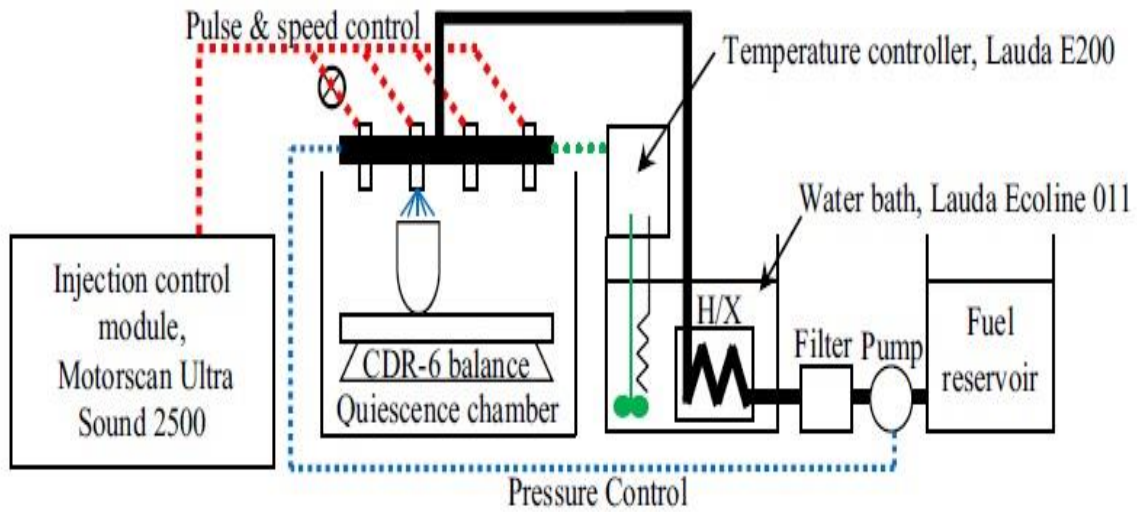


Figure.2.5. Fuel injector test cell. [11].

The fuel injection control module from Motor scan model Ultra Sound 2500 was employed to supply pulse and speed signals by electronic control to injectors. There were two types of fuel used in the test, ethanol and gasoline.

2.6.1. Effects of pressure drop on fuel flow rate:

At a temperature, fuel mass flow rate is dependent on pressure difference across the injector nozzle as shown in Figure. 2.6.

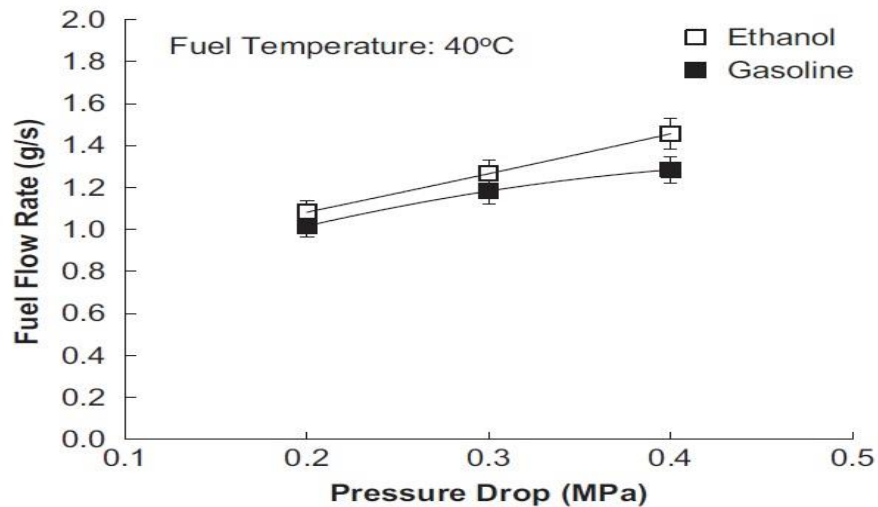


Figure 2.6. Fuel mass flow rate dependency on pressure drop across injector nozzle at 40°C fuel temperature. [11].

The fuel mass flow rate increased with the injection pressure. It is clear in Figure.2.6 that the relation between the fuel mass flow rate and the pressure drop follows $\dot{m} \propto \sqrt{\Delta p}$. With the same value of pressure drop, the injector delivered higher rate of ethanol than gasoline. This may be due to the difference in fuel density.

2.6.2. Effects of temperature on fuel flow rate

Fuel mass flow rate is also dependent on injection temperature as shown in Figure 2.7 for 0.4M Pa pressure drop across the injector nozzle. The variations in fuel mass flow rate were different for fuel type, depending on fuel temperatures. When elevating the fuel temperatures from 40 °C up to 60 °C, the injection of ethanol delivered greater fuel flow rate than gasoline. However, the increment of the fuel temperatures of up to 80°C caused the fuel mass flow rate declined for all type of fuels compared to those at 60 °C. This behavior can occur when ethanol absorbed external heat that changes the density of the fuel itself, causing the injector delivering lesser fuel throughout its nozzle.

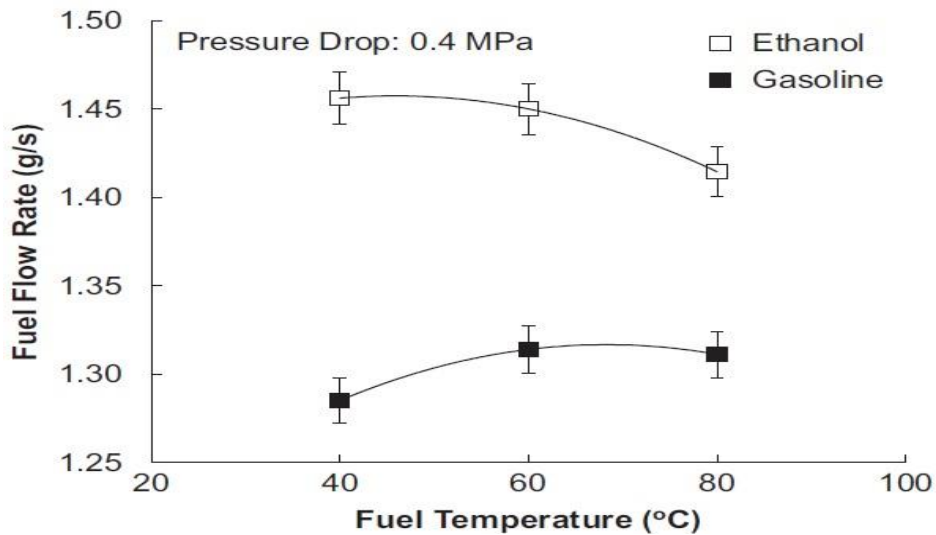


Figure 2.7. Fuel mass flow rate dependency on fuel injection temperature at 0.4 MPa pressure drop [11].

2.6.3. Discharge coefficient

The temperatures of the injected fuels are shown to affect the discharge coefficients as shown in Figure 2.8 for 0.4 MPa. Pressure drop across the nozzle. At the same pressure drop, the discharge coefficients for the injection of the ethanol were greater than gasoline. However, the variations in discharge coefficients were different for fuel type, depending on fuel temperatures. The greatest difference in discharge coefficient of up to 10% for ethanol compared to gasoline was observed at 40 °C.

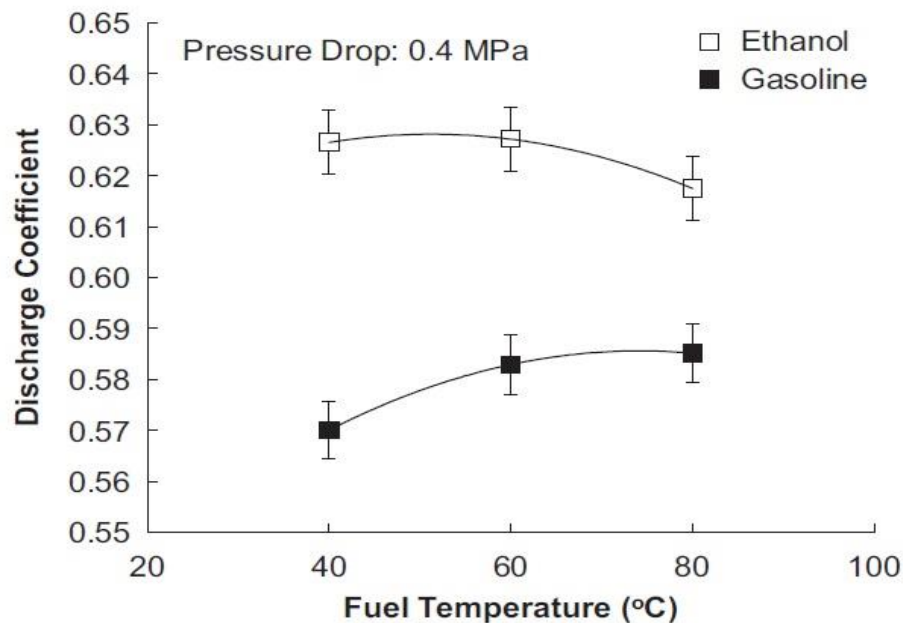


Figure 2.8. Discharge coefficient variation with fuel injection temperature at 0.4 MPa pressure drop. [11].

This is mainly derived from the larger fuel mass flow rate of ethanol than gasoline at 40 °C. When the fuel temperatures were climbed up from 40 °C to 80 °C, the discharge coefficients for the injection of ethanol were declined that contrasts to those of gasoline. This occurrence can be observed in parallel with the fuel mass flow rate.

The results showed that: At constant fuel temperature, ethanol delivered greater fuel amounts than gasoline.

Both fuels showed greater flow at higher pressure drop across the injector nozzle.

Higher discharge coefficients were observed for ethanol. By the conditions used in the test, the heated ethanol up to 60°C benefits for both terms of mass flow rate and discharge coefficient.

2.7. Effect of ethanol–gasoline blends on cold start emissions in SI engines:

In recent years, advances in internal combustion engines (such as the common rail, the adoption of improved lubricants, the development of the control electronics and the use of catalytic converters) allowed to reduce considerably both fuel consumption and pollutants emission. These relate definitely steady operation of the engines, but there is still some way to go with regard to engine cold starting, the phase in which the environmental performance is not optimal due to low temperature of engine components and lubricants this occurs mainly for the following reasons: Partial combustion, Catalyst inefficiency, and increased friction.

Iodice et al investigated the effect of ethanol–gasoline blends on cold start emissions in SI engines [12] for this purpose they equipped motorcycle with a four stroke SI engine with a displacement of 1000 cm³. which belongs to Euro-3 legislative category This engine is fitted with a very efficient electronic fuel injection system, allowing the control of fuel feeding and enhancing catalyst efficiency also in cold transient. Five testing fuels were used in the experimental activity first fuel (E0) is commercial gasoline with oxygenated additive (8.1% v/v) and a research octane number (RON) of 95.5. Second fuel is unleaded gasoline without any oxygenated additive (G0), that is also used as a reference and base fuel for the composition of ethanol– gasoline blends; the other fuels (G10, G20, G30) are ethanol–gasoline blends containing 10%, 20% and 30% ethanol v/v, respectively.

Each experimental tests were performed in cold-start conditions and, for each blended fuels, the motorcycle was kept at a relatively constant temperature around 20 C° for at least 6 h.

By employing the calculation procedure it's obvious the results obtained in this study show clearly that using ethanol–gasoline blends, CO and HC cold-start extra emissions decrease with increases in ethanol concentration, until 20% v/v ethanol content, because more ethanol in the blends supplies additional oxygen during the cold transient for more efficient combustion process in the fuel rich regions of engine. Besides, the higher volatility of the

20% ethanol blend improves fuel vaporization during the transient time, thus decreasing CO and HC cold emission levels.

On the other hand, higher ethanol concentration blend (30% v/v ethanol content) was characterized by higher CO and HC cold emissions than those of lower content blends, because with even more ethanol in the blends, the heating value decreases while the latent heat of evaporation increases, so resulting in lower combustion temperature and burning velocity, leading to partial combustion process.

Besides, for higher ethanol percentage (>15% v/v) the volatility of blend fuel decreases, and over a definite lean limit, partial combustion could happen during the cold transient time, leading to numerous misfires and then with resulting increased cold emissions.

2.8. Effect of ethanol–gasoline blend on NO_x emission:

Many studies have been done on SI engines as well as flex-fuel vehicles using either pure ethanol or ethanol–gasoline blends as a fuel.

2.8.1. Formation of NO_x:

NO_x is a mixture of such compounds: Nitric oxide(NO), nitrogen dioxide (NO₂), nitrous oxide(N₂O),dinitrogen trioxide (N₂O₃),dinitrogen tetroxide.(N₂O₄),and dinitrogen pentoxide (N₂O₅).

Among them, nitric oxide (NO) and nitrogen dioxide (NO₂) are most prominent.

The other five nitrogen oxides are known to exist, but in very small quantities. Nitric oxide is a colorless, odorless gas. Its ambient concentration is usually far less than 0.5ppm. Nitrogen dioxide is a corrosive, toxic, and reddish- brown gas. It is quite visible insufficient amounts Oxidation of nitrogen molecules at high temperature inside the cylinder is the cause of NO_x formation as a byproduct. The pathways of formation of oxides of nitrogen such as Thermal, Prompt, Fuel NO_x and N₂O intermediate mechanisms are discussed here. [13]

2.8.2. Effect of blend concentration

Researchers have tested ethanol–gasoline blends from 5 vol% ethanol to as high as 100 vol% i.e.pure ethanol in SI engines.

The physicochemical properties of different ethanol – gasoline blends are summarized in Table 5. These results presented have been obtained by different test methods as done by the researchers. From Table 2.1 it can be seen that the addition of ethanol to gasoline simultaneously increases the octane number, density, and latent heat of vaporization and decreases the heating value of the ethanol–gasoline blend. Many investigations have been carried out to identify the effect of these changes on emission characteristics especially on NO_x emission due to variation in ethanol contents.

Table 2.1. Properties of different gasoline-ethanol blended fuels.[13]

| Property | E0 | E5 | E10 | E15 | E20 | E25 | E30 | E40 | E50 | E60 | E100 |
|-----------------------------|------------|-------------|-----------|------|-----------|------|-----------|-------|-------|------|-------|
| Density(kg/m ³) | 757 | 759 | 760 | 776 | 764 | 775 | 768 | 780 | 751 | 789 | 792 |
| RVP(KPA) | 53 | 59 | 59 | 58 | 58.3 | | 56 | 63 | 45 | 57 | 37 |
| RON | 95.4 | 96.7 | 98.1 | 98.5 | 100.7 | 100 | 102 | 90 | 101 | 92 | 101 |
| (a)Initial Boiling Point | 35.5-38.8 | 36.5 | 37.8 | 37.9 | 36.7-38.7 | | 37.2-39.5 | 39.6 | 32.83 | | 31.86 |
| (b)10% Vol | 54.5-56.1 | 49.7 | 50.8-52.9 | 51.7 | 51.3-52.8 | 58.1 | 52.1-54.8 | 53.4 | | | 73.9 |
| (c)50% Vol | 94-109 | 88 | 71-95 | 72.6 | 70-73 | 71 | 72-74 | 72.5 | 52 | | 78 |
| (d)90% Vol | 167-206 | 167 | 157-166 | 165 | 165-163 | | 154-159 | 152 | 57.4 | 78.7 | |
| (e)End point | 197 | 202 | 197-208 | 198 | 198-203 | 177 | 198-205 | 204 | | | 79.9 |
| Heating Value(MJ/Kg) | 42.58-42.7 | 40.55-41.78 | 39.79-41 | 41.6 | 38.-39 | 38.2 | 36.30-37 | 33-36 | 33 | 26 | 29 |

Many literatures have showed that, NO_x emission decreases with the increase in content of ethanol. Turner et al. [14] investigated NO_x emission in a direct injection spark ignition (DISI) engine on a 1500 rpm and 3.4 bar indicated mean effective pressure (IMEP) with ethanol – gasoline blends. When the ethanol portion increased up to 85% in the blend, NO_x emission was reduced. They attributed this reduction to reduction in flame temperature, which was corroborated by a reduction in exhaust temperature. The NO_x level then increased slightly for pure ethanol because combustion was advanced, leading to a higher in-cylinder pressure and temperature compared to those of 85% ethanol. Here the maximum in-cylinder pressure was reduced with an ethanol blend of up to 85% and then increased for pure ethanol. Bielaczyc et al. [15] also found decreased NO_x for 10–85% ethanol blends. They evaluated the possibility of using gasoline–ethanol blends in a modern Euro4 vehicle without substantial engine modification. NO_x emission from the engine was found to give a perfect linear fit with the ethanol content of the blend over the range 10–85%. Oh et al. [16] studied a DISI engine with 25%, 50% and 85% ethanol–gasoline blends. They found that HC emissions increased and NO_x emissions decreased with increase of ethanol percentage in blend due to the decreased peak in-cylinder temperature resulting from the combustion retardation.

Ioannis et al. [17] investigated NO_x emission with different blends at 1500 rpm in wide open throttle (WOT) condition. From figure.2.9, it is seen that, NO_x emission decreased with increasing ethanol concentration. Because of the higher heat of vaporization of ethanol compared to gasoline, the combustion temperature of the blend decreases. In case of HC emission, up to certain concentration of ethanol, HC emission is reduced as the oxygen content of ethanol causes the reaction to move towards complete combustion. However, a greater concentration of ethanol in the gasoline reduces the flame temperature, which increases HC emission. It is seen that E40 is a good option for reduced HC emission and E80 is suitable for lower NO_x emission.

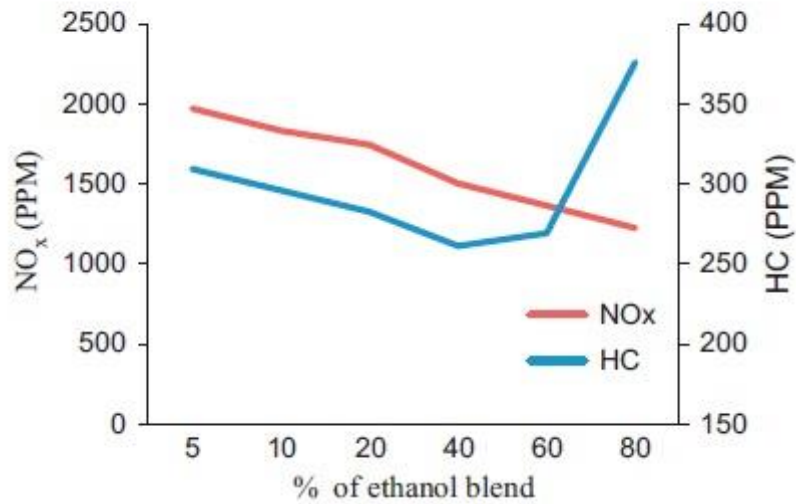


Figure 2.9.Correlation of NO_x and HC emission with ethanol percentage at 2000 rpm [17].

In a four-cylinder, multi-port injection system engine, Canakci et al. [50] found that NO_x emission decreased as the ethanol percentage of the blend increased. With the use of alcohol in gasoline, the combustion temperature decreased due to the high latent heat and lower heating value, which led to the reduction of NO_x emission. When comparing the exhaust emission of gasoline with pure ethanol, Balki et al. [18] found lower NO_x emission for ethanol than gasoline. They attributed this reduction to the higher heat of vaporization of ethanol, which reduces the combustion temperature. Yao et al. [19] Found similar results. They ascribed this to lower flame temperature because of the higher latent heat of evaporation of ethanol.

Considering a DISI engine, Storey et al. [20] analyzed the effect of ethanol addition and concluded that NO_x emission decreased with increased ethanol concentration because of the lower energy density of the ethanol blend. Lin et al. [21] experimented on a small engine generator to observe the effect of ethanol–gasoline blend on exhaust emission and efficiency. Ethanol–gasoline blend led to a significant reduction in NO_x emissions by approximately 35%, 86 % and 77% on average with E3, E6, and E9 fuels respectively.

The best results were obtained with E6 fuel in term of exhaust emissions and E9 fuel for engine performance. Broustail et al. [22] found a slight reduction in NO_x using ethanol with gasoline than compared to pure gasoline. Using a motorcycle engine Chen et al. [23] investigated the effect on emission of ethanol–gasoline blends (E3, E5, E10, E15, E20, E25 and E30). With an increase in the ethanol concentration, the particle diameter of the accumulation mode becomes smaller. The aerosol number concentration decreases with increases in ethanol concentration which causes combustion to become complete. For this reason, CO and NO_x emission decreased with increases in ethanol concentration. The emission reduction rates as high in low ethanol concentration blend (E15) compared to high ethanol concentration blend (E20).

In contrast, some researchers have found increased NO_x emission. Using a single cylinder SI engine, Schifter et al. [24] investigated the effect of using gasoline–ethanol mid-level blends (0–20% ethanol) on engine performance and exhausts emissions. It is seen that NO_x emission increased with the addition of ethanol to gasoline compared to gasoline. With the addition of ethanol, NO_x emission is higher for a higher heat release of ethanol.

The performance and the pollutant emissions of a four-stroke SI engine operating on ethanol–gasoline blends of 0%, 5%, 10 %, 15 % and 20 % were investigated by Najafi et al. [25]. They also found a higher NO_x concentration when the ethanol percentage increased, as shown in Figure. 3.

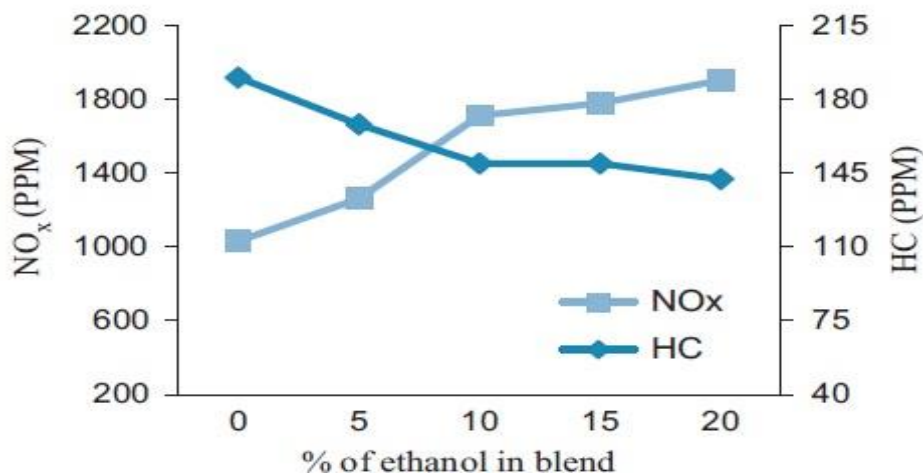


Figure 2.10. Correlation of NO_x and HC with the percentage of ethanol at 3500 rpm [25].

Another significant reason for this increase is that the oxygen content in the ethanol-blended fuels increased the oxygen to fuel ratio in the fuel rich regions.

The most significant parameter affecting NO_x concentration is the relative air–fuel ratio. The actual air–fuel ratio approaches to stoichiometric as the ethanol content of the blended fuel increases, and consequently combustion becomes complete. This complete combustion increases the in-cylinder temperature as well as NO_x emission.

With a higher oxygen concentration in ethanol, Keskin and Guru [26] also found higher NO_x emission with the addition of ethanol. Zhuang et al. [27] varied the ethanol/gasoline energy ratio from 0% to 60.1%. NO_x emission increased with the addition of up to 24.3% ethanol to gasoline after which it decreased with increasing ethanol percentage. With regard to increasing NO_x, they reported that, ethanol improved the combustion inside the cylinder resulting in an increased in-cylinder temperature. In the case of reduced NO_x, they explained that a higher percentage of ethanol in gasoline reduces the in-cylinder temperature. They attributed this reduction to two factors. One is the high latent heat of vaporization of the ethanol fuel, which decreases the in-cylinder temperature when it vaporizes. The other factor is that there are more triatomic molecules in the combustion products of ethanol fuel than in those of the gasoline fuel. The more triatomic molecules are produced, the higher the gas heat capacity and the lower the combustion gas temperature will be. However, the low in-cylinder temperature can also lead to an increment in the unburned combustion product.

2.8.3. Effect of hydrous ethanol:

The water absorbs heat and lowers the pressure as the charge is compressed reducing the compression stroke work. Additionally, during the combustion itself, water absorbs heat as it vaporizes reducing the peak temperatures and then reducing NO_x emissions. This peak temperature reduction diminishes the heat flux to the cylinder wall. As a result of the reduced intake air temperatures and the effects on the combustion process itself, fuel blends of gasoline with hydrated ethanol present slightly lower exhaust gas temperatures. As distillation of hydrous ethanol to get anhydrous ethanol is costly, there is scope for hydrous ethanol. Also, few researches have dealt with hydrous ethanol so far. Schifferetal. [28] Compared mid-level (0–40% volume water) hydrous ethanol–gasoline blend with anhydrous

gasoline blend. They found 2% lower NO_x emission for hydrous ethanol–gasoline blends than for anhydrous ethanol–gasoline blend. Water in the hydrated ethanol decreases the temperature, combustion speed, and peak pressure compared to anhydrous ethanol, therefore improving the NO_x emission, especially for 30% and 40% ethanol contents. Water slows the combustion process but keeps the quantity of energy produced per cycle constant, the amount of work obtained is therefore the same and the same amount of heat is released, but more efficiently. Kyriakides et al. [29] also get lower NO_x for 40% hydrous ethanol blend compared to 40% anhydrous ethanol. They explained, water content of hydrous ethanol lowered the peak temperature and slowed the combustion rate that resulted lowers NO_x emission.

Costa and Sodre [30] compared the performance and emissions of E22 with hydrous ethanol (6.8% water content in ethanol). The NO_x emission of hydrous ethanol was more than those of E22. For higher NO_x of hydrous ethanol, they explained, a faster flame speed of hydrous ethanol favors the production of higher peak pressure and, therefore a higher peak temperature in the combustion chamber. considering a small SI engine, Munsen et al. [31] studied the effect of hydrous ethanol (up to 40 % water in ethanol) on performance and emission. The addition of 20–40% water to ethanol resulted in incomplete combustion, which increased CO and HC emission and reduced NO_x emission. They determined the combustion temperature by measuring the spark plug temperature. The spark plug temperature was found to decrease with increases in the water content in ethanol. The lower combustion temperatures of hydrous ethanol affect the thermal NO_x formation.

2.8.4. Effect of compression ratio

It was found that a high CR can increase the efficiency of ethanol fuel blends, and as a result, the fuel economy penalty associated with the lower energy content of E85 can be reduced by about 20% [32]

The relatively high burning rate of the overall rich mixture combustion and a high-temperature environment contribute to the increase in the NO_x emissions with increasing CR at high engine loads to improve engine power, Al-Baghdadi [33] used the high useful compression ratio (HUCR), which is a variable compression ratio that is directly proportional

to the ethanol percentage in the blend. The compression ratio varies from 8 to 9.25 as the ethanol percentage increases from 0% to 30%. The NO_x emission decreased with increases in ethanol although the CR was increased.

Celiketal.[34] increased the compression ratio from 6:1 to 10:1 by adding 50% ethanol to gasoline. When running with E50 at a high compression ratio (10:1), NO_x decreases by 19% compared to the case of E0 fuel at a compression ratio of 6:1. NO_x emission is reduced here owing to the fact that the heating value of ethanol is lower than that of gasoline.

Koc et al. [35] used 0%, 50% and 85% ethanol with gasoline on compression ratios of 10:1 and 11:1. NO_x emission decreased with the increase of ethanol. NO_x emission of gasoline at CR10:1 is also higher than those of ethanol–gasoline blend at a CR of 11:1.

The high latent heat of vaporization of ethanol lowers the flame temperature, which results in lower NO_x emissions. However, the NO_x emission may change depending on the percentage of ethanol in the blend and operating conditions. The oxygen concentration and combustion temperature and combustion duration are the main parameters affecting the NO_x emissions. However, for the same blend, NO_x was higher for a higher CR.

2.8.5. Effect of engine load

Engine load plays a very important role in NO_x formation. More fuel or a richer mixture is needed to increase the engine load, which results in a higher in-cylinder temperature as well as higher NO_x formation. The flame speed of fuel is an important factor for complete combustion in rich-mixture conditions as well as high engine load. Using a 1.4L flex-fuel engine, Melo et al. [36] tested 0–100% hydrous ethanol with gasoline at two different loads. At a low load (60 Nm), NO_x emission decreased with ethanol addition. But at the same speed with a higher load (105 Nm), NO_x increased with the addition of ethanol.

They explained that the higher flame speed of ethanol compared to gasoline was the cause of the NO_x emission increase when using ethanol at high load. A higher flame speed assists in complete combustion. It is also seen that the CO emission reduction with the addition of ethanol at high loads is higher than that at low loads.

At a high load, Keskin and Guru [37] also found higher NO_x emission for adding ethanol. They did experiment with 0%, 4%, 8%, 12%, 16%, and 20% ethanol in gasoline at different

loads (800, 1600, 2400 kW). At lower load conditions, NO_x emissions were the same for all blends but at higher loads, NO_x emissions were higher for ethanol-blended fuel.

Gomes et al. [38] focused on the operation of ethanol blends up to E100 at high loads of up to 30 bar IMEP. At comparatively lower loads, NO_x emissions were lower for high ethanol content blends. They explained that ethanol lowered the peak temperature slightly, which reduces NO_x at lower loads. However, at comparatively higher loads, NO_x emissions were the same for all of the blends as high flame speed of ethanol fuel results in similar peak temperatures. No significant change in NO_x emissions was observed at different engine loads (3–161 Nm torque) by Pang et al. [39], when they compared gasoline and 10% ethanol blended gasoline. However, for lower heating values, fuel consumption was greater for ethanol-blended fuel.

2.8.6. Effect of equivalence ratio

The stoichiometric air–fuel-ratio of gasoline is 1.6 times higher than that of ethanol.

Since at fixed throttle opening and a fixed engine speed, the amount of air intake is a constant; to obtain the same λ , more volume flow rate of ethanol–gasoline blend is required than base gasoline which produces the leaning effect.

Leaning of fuel/air ratio causes the flame temperature to blow enough to reduce NO_x as well as other emissions [40].

Theoretically, the hottest flame comes from stoichiometric air/fuel mixtures; however, NO_x peaks at slightly leaner fuel/air ratios. Leaning of fuel/air ratio causes the flame temperature to below enough to reduce NO_x as well as other emissions.

Hsieh et al. [13] also found higher NO_x emission in stoichiometric air– fuel ratio as complete combustion led to a high combustion temperature. However, at an equivalence ratio lower than 1.0, the effect of addition of ethanol on NO_x emissions was insignificant.

They concluded that NO_x emissions depend on the engine operating conditions rather than on the ethanol content. Using a six-cylinder test engine, Al-Farayedhi [13] found maximum NO_x emission in the equivalence ratio of 0.9 for using gasoline, E10, E15, and E20 as fuel. NO_x emissions increased as the ethanol concentration of the blend increased except at the equivalence ratio of 0.8. The availability of oxygen and high combustion temperature were

the cause of these NO_x emissions. However, for very lean mixtures, NO_x concentration decreased for higher content of ethanol.

Zervasetal. [13] investigated the effect of different equivalence ratios ($\lambda=0.83-1.25$) on exhaust emissions. They found, the difference in equivalence ratios did not lead to a large change in NO_x emissions. With different values of λ , NO_x varied from 15 % to 30%. In stoichiometric and lean conditions, emissions of CO decreased. The addition of an oxygenated compound is more important than the percentage of oxygen in the fuel, which means that CO emissions decreased because the oxygen concentration was higher. However, for E5 fuel, HC emissions are almost independent of λ . For E20 there are two zones: a 9–28% decrease in HC emissions in the lean condition and a 46–48% decrease in HC emissions in the stoichiometric and rich conditions.

2.8.7. Effect of speed:

Engine speed also affects NO_x emissions. Some authors [31] have reported that NO_x increases with engine speed as more fuel is burnt resulting in high in-cylinder temperature at high speeds. Few authors [13] have also reported low NO_x emission because of less available time for combustion at high speeds. At higher speeds, lower combustion time is available for burning higher amount of fuel than lower speeds. Flame speed is an important factor to complete the combustion in short time. As flame speed of ethanol is higher than that of gasoline, it assists in completing the combustion at high speeds, which results in higher NO_x emission for ethanol. Costa and Sodr  [18] found higher NO_x emission for 100% hydrous ethanol than E22 at high speeds as it has more ethanol content than E22. However, at low speeds (2500–3000rpm) there was no significant change for these fuels. Koç et al. [38] found different results for ethanol blended fuel at high speeds. They found 42%, 41% and 11% NO_x increase for E0, E50 and E85 respectively within speed range of 1500–5000 rpm. Increase in NO_x emission with speed was relatively lower for E85 than E0. Lower heating value combined with low combustion time can be the reason of lower NO_x for ethanol in high speeds.

2.8.8. Application of thermal barrier coating:

A thermal barrier coating (TBC) is applied to minimize heat transfer from the combustion chamber by insulating the piston and cylinder wall with an adherent layer of a low thermal conductivity material. This type of engines is known as a low heat rejection (LHR) engine. This insulation reduces the heat flux into the piston and thus heat transfer to the coolant is reduced [41]. Because of the lower heat loss, TBC affects the combustion process and hence changes the performance and emission characteristics. NO_x emission is significantly higher in the coated pistons engine, which is evident due to the higher cylinder temperature due to the lower heat loss. As the heating value of ethanol is a lower, there is growing interest in thermal barrier coated engines with ethanol blended fuel and a few works have already been done. Srinivasan and Saravanan [41] investigated the use of gasoline, E 60+2.0 Iso-heptanol, and E50+1.0 Iso-heptanol blends in a multi-cylinder gasoline engine with and without alumina titania coated pistons. In both cases, they found lower NO_x emissions for ethanol blends than for gasoline. Moreover, ethanol blends in the coated pistons condition produced lower NO_x emissions than gasoline fuel in the non-coated pistons condition. The lower heating value of ethanol is the reason for its lower NO_x emissions compared to gasoline.

Kumar and Nagarajan [42] investigated the emissions and performance of an SI engine using E20 fuel with and without TBC on the cylinder head, inlet, and exhaust valves. As TBC reduced the heat loss from the combustion chamber, it increased the peak in- cylinder temperature as well as NO_x formation. As a result, NO_x emissions were higher for the coated than the uncoated cylinder for all types of fuel blend. However, the additional oxygen of E20 fuel accelerates NO_x formation with higher in-cylinder temperature for thermal coating. Therefore, they found a 46% increase in NO_x emission for E20 than for gasoline.

2.8.9. Effect of separate aqueous ethanol injection:

It was hypothesized that the primary effect of the water was to reduce flame temperatures, thereby obstructing the thermal formation of NO_x. Avoiding the phase separation of ethanol–gasoline blend requires high purity ethanol so it is costly, and better performance of the engine depends on the best ethanol–gasoline ratio, which varies for different engine speeds

and torques. To solve this problem, an independently controlled separate set of aqueous alcohol injector was used. Chen et al. [13] installed a set of independently controlled separate aqueous alcohol injectors alongside the gasoline injector at the manifold. Aqueous ethanol with a high water content (ethanol purity: 99.7%, 75% and 50%) was injected as a fuel substitute through them. They selected two operating regimes: high way running and high load running. During high way running, engine control unit cut down the flow of gasoline when aqueous ethanol was injected by receiving feedback from the exhaust oxygen sensor, but in high load running, nothing happened. Aqueous alcohol reduced the combustion temperature and thus reduced NO_x formation. They concluded that the water content in the fuel mixture dominated the NO_x reduction rather than the ethanol content. With a 16% water content in the fuel mixture, NO_x emission can be reduced by 30% with little adverse effect on the torque compared to gasoline.

On the other hand, to compare the effect of different injection strategies on engine emissions, Anderson et al. [43] performed two sets of experiments using premixed ethanol–water blends and separately injecting water and ethanol into the blends on a modified Co-operative Fuels Research (CFR) engine at a constant compression ratio of 10:1. Three types of ethanol–water blended fuels were used: 20 vol % water + 80 vol % E100 (80/20), 10 vol % water + 90 vol % E 100 (90/10), and 30 vol % water + 70 vol % E 100 (70/30). They measured NO_x emissions, first by injecting the premixed blend and then injecting water and ethanol separately. Premixed ethanol – water blends showed a higher reduction in NO_x compared to separate injection of water and ethanol for blends with ethanol/water ratios of up to 70/30, as shown in Figure 2.11. More immediate contact between the water molecules and ethanol under premixed conditions appears to have a strong influence on combustion chemistry, which in turn produces better NO_x emission characteristics.

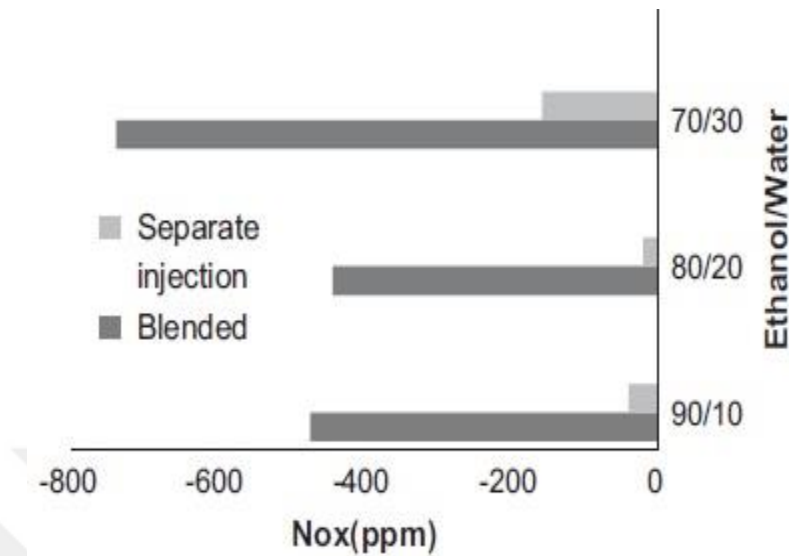


Figure 2.11. NOx emission changes for ethanol / water fuel with respect to gasoline [43].

2.8.10. Effect of different vehicles:

The use of ethanol in vehicles is increasing day by day. More than 95% of the gasoline in the U.S. contains ethanol in an approximately 10 percentage blend [44]. Ethanol is also available in higher concentration blends marketed as E85 (also known as flex-fuel).

The use of low concentration ethanol is possible in ordinary vehicles without any problem. However, use of higher concentration ethanol is somewhat questionable. Because of its corrosiveness, it degrades arrange of the materials found in specific components of the engine, and fuel supply systems [44].

New generation engines are designed to work with higher biofuel blends, which allow the engine to be modified to maximize the benefits of the higher oxygen content and improved fuel efficiency with low emissions. Figure. 2.12 shows the variation of different generations of Flexible fuel vehicle (FFV) in Brazil. FFVs are among the modern vehicles designed to use up to 85% ethanol, and they were developed with better fuel efficiency with higher compression ratios. The specialty of this vehicle is that its fuel sensor automatically detects the ethanol–gasoline ratio to adjust fuel ignition and injection timing according to the ethanol–gasoline ratio. In the US vehicle market alone, more than 10 million FFVs were in operation in mid-2012.

Zhai et al. [45] compared the fuel consumption and emission of FFVs with E85 and gasoline fuel. They used data from different data sources, such as portable emissions measurement system (PEMS) data, Environmental Protection Agency (EPA) certification data, and US Department of Energy (DOE) dynamometer tests. In higher vehicle specific power (VSP) modes, from PEMS data, NO_x emission was found to be higher for E85 than for gasoline. From the dynamometer and certification data, NO_x emission was seen to depend on the vehicle condition and not on the fuel. On a fleet basis, NO_x and other emissions were lower for E85 than for gasoline. On a life-cycle basis, NO_x emission was 82 % higher for E85 than for gasoline.

| Ethanol Blend | Carburettor | Fuel Injection | Fuel Pump | Fuel Pressure Device | Fuel Filter | Ignition system | Fuel Tank | Catalytic Converter | Basic Engine | Motor Oil | Intake Manifold | Exhaust system | Cold Start System |
|---------------|-------------|----------------|-----------|----------------------|-------------|-----------------|-----------|---------------------|--------------|-----------|-----------------|----------------|-------------------|
| ≤5% | | | | | | | | | | | | | |
| 5-10% | ■ | ■ | ■ | ■ | ■ | ■ | ■ | ■ | ■ | ■ | ■ | ■ | ■ |
| 10-25% | ■ | ■ | ■ | ■ | ■ | ■ | ■ | ■ | ■ | ■ | ■ | ■ | ■ |
| 25-85% | ■ | ■ | ■ | ■ | ■ | ■ | ■ | ■ | ■ | ■ | ■ | ■ | ■ |
| ≥85% | ■ | ■ | ■ | ■ | ■ | ■ | ■ | ■ | ■ | ■ | ■ | ■ | ■ |

■ - For special designed vehicle ■ - For vehicles up to 15-20 years old □ - For any vehicle

Figure 2.12. Necessary modification to the engine to increase ethanol–gasoline blend [45].

Karavalasik et al. [13] investigated the impact of ethanol blends on different vehicle models ranging from 1984 to 2007 including FFVs. NO_x emission increased with increase in ethanol content for a few old model vehicles, which can be attributed to differences in catalyst technology, aging or effectiveness. As old model vehicles do not have sophisticated engine control technology, the leaning effect cannot be very pronounced with the change of fuel type here. Yao et al. [46] tested various ethanol–gasoline blends (E0, E3, E10 and E20) in a low mileage (about 21750 mile) and a high mileage (about 87,000 mile) passenger car. Both cars operated well with ethanol blends of up to 20%. In this experiment, it was seen that NO_x

emission was lower when using ethanol blend, especially in the low-mileage vehicle fueled with E20. The low mileage vehicle had NO_x emission of 0.072g/km, 0.71g/km, 0.068g/km, and 0.061g/km respectively, for E0, E3, E10 and E20 fuels, while the high-mileage vehicle's NO_x emission was 0.471g/km, 0.472g/km, 0.451g/km and 0.417g/km, respectively, for E0, E3, E10 and E20 fuel. Durbin et al. [34] used 12 different vehicles to find the effect of different ethanol-gasoline blends and volatilities on emission. The vehicles included present day technologies. They found an increase in NO_x emission with a 10% ethanol-gasoline blend compared to gasoline. Mayotte et al. [46] investigated emission in a 1990 model or equivalent vehicles. They found that the sulfur concentration of fuel affects the HC and NO_x emission of these vehicles. Some authors reported that the operation of small engines using a lower ethanol percentage (10–15%) with gasoline causes HC and CO emissions to decrease and NO_x emissions to increase. The USDOE reported that in small engines using ethanol contents of 10–15% with gasoline, NO_x emissions increased by 50–70%. Small engines have no oxygen-sensing feedback control like modern cars. When ethanol is added to gasoline, an engine operated under lean or oxygen rich conditions experiences over-heating. This high temperature causes more NO_x formation. Knoll et al. [19] compared some small non-road engines and observed the emissions for different ethanol-gasoline blends. From Figure. 2.13 it can be seen that NO_x increases with the increase in ethanol percentage. In a Stihl Line Trimmer engine, NO_x emissions were lower when using E20 due to poor combustion. Emissions were lower in a Poulan Blower engine as it was equipped with a three-way catalyst. Hilton and buddy [25] used 10 cars (1994 to 2004 models) to compare the tail pipe emissions of E20 and gasoline. Among the 10 cars, five produced higher NO_x emissions and five produced an average of 2.4% lower NO_x emissions when using E20 compared to gasoline. For most of the cars, HC and CO emissions were lower for E20 than for gasoline. They discussed some reasons for emissions degradation of vehicles such as degradation of the catalyst, material compatibility of fuel system components, and so on.

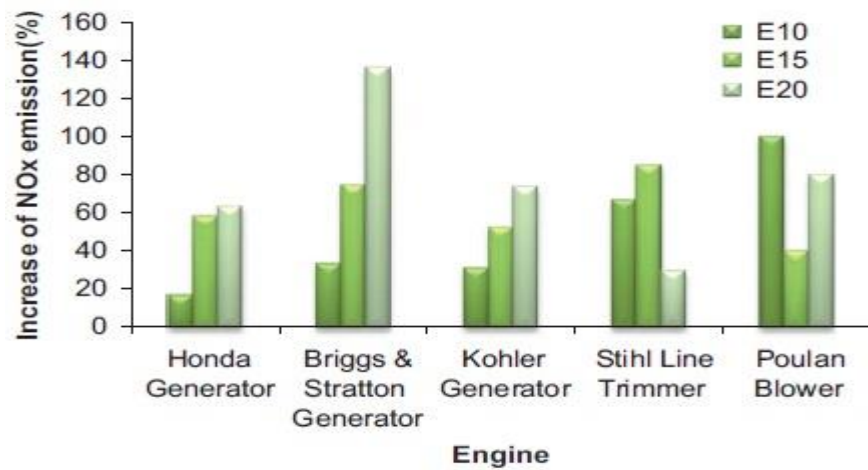


Figure. 2.13. Increase of NOx emission than gasoline fuel versus different engines for ethanol–gasoline blend [25].

2.9. Combustion in SI engines:

In the study of Moxey he evaluated the effect of ethanol fuels in turbulent flame development [47]. He compared the following four fuels pump grade gasoline, iso-octane, pure ethanol and E10 to obtain the effect of high and low ethanol content fuels on the performance he used A customized single cylinder research engine with a unique optical arrangement the combustion chamber and schematic views are shown in Figure 2.14 and figure

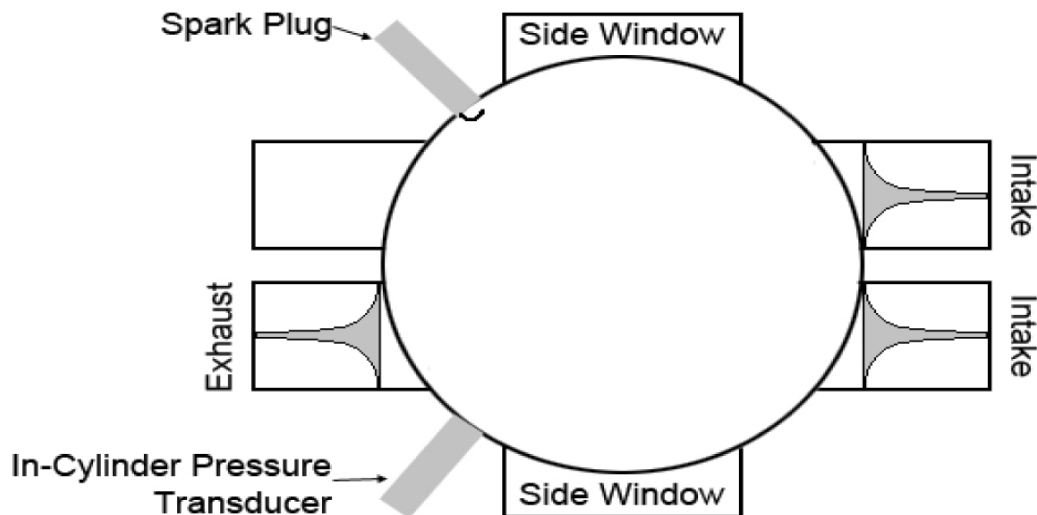


Figure 2.14. Overhead view of combustion chamber with the deactivated exhaust valve shown missing [47]

The studies showed that E10 has the slowest burning; slower burning than pure iso-octane also, the slower burning fuels were shown to exhibit the widest ranges of in cylinder pressure development.

The faster burning with the pure ethanol fuel was shown to be the result of marginally higher initial laminar-like burning providing a “head start” to the turbulent flame development process, with the turbulent spectrum thereafter more quickly encroached. In turn this led to faster in-cylinder pressure development and the slower burning iso-octane and E10 fuels were shown to exhibit a higher degree of bulk flame distortion as quantified directly from the flame images and expressed in terms of flame shape factor.

Aleiferis and Behringer did the flame front analysis of ethanol, butanol, iso-octane and gasoline in a SI engine for this purpose they employed direct-injection spark-ignition engine run at 1500 RPM and they used early intake stroke fuel injection for homogeneous mixture preparation method [48].

Flame chemiluminescence imaging was used to characterize the global flame behavior and double-pulsed Laser-sheet flame tomography to quantify the local topology of the flame front.

Four fuels were investigated: a typical commercial grade gasoline (RON95) without oxygenates, iso-octane, ethanol and n-butanol (1-butanol). The results showed that the flame tomography experiment was conducted to obtain planar details of the flame front on the horizontal swirl plane that could not be identified by chemiluminescence imaging due to the projected line of sight nature of the latter technique.

The flame roundness was ~10–15% from tomography images, with largest values for ethanol then for butanol, gasoline and finally iso-octane. This reflects the fact that the hydro carbon fuels exhibited more often multiple flame clusters and stronger flame distortion. The chemiluminescence images showed same order of roundness in terms of fuel sequence but with levels of ~18–25%.

2.10. Spray and evaporation characteristics of ethanol and gasoline:

Huang et al investigated Spray and evaporation characteristics of ethanol and gasoline [49]. The fuel evaporation process strongly affects the consequent mixture formation, combustion and emission processes. This is because the droplets must vaporize before they can burn also ethanol has a faster vaporization rate due to its higher vapor pressure in high Temperature conditions in experiments and numerical studies showed that the evaporation rate of ethanol direct injection was lower than that of gasoline in naturally aspirated SI engines.

In this study, authors diagnosed the effect of fuel temperature on the ethanol and gasoline spray characteristics from a multi-hole in a constant volume chamber as part of investigation of a novel fuel system, ethanol direct injection plus gasoline port injection (EDI + GPI). The fuel temperature varied from 275 K (non-evaporating) to 400 K (flash boiling) which corresponded to cold-start and running conditions that the injector may have in real engines. The ethanol fuel investigated in this study was the absolute ethyl alcohol with a purity of 99.9%. The gasoline fuel tested was a commercial unleaded gasoline with an octane number of 97.

The fuel injection pressure of 6 MPa was achieved using compressed nitrogen. 6 MPa was the direct injection pressure of the ethanol fuel applied in the experiments on the EDI + GPI research engine.

The results showed that ethanol and gasoline sprays showed the same patterns in non-evaporating conditions. As fuel temperature increased, it had greater effect on gasoline spray structure than on ethanol's, indicated by lower spray collapse temperature of gasoline than that of ethanol.

The effect of fuel temperature on macroscopic characteristics was insignificant for non-flash boiling sprays, but significant for flash-boiling sprays whose spray angles and projected areas became much smaller and the spray tip penetrations were slightly longer. And ethanol evaporated more slowly than gasoline did in low temperature environment (<375 K), but they reached a similar evaporation rate when the fuel temperature was higher than 375 K. The sprays could be considered as no evaporating when the vapor pressure was smaller than 30

kPa, demonstrated by the low evaporation rates at temperature lower than 325 K for ethanol and 300 K for gasoline.

The evaporation rates increased significantly when temperatures were further increased. The low evaporation rate of ethanol fuel in low temperature environment implied that EDI should only be applied in high temperature engine environment.

Not only the spray evaporation modes but also the breakup mechanisms changed with the fuel temperature. The ethanol spray went through all the three breakup mechanisms within the temperature range from 275 K to 500 K, while gasoline spray only went through the bag breakup and stripping breakup regimes.

2.11. Spark knock or knock:

Knock is the name of the noise transmitted through the engine structure when essentially spontaneous ignition of a portion of end-gas – the fuel, air, residual gas, mixture ahead of the flame front – occurs. When knock takes place, there is an extremely rapid release of much of the chemical energy in the end-gas, causing very high local pressures and the propagation of pressure waves of substantial amplitude across the combustion chamber.

2.11.1. The Effect of Alcohols–gasoline Dual-Fuel on knock suppression:

Wang et al studied Alcohols–gasoline blend on knock suppression on SI engine [50]. For this purpose, Alcohols–gasoline Dual-Fuel Spark Ignition (DFSI) is organized using a port-fuel-injection (PFI) and direct injection (DI) for gasoline injection. Figure (2.15)

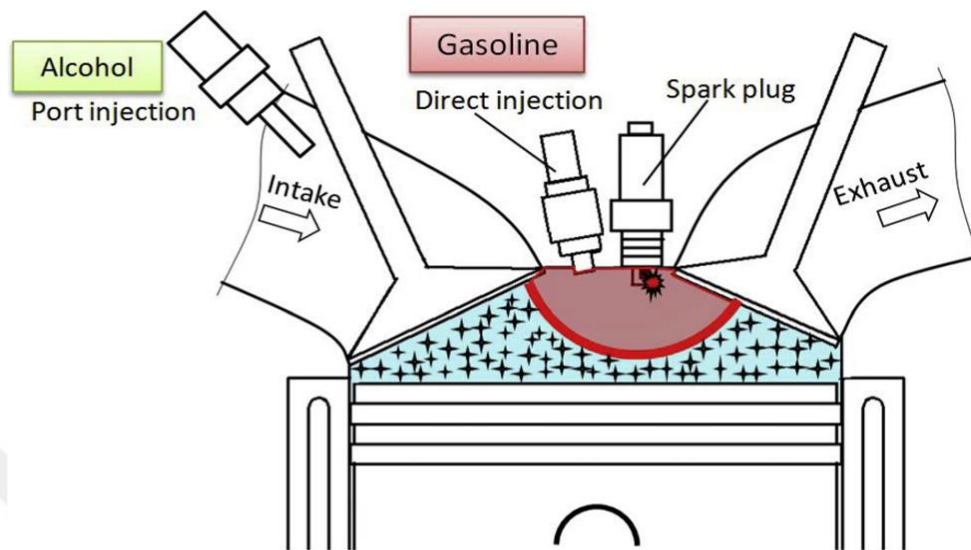


Figure 2.15. Schematic of Alcohols–Gasoline Dual-Fuel Spark Ignition Combustion. [50]

This work systematically compares the potentials of Alcohols–gasoline DFSI combustion fueled with different alcohols and gasoline on knock suppression.

Three different Alcohols–gasoline combustion modes were studied, including M–G (PFI-Methanol and DI-Gasoline), E–G (PFI-Ethanol and DI-Gasoline) and E85W15–G (PFI-15% water and 85% ethanol and DI-Gasoline) DFSI, while G–G (PFI-Gasoline and DI-Gasoline) DFSI was selected as the reference. The PFI to DI fuel ratios are flexibly controlled on-line. Systematical comparison about the effect of stoichiometric M–G, E–G, E85W15–G and G–G DFSI on engine knock suppression was conducted by experiments. The engine was natural aspirated with high compression ratio of 13:1. In each test, the percentage of alcohols injection was varied from 0% to 100%.

The test process was presented as follows. First of all, gasoline was injected direct into cylinder (without PFI-Alcohol) and all operating parameters, including injection and ignition parameters, etc., were taken from the original engine calibration. This test point was marked as the ‘baseline’. Secondly, systematical comparison about the effect of stoichiometric M–G, E–G, E85W15–G and G–G DFSI on engine knock suppression was conducted. The engine was set at stoichiometric condition, the ignition timing was adjusted at MBT (Minimum spark advance for Best Torque) point and the percentage of PFI-Alcohol was varied from 0% to 100%.

Results show that Alcohols–gasoline DFSI could extend the knock-limit effectively when compared to the baseline. No matter the PFI-Alcohols is methanol, ethanol, or E85W15, its higher latent heat of vaporization causes lower mixture temperature and the subsequent lower compression temperature near TDC, which suppresses knock.

The higher octane number of alcohols also leads to improved anti-knock performance. Moreover, the flame speed of alcohols is higher than that of gasoline. Higher burning speed also reduces knock tendency with the same percentage of PFI-Alcohols, the BMEP subsequence from high to low is M–G, E–G, E85W15–G and G–G. The reason could be that the latent heat of vaporization, the octane number and the laminar flame speed of the alcohols used in these combustion modes are also in this subsequence

Higher latent heat, octane number and laminar speed allow higher anti-knock ability, causing reduced knock tendency and higher knock-limit.

2.12. Regulations to prevent vapor lock:

To prevent vapor lock and environmental issues, automotive fuel specification ASTM_D4814 requires that gasoline is tested according to ASTM D5188. This standard is governing the assessment of vapor-liquid ratio temperatures. In automotive fuel speculations, the temperature, at which a ratio of 20 (vapor) to 1 (liquid) is reached (commonly referred to as $T(V/L) = 20$), indicates the risk of the fuel to form a vapor lock. This tendency is higher in hotter climate and in higher altitude.

2.12.1. The effect of ethanol on vapor lock:

Blending of ethanol into gasoline at 10 volume percent causes the RVP to increase by about 1 psi despite the fact that fuel grade ethanol has a lower vapor pressure than gasoline (Figure 2.16) The low vapor pressure of fuel grade ethanol is caused by attractive forces between the ethanol molecules. The strongly electronegative oxygen atom in each ethanol molecule is attracted to the somewhat positive hydrogen atoms in other ethanol molecules. The attraction between ethanol molecules means that it has a stronger tendency to stay as a liquid and not vaporize into the more dispersed gaseous state. However, when blended into gasoline at relatively low concentrations the more numerous gasoline molecules disrupt the attractive forces between ethanol molecules

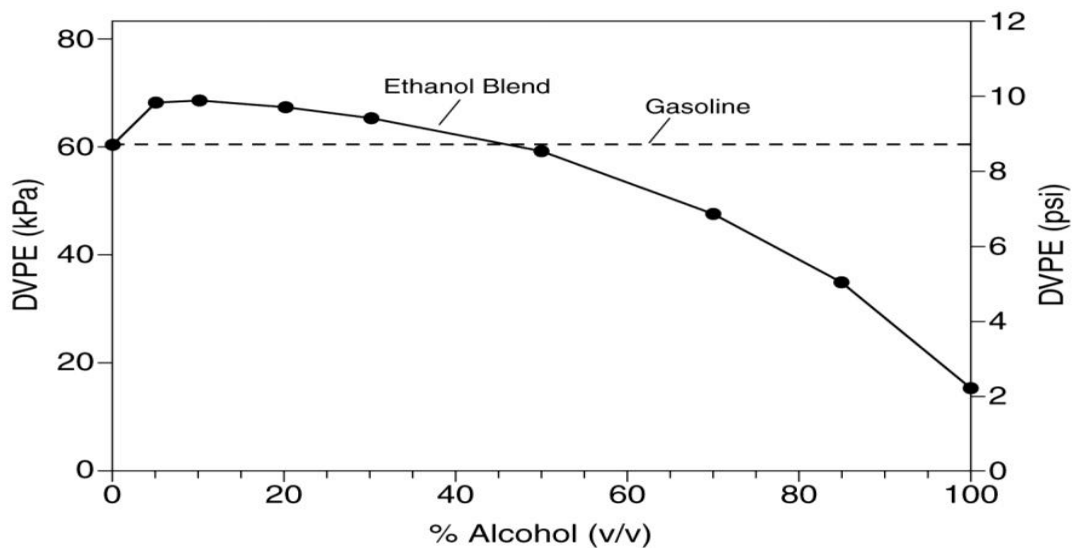


Figure 2.16. Effect of ethanol blending on vapor pressure of gasoline.

and allow the ethanol to readily evaporate, raising the vapor pressure of the blend. Not surprisingly this increase in vapor pressure with ethanol is more marked with the lower RVP hydrocarbon blend stocks. This would be true with the addition of any component which raises vapor pressure, as the final pressure is a weighted average of the pressure contributions of all of the components. As ethanol content is increased above about 20% the vapor pressure increase becomes less, and above about 50% ethanol vapor pressure for the blend is less than that of the gasoline.

2.12. Biofuels:

Biofuels are combustible materials, which derived directly or indirectly from biomass generally produced from plants animals and micro-organisms and also from organic wastes Biofuels are available in various forms such as solid, liquid or gaseous and includes all kinds of biomass and derived products used for energetic purposes. Biofuels are classified in three generations:

2.12.1. First generation biofuels:

This kind of biofuels are mostly produced using conventional technologies the most common first generation biofuel is bioethanol the main feedstock's are seeds grains or hole plants from corps such as corn, sugar cane, sunflower seeds or oil palm.

2.12.2. Second generation of biofuels:

This kind of biofuels can be produced from various non-food sources which includes waste biomass the stalks of wheat corn Stover and biomass crops'. Second generation biofuels use biomass to liquid technology by thermochemical conversion or fermentation.

2.12.3. Third generation biofuels:

This kind of biofuels includes alcohols like bio-propanol or bio-butanol which due to lack of production experience are usually not considered to be relevant as fuels in the market before 2050 though incising Investment could accelerate their development. As a transport, fuel butanol has properties closer to gasoline than bioethanol but as reminded it needs some more time to become a transportation fuel. [51]

2.13. Ethanol:

Ethanol is a volatile, colorless and flammable matter, and is in liquid phase at STP. (Standard Temperature and Pressure). Ethanol fuel, also known as E100; contains 96,4% of ethanol and the remaining fraction as water, which is the highest purity level that can be obtained by distillation. Fuel ethanol is produced by various methods but the most known one is the dry mill process method. This method accounts for almost 75% of the current fuel ethanol production in the world this method produces ethanol as the main product but remarkable amount of co-products also be produced in this method.

2.13.1. Dry Milling:

The major steps of dry milling are outlined below:

2.13.1.1 Milling:

After the corn (or other grain or biomass) is cleaned, it passes first through hammer mills which grind it into a fine powder.

2.13.1.2 Liquefaction:

The meal is then mixed with water and an enzyme (alpha amylase), and passes through cookers where the starch is liquefied. A pH of 7 is maintained by adding sulfuric acid or sodium hydroxide. Heat is applied to enable liquefaction. Cookers with a high temperature stage (120°-150° C) and a lower temperature holding period (95° C) are used. The high temperatures reduce bacteria levels in the mash.

2.13.1.3. Saccharification:

The mash from the cookers is cooled and the enzyme gluco amylase is added to convert starch molecules to fermentable sugars (dextrose).

2.13.1.4 Fermentation:

Yeast is added to the mash to ferment the sugars to ethanol and carbon dioxide. Using a continuous process, the fermenting mash flows through several fermenters until the mash is fully fermented and leaves the tank. In a batch fermentation process, the mash stays in one fermenter for about 48 hours.

2.13.1.5 Distillation:

The fermented mash, now called “beer,” contains about 10 percent alcohol, as well as all the non-fermentable solids from the corn and the yeast cells. The mash is then pumped to the continuous flow, multi-column distillation system where the alcohol is removed from the solids and water. The alcohol leaves the top of the final column at about 96 percent strength, and the residue mash, called stillage, is transferred from the base of the column to the co-product processing area.

2.13.1.6. Dehydration:

The alcohol then passes through a dehydration system where the remaining water is removed. Most plants use a molecular sieve to capture the last bit of water in the ethanol. The alcohol at this stage is called anhydrous (pure, without water) ethanol and is approximately 200 proof.

2.13.1.7. Denaturing:

Ethanol that is used for fuel is then denatured with a small amount (2-5%) of some product, like gasoline, to make it unfit for human consumption. [51]

2.13.2. Net Energy:

One of the most controversial issues relating to ethanol is the question of “net energy” of ethanol production. According to the Institute for Local Self Reliance research in 2007 and studies made by the U.S. Department of Agriculture in 2009 and Michigan State University in 2012, the production of ethanol from corn is a positive net energy generator. If corn farmers use energy efficient farming techniques, then the amount of energy contained in a gallon of ethanol and the other co-products is more than twice the energy used to grow the corn and convert it into ethanol. These studies indicated an industry average net energy gain of 1.38 to 1. The industry-best existing production net energy ratio was 2.09 to 1. If farmers and industry were to use all the best technologies and practices the net energy ratio would be 2.51 to 1. In other words, the production of ethanol would result in more than 2-1/2 times the available energy than it took to produce it. [52]

2.13.3. Fuel properties:

Ethanol(C_2H_5OH) also known as ethyl alcohol apart from being a renewable fuel has properties that can enhance the performance of spark ignition (SI) engines. The use of neat ethanol (100%) is reported to improve the torque and efficiency at wide open throttle (WOT) as compared to gasoline. Ethanol also increases the ratio of specific heats of combustion products and results in an increase in the number of moles of products of combustion as compared to gasoline operation. [52]

Table 2.2 Properties of Ethanol [52]

| Property | Gasoline | Ethanol |
|---|---------------------------------|----------------------------------|
| Chemical Formula | C ₈ -H ₁₈ | C ₂ H ₅ OH |
| Composition(C,H,O)(mass %) | 86,14,0 | 52,13,35 |
| Lower heating value (MJ/kg) | 42,7 | 26.8 |
| Density (kg/m ³) | 745 | 790 |
| Octane number((R+M)/2) | 90 | 100 |
| Boiling temperature (C°) | 25-215 | 78 |
| Latent heat of vaporization (25C°)(kJ/kg) | 380-500 | 904 |
| Self-ignition temperature (°C) | 300 | 420 |
| Stoichiometric air/fuel ratio | 14.7 | 9.0 |
| Laminar flame speed 1bar , 390 K | 52 | 59 |
| Mixture calorific value (MJ/m ³ , Ø=1) | 3.75 | 3.85 |
| Ignition limit in air (vol%) | | |
| Lower limit | 0.6 | 3.5 |
| Upper limit | | 15 |
| Solubility in water at 20 °C (ml/100 ml H ₂ O) | fully miscible | |

Comparison of physicochemical properties:

The physical and chemical properties indicate the quality of fuel to be combusted in an engine. Engine combustion quality, performance and emission characteristics are dependent on them.

1. Heating value of ethanol is approximately 1/3 times lower than that of gasoline. Thus, to achieve same engine power output more amount fuel is required for ethanol.
2. An oxygen content of 34.7 wt % in ethanol promotes combustion efficiency as well as high combustion temperature.
3. Heat of vaporization of ethanol is higher than gasoline. Thus, charge requires more heat to evaporate which is taken up from in-cylinder environment. This in turn increases the volumetric efficiency of the engine.
4. Ethanol has no mono-aromatic or poly-aromatic hydrocarbons.

5. Lower C/H atom ratio of ethanol reduces the adiabatic flame temperature.
6. Ethanol has higher octane number (ON) than gasoline. The higher the octane number, the more compression the fuel can withstand before detonating. Premature fuel ignition can damage engine, which is a common phenomenon for lower ON fuel.
7. Ethanol has a higher laminar flame propagation speed than gasoline, which makes combustion process finish earlier and thus improving the engine thermal efficiency.
8. Using ethanol with gasoline can reduce costs of gasoline refineries as they can produce low-grade gasoline with lower ON.

2.14. Fuel Quality:

The quality of fuel used in any motor vehicle engine is very important to its long life and proper operation. If the fuel is not right for the air temperature or if fuel changes to a vapor incorrectly, drivability will suffer. Gasoline is a complex mixture of approximately 300 various ingredients, mainly hydrocarbons, refined from crude petroleum oil for use as fuel in engines.

2.14.1. Volatility and Vapor Pressure:

Gasoline is metered in liquid form through the fuel injectors or the carburetor and is atomized (mixed with air) and vaporized before entering the cylinders. It is very important to control a fuel's tendency to evaporate. This tendency to vaporize or change from a liquid to a vapor is referred to as the fuel's volatility. If volatility is too low (not volatile enough), symptoms could include: Poor cold start, poor warm up performance, poor cool weather driveability, unequal fuel distribution, or increased deposits in the crankcase, combustion chamber, and spark plug. If volatility is too high and too much vapor is formed, it could cause a decrease of fuel flow resulting in vapor lock, loss of power, rough running or stalling, decreased fuel mileage, or increased evaporative emissions leading to overloading the fuel evaporative canister. Refiners are required to deliver the correct volatility of fuel for winter, summer, and fall/spring. [38] According to Ahmadi adding ethanol to gasoline will increase the volatility, decrease the 50% distillation point (T50), and affect both the drivability index and vapor lock

protection. Vapor pressure. Is measure of “frontend” volatility, and a fuel with extremely high vapor pressure may cause problems with hot start ability, hot drivability and vapor lock.

2.15. Previous studies:

Najafi et al.[52] studied spark ignition engine with gasoline-ethanol blended fuels using response surface methodology RSM for this purpose they employed normal KIA 1.3 SOHC, four cylinders, and four strock and SI (spark ignition) gasoline engine as fuel they used E5, E7.5, E10, E12.5 and E15.

In this study, RSM (response surface methodology) has been employed to optimize of the engine power, torque, bsfc (brake specific fuel consumption), and emission components based on various gasoline-ethanol blends and speeds. The main objective of this research is to investigate the ability of RSM for optimization of engine performance parameters and exhaust emissions, and compare their performances in modelling when the engine runs on gasoline-ethanol blend.

In the experiments, the engine ran at various speeds for each test fuel and 45 different conditions were constructed

In statistics, RSM (response surface methodology) explores the relationships between several explanatory variables and one or more response variables. The method was introduced by G. E. P. Box and K.B. Wilson in 1951. The main idea of RSM is to use a sequence of designed experiments to obtain an optimal response. Box and Wilson suggest using a 2nd degree polynomial model to do this. RSM (response surface methodology) consists of a group of mathematical and statistical techniques used in the development of an adequate functional relationship between a response of interest (y) and a number of associated control (or input) variables denoted by x_1, x_2, \dots, x_k . In general, such a relationship is unknown but can be approximated by a low-degree polynomial model of the form:

$$Y=f(x)\beta+\varepsilon$$

where $x=(x_1, x_2, \dots, x_k)$, $f(x)$ is a vector function of p elements that consists of powers and cross-products of powers of x_1, x_2, \dots, x_k up to a certain degree denoted by $d (>1)$, b is a vector of p unknown constant coefficients referred to as parameters, and ε is a random

experimental error assumed to have a zero mean. This is conditioned on the belief that model (1) provides an adequate representation of the response.

Two important models are commonly used in RSM. These are special cases of model (1) and include the first-degree model (d=1):

$$Y = \beta_0 + \sum_{i=1}^k \beta_i x_i + \varepsilon$$

And the second-degree model (d=2):

$$Y = \beta_0 + \sum_{i=1}^k \beta_i x_i + \sum_{i,j} \beta_{ij} x_i x_j + \sum_{i=1}^k \beta_{ii} x_i^2 + \varepsilon$$

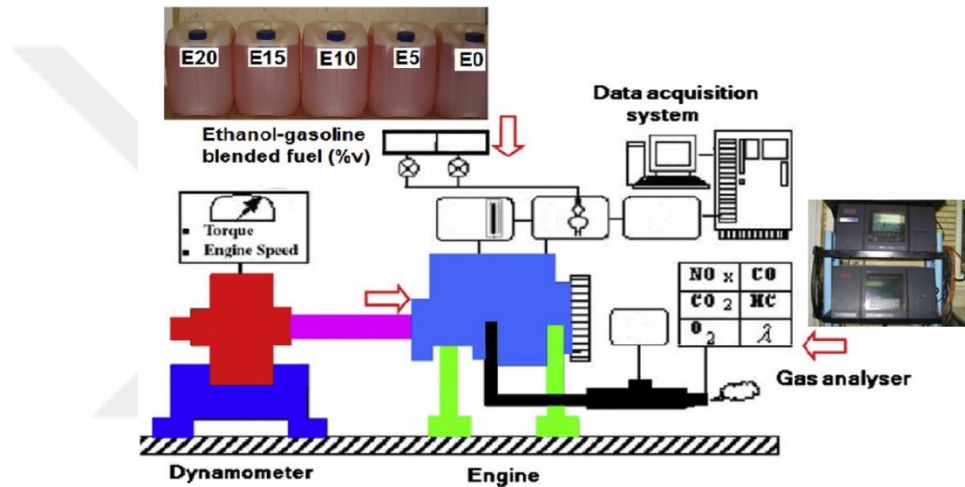


Figure 2.17. Engine test set-up and test instruments [52]

The purpose of considering a model such as (1) is threefold

1. To establish a relationship, albeit approximate, between y and x_1, x_2, \dots, x_k that can be used to predict response values for given settings of the control variables.
2. To determine, through hypothesis testing, significance of the factors whose levels are represented by x_1, x_2, \dots, x_k .
3. To determine the optimum settings of x_1, x_2, \dots, x_k that result in the maximum (or minimum) response over a certain region of interest.

They found out that according to our experiments and results obtained by the proposed methods, the results are as follows:

1. Experimental results indicate that CO_2 concentration increases as the bioethanol concentration increases. CO_2 emission depends on relative air fuel ratio and CO emission concentration. As a result of the lean burning associated with increasing bioethanol, the CO_2 emission increased because of the improved combustion. Blending of bioethanol with

gasoline fuel can significantly reduce HC emissions. The concentration of HC emission decreases with the increase of the relative air fuel ratio, the reason for the decrease of HC concentration is the use of oxygenated additives promote complete combustion and the cause for the hydrocarbon emission reduction CO₂ concentration increases as the ethanol concentration increases. CO₂ emission depends on relative air fuel ratio and CO emission concentration. Because of the lean burning associated with increasing ethanol, the CO₂ emission increased because of the improved combustion.

2. RSM can be employed to optimize the engine performance and exhaust emissions.
3. The performance parameters for different biofuel-gasoline blends were found close to gasoline, and emission characteristics of the engine improved significantly.

The two most outstanding benefits of the study are as follows: First, the practical data from the SI engine fueled with bioethanol-gasoline blends over a wide range of engine speeds and loads are revealed; and the second one the details of the technique are discussed. Even though the new approach (RSM) is complicated, it provides higher flexibility and accuracy with less complicated experimentation, as the response surfaces and mathematical models can forecast the results in-depth.

In a similar study Najafi et al studied the performance of four cylinders, and four stroke and SI (spark ignition) gasoline engine fueled with gasoline –ethanol blend the authors used E0, E5, E10, E15 and E20 fuels and this time they employed artificial neural network (ANN) method. [53] The properties of bioethanol were measured based on American Society for Testing and Materials (ASTM) standards. ANN is an analytical method for simulating system performance.

The Schematic diagram of experimental setup is clear in figure 2.18

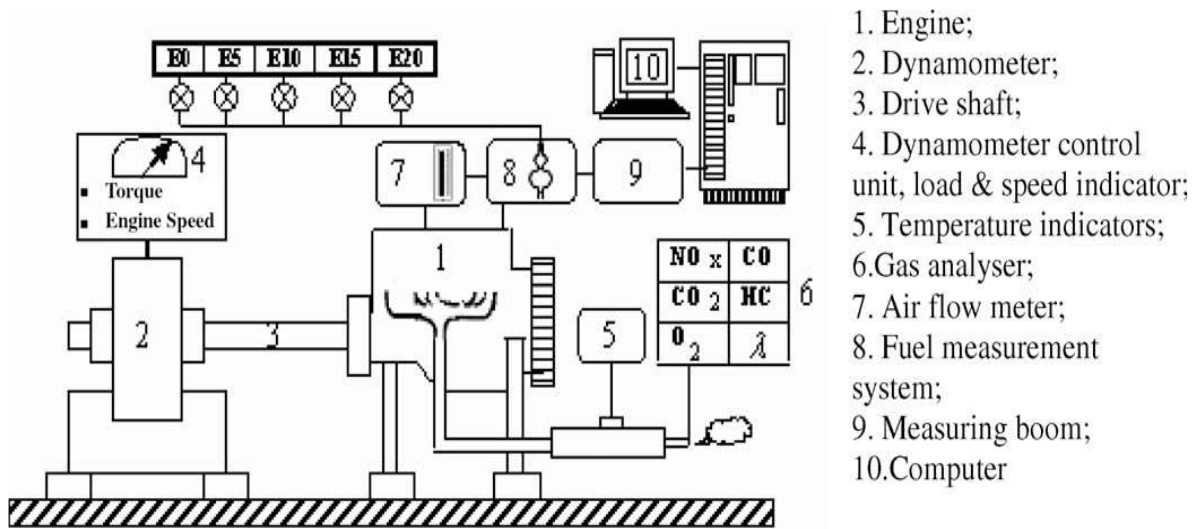


Figure 2.18. The Schematic diagram of experimental setup. [53]

The method relies on experimental data that is used to ‘train’ the ANN so that it can precisely predict the system performance at other conditions. This technique has found application in situations where the simulation of complex systems is required but limited experimental data is available. ANN is a powerful, nonlinear tool and since many phenomena in industry have non-linear characteristics, ANN has been applied widely. The performance of the ANN-based predictions is evaluated by regression analysis of the network outputs (predicted parameters) and the experimental values

In this case an ANN model was developed to predict a correlation between brake power, torque, brake specific fuel consumption, brake thermal efficiency, volumetric efficiency and emission components using different gasoline–ethanol blends and speeds as inputs_data. The results showed that the use of ethanol–gasoline blended fuels would marginally increase the brake power and decrease the brake specific fuel consumption. It was also found that the brake thermal efficiency and volumetric efficiency increase when ethanol–gasoline blends are used. Analysis of the experimental data by the ANN revealed that there is a good correlation between the ANN-predicted results and the experimental data. Therefore, ANN proved to be a useful tool for correlation and simulation of engine parameters. ANN provided an accurate and simple approach in the analysis of this complex, multivariate problem, the analysis of the SI engine performance and emissions. From emission point It can be seen that when ethanol percentage increases, the CO concentration decreases which means the

combustion is tuned to be completed. The CO concentration in the exhaust gas emission at 3000 rpm for gasoline fuel was 4.69 (%V), while the CO concentration of E5, E10, E15 and E20 at 3000 rpm was 4.05, 3.55, 3.38 and 2.56 (%V), respectively.

The CO concentrations at 3000 rpm using E5, E10, E15 and E20 was decreased by 13.7%, 24.31%, 27.93% and 45.42%, respectively in comparison to gasoline.

The reduction in CO concentration using blended fuels is due to the fact that ethanol (C_2H_5OH) has less carbon than gasoline (C_8H_{18}). Another significant reason of this reduction is that the oxygen content in the blended fuels increases the oxygen-to-fuel ratio in the fuel-rich regions. The most significant parameter affecting CO concentration is the relative air-fuel ratio (λ). Relative air-fuel ratio (λ) approaches 1 as the ethanol content of the blended fuel increases, and consequently combustion becomes complete.

And in CO_2 case, CO_2 concentration increases as the ethanol percentage increases. CO_2 emission depends on relative air-fuel ratio and CO emission concentration. The CO_2 concentration in the exhaust gas emission at 3000 rpm for gasoline fuel was 12.4 (%V), while the CO_2 concentration of E5, E10, E15 and E20 at 3000 rpm was 12.9, 13.2, 13.3 and 13.8 (%V), respectively. The CO_2 concentrations at 3000 rpm using E5, E10, E15 and E20 was increased by 3.87%, 6.06%, 6.76% and 10.14%, respectively in comparison to gasoline. As a result of the lean burning associated with increasing ethanol percentages, the CO_2 emission increased because of the improved combustion.

The HC concentration in the exhaust gas emission at 3000 rpm for gasoline fuel was 183 ppm, while the HC concentration of E5, E10, E15 and E20 at 3000 rpm was 152, 139, 137 and 125 ppm, respectively. The HC concentration at 3000 rpm using E5, E10, E15 and E20 was decreased by 16.94%, 24.04%, 25.14% and 31.69% at 3000 rpm, respectively in comparison to gasoline. This result indicates that ethanol can significantly reduce HC emissions. The concentration of HC emission decreases with the increase of the relative air-fuel ratio, the reason for the decrease of HC concentration is similar to that of CO concentration described above.

From one dimensional point Iliev studied the performance of a four stroke gasoline engine by employing AVL boost software[54] he compared the performance of engine under various contents of gasoline-ethanol (E0, E5, E10, E20, E30 and E50) and gasoline-methanol blends

(M0, M5, M10, M20, M30 and M50) for this purpose, a simulation of calibrated gasoline engine model was used as basic operating condition and the laminar burning velocity correlations of ethanol–gasoline and methanol– gasoline fuel blends for calculating the changed combustion duration. The engine performances: torque and specific fuel consumption were compared and discussed.

He employed AVL BOOST at full load conditions for the speeds ranging from 1000 - 6500 rpm in the steps of 500rpm.

The results shows that when the ethanol content in the blended fuel was increased, the engine brake power decreased for all engine speeds. When the methanol content in the blended fuel was increased (M5 and M10), the engine brake power slightly increased and when the methanol content in the blended fuel was increased (M30 and M50), the engine brake power decreased for all engine speeds. The BSFC increased as the ethanol (methanol) percentage increased. Gasoline blended fuels show lower brake power and higher BSFC than those of gasoline. Also, a slight difference exists between the BSFC when using gasoline and when using gasoline blended fuels (E5 (M5), E10 (M10) and E20 (M20)).

When ethanol and methanol percentage increases, the CO and HC concentration decreases. Thangavel et al used two separate injectors were used to simultaneously inject ethanol and gasoline in the intake port of a single cylinder SI engine. [55]

This work is aimed at developing and evaluating the potential of a system that can vary the relative amounts of ethanol and gasoline in a SI engine based on the operating condition and availability of ethanol. Both these fuels were injected into the intake manifold through two separate injectors. The amounts of ethanol and gasoline could be varied from 0 to 100% using a real time engine controller, which is difficult in the case of pre-blended ethanol-gasoline. The two fuel sprays were targeted at two different portions of the intake valve to improve evaporation. The experiments were conducted to study the performance, emission and combustion characteristics of the engine with this dual injection system.

The efficiency and emission characteristics have been reported with simultaneous injection of ethanol and gasoline using dual injection system at different torque conditions.

The main advantages of the dual injection system are:

i The proportion of alcohol and gasoline can be varied based on the operating condition for good performance.

ii. Use of alcohols in limited quantities at suitable operating conditions where the performance and emission benefits are significant can be possible with this system in countries where the availability of the alcohol is less.

iv. Methanol and ethanol will separate from gasoline without additives after they are blended with gasoline due to their hydroscopic nature.

v. Cold starting and warming up can be done by using gasoline alone and thereby reducing the emissions at starting with this system.

vi. High amount of alcohols can be used only during knock period to boost the engine power and it could avoid knocking with change in ambient temperatures.

vii. Hydrous ethanol with very high water content can be used along with gasoline since no phase separation issue with simultaneous injection system.

ix. Part load efficiency can be improved by increasing the compression ratio of the engine with this dual injection system; further, more alcohol can be injected at full torque conditions to mitigate knock

with the dual injection system high amounts of ethanol can be used during acceleration (transient condition) alone for ensuring knock free operation even with stoichiometric mixtures and thermal efficiency and torque are better with dual injection of ethanol and gasoline as compared to conventional pre-blended injection and its possible to say that emission benefits are observed with dual injection case

On the whole, the developed dual injection can effectively utilize ethanol based fuels on the operating condition in a SI engine for improved performance and reduced emissions.

Hsieh et al investigated the effect of gasoline- ethanol blends on engine performance and they factored in various throttle valve opening conditions [56] Their experimental apparatus included three major systems, engine system, power measurement system and exhaust measurement system. The engine system used in this experiment is a commercial engine, New Sentra GA16DE, which is a 1600 cm³ multi-point injection gasoline engine with cylinder bore and stroke being 76.0 and 88.0 mm, respectively, and the compression ratio being 9.5.

The selected operation conditions for this experiment were as follows: the engine speeds were at 1000, 2000, 3000 and 4000 rpm; throttle valves were at 0%, 20%, 40%, 60%, 80% and 100% (wide open throttle, WOT) opening.

From WOT point for a fixed engine speed, a higher throttle opening can provide more fuel for burning more energy input. Therefore, the torque output is increased with the increase of the throttle valve opening.

The torque output of pure gasoline (E0) is slightly lower than those of E5–E30, especially for low throttle valve openings Figure. 2.19 presents the influence of the blended fuels on the increase of engine torque output. It can be observed from the figure that at lower throttle valve openings, the torque output is either increased or decreased by adding the ethanol content. However, at higher throttle valve openings (60%, 80%, 100%), the increase of torque output grows with the ethanol content ranging from 2% to 4%.

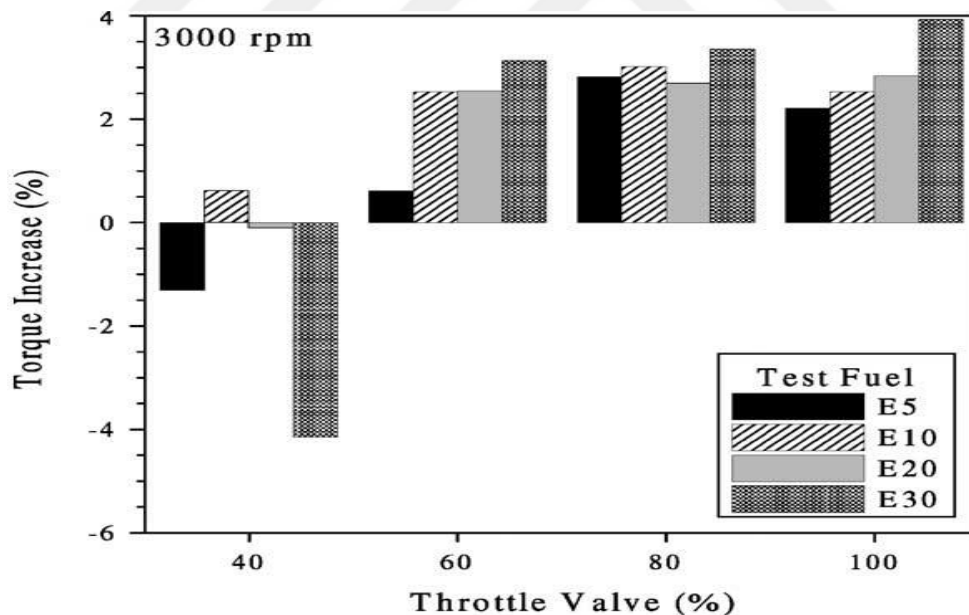


Figure 2.19. Influence of the blended fuels on the increase of engine torque output (relative to pure gasoline) at 3000 rpm. [56]

Under the conditions of low, throttle valve openings or high engine speeds, the original fuel injection strategy tends to operate the engine in fuel- rich burning conditions. Therefore, the added ethanol will produce the leaning effect to increase the air–fuel equivalence ratio (λ) to

a higher value, and make the burning closer to be stoichiometric. Its final result is that better combustion can be achieved and higher torque output can be acquired as a consequence.

From bsfc point the bsfc remains constant at low engine speeds (1000, 2000 rpm) with throttle valve openings >20%, or at high engine speeds (3000, 4000 rpm) with higher throttle valve openings (above 40%).

Wang et al diagnosed the SI engine performance fueled with hydrous ethanol gasoline blend for this purpose they employed four-cylinder, port injection, and electronic controlled automotive engine [57]. The engine was loaded with a GW160 eddy current dynamometer the used fuel is the engine was tested and fueled with commercially available pure gasoline which also was the base fuel, 10% anhydrous ethanol-90% gasoline and 10% hydrous ethanol (containing 5% water by volume)-90% gasoline.

The tests in this experiment were conduct data fixed speed of 2000rpm the peak in-cylinder pressure of E0 was the highest at the low and medium loads, then E10W and E10. At high load, the peak in-cylinder pressure of E10W was the highest, while E10 and E0 came second and third, respectively. At low and medium loads, gas temperature in the cylinder is lower than that at high loads. Higher latent heat of evaporation of blended fuels reduces the intake air temperature, which results in a worse fuel atomization and fuel-air mixture. In addition, the evaporation of ethanol or hydrous ethanol obviously decreases the gas temperature in the cylinder, leading to a lower peak in-cylinder pressure. This explains why the peak cylinder pressure of pure gasoline is higher than those of blended fuels for low and medium loads. Gas temperature in the cylinder increases with the increase of engine load. In the case of high load, the negative effect of higher latent heat of evaporation of blended fuels on peak in-cylinder pressure reduces, which results in high peak cylinder pressures of blended fuels. Meanwhile, on the premise of the same fuel-air equivalent ratio, the present oxygen of blended fuels accelerates the speed of flame propagation and combustion, thereby leading to high peak cylinder pressures.

At all the operating conditions, E10W exhibits higher peak in cylinder pressures than E10 does. The reason behind it is water in hydrous ethanol expedites the fuel mixing with air, and leading to a faster flame propagation and combustion [16]. Additionally, water in hydrous

ethanol promotes the formation of radicals H, O, OH and HO₂, which enhances the combustion process

From heat release rate point that the peak heat release rates of E0 are higher than those of E10 while lower than those of E10W at low and medium loads. At high load, both of peak heat release rates of E10 and E10W are higher than that of E0.

This behavior may be explained by the reduction of excess air coefficient with the increase in engine load, thereby leading to an increase of fuel density within the reaction zone due to richer fuel–air mixture. Thus, a faster flame propagation and combustion process decreases heat transfer loss, resulting in a higher combustion temperature, peak in-cylinder pressure and heat release rate.

At all operating conditions, a higher NO_x emission level is observed for the blended fuels. Due to higher latent heat of evaporation and lower heating value of the blended fuels, their cooling effect could reduce the combustion temperature and thereby reduce the formation of nitrogen oxides. However, the presence of oxygen in blended fuels provides relative oxygen-enrichment in the reaction regions, which promotes the oxidation of N₂ and the formation of the NO_x. In addition, a faster flame propagation and combustion process caused by ethanol increases the combustion temperature in the cylinder, thereby leading to an increase of the NO_x emission. For the blended fuels, the combination effect of these factors results in the overall reduction of NO_x emission. Compared with E10, for E10W, a slight drop of NO_x emission can be observed at all the operating conditions. This can be explained by the presence of water in hydrous ethanol which absorbs heat to evaporate, reducing the combustion temperature in the cylinder, and hence, NO_x emission reduces slightly.

HC emissions of the tested engine powered by E10W and E10 decrease by 40% and 44.24%, respectively. When the engine is operating at high load conditions, HC emissions for three fuels decrease. HC productions, primarily caused by unburned mixtures, are located around the periphery of the reaction regions.

At low loads, leaner mixture and lower combustion temperature increase HC emission caused by flame quenching on the chamber walls. With the addition of ethanol (or hydrous ethanol), the presence of oxygen reduces the zone of ‘lean outer flame’, which results in a reduction of HC formation.

This explains why a significant drop of HC emissions can be observed for E10W and E10 at low load conditions. Turbulence intensity of gas in the cylinder increases with the increasing engine load, which makes fuel–air mixture more homogenous. Hence, engine load increases, leading to a higher combustion temperature and efficiency. When the engine is operating at high load conditions, air–fuel equivalence ratios for three fuels are slightly higher than 1. The excess air in the cylinder reduces the residual gas coefficient, leading to a more efficient combustion and lower HC emission.

Compared with E10, the addition of water in E10W absorbs heat to evaporate, reducing the combustion temperature in the cylinder. At low loads, on the basis of a lower combustion temperature, the level of HC emissions for E10 is lower than that of E10W.

At low loads, CO emissions of E10W are more than those of E10. This can be explained by the addition of water reduces the combustion temperature, restraining the oxidation of CO, and hence, CO emission increases. At medium and high loads, the breakdown of water in E10W into the hydroxyl radical ($-OH$) and the hydrogen radical ($-H$) promotes the oxidation of CO at high temperature conditions. In addition, according to chemical kinetics, moderate addition of water promotes the oxidation of CO on the condition of sufficient reaction. These two reasons explain why E10W has fewer CO emissions at medium and high loads.

Compared to pure gasoline, the addition of ethanol reduces carbon–hydrogen ratio of the blended fuels, resulting in a lower CO_2 production for E10 and E10W at low and medium loads. At high loads, to export comparable power, more blended fuels are injected into the cylinder, which increases the formation of CO_2 . Thus, CO_2 emissions for three fuels are comparable under high load conditions

Balki et al used Taguchi method to optimize the performance of a SI engine fueled with pure gasoline, ethanol and methanol [58]. In this study, Taguchi's design of experiment method and analysis of variance (ANOVA) were applied in order to find optimum operating parameters giving the best engine performance and exhaust emissions with a minimum number of the engine tests in a spark ignition (SI) engine fueled with pure gasoline, ethanol and methanol. For this purpose, the optimum operating conditions are searched under three different CR, IT and engine speeds with three levels. In addition, the engine performance and regular brake specific exhaust emission values obtained from the

optimized engine have been compared with results of the baseline engine.

Taguchi is a statistical method developed by Genichi Taguchi to investigate the effect of different parameters on variance of performance characteristic that determines the suitable operating conditions of the process. Taguchi method making statistical design by using the orthogonal array also offers an opportunity to reduce the number of experiments. Taguchi technique computes a signal-to-noise (S/N) ratio based on experimental data. This ratio defines an experiment level which gives the best performance in the test variables. In addition, the effect of test parameters on the experiment outputs is statistically demonstrated by ANOVA analysis. Therefore, with the help of both S/N ratio and ANOVA, engine operating parameters can be determined to provide optimum performance. S/N ratios (dB) obtained from Taguchi method are used to achieve the optimization of operating parameters. S/N ratios are logarithmic functions of the expected experimental outcome which is to provide a healthy optimization ANOVA is a statistical method which is used to define the individual interactions into the test results of all the operating parameters.

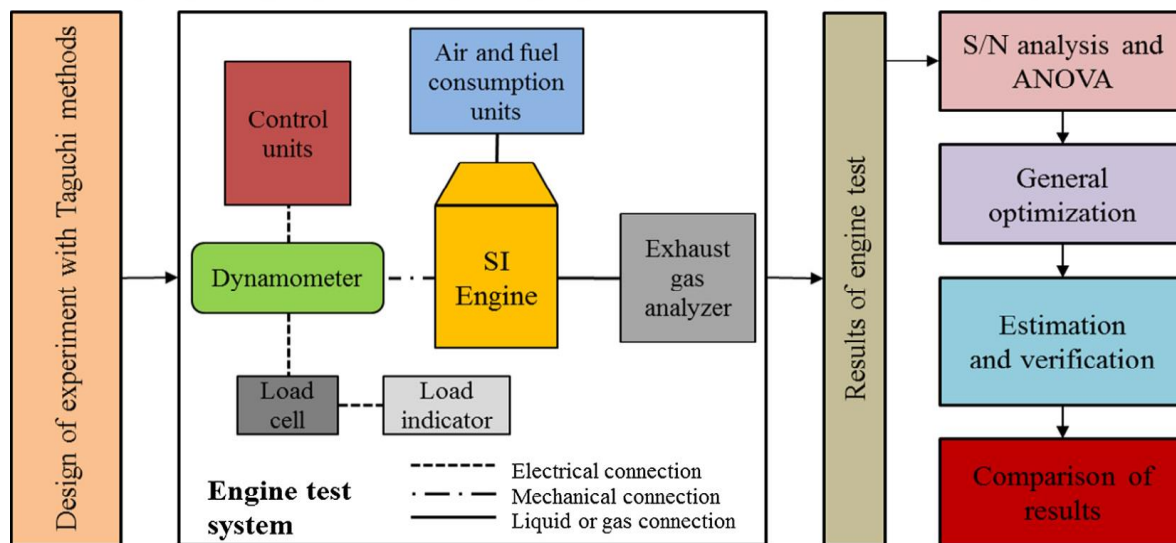


Figure.2.20. The test procedure followed in the study. [58]

The results show that According to the general optimization results obtained from ANOVA, engine speed and CR values, providing the best engine performance for gasoline, pure ethanol and methanol are 2400 rpm and 9.0 of CR. In addition, while optimal IT for ethanol and methanol is 20° CA, it is 26° CA in gasoline. BEP and BTE values with pure gasoline,

ethanol and methanol at optimized engine are found to be higher than that of gasoline at baseline engine. Also, the highest value of the BTE (about 32.5%) reached with using methanol at optimized engine. BSFC with the use of pure ethanol and methanol as compared to gasoline increases in general. However, with optimized engine, BSFC decreases on average 15.64% compared to that baseline engine for all fuel types. Exhaust emission levels in the engine are important in terms of environmental pollution. The alternative fuels are expected to give good performance in the internal combustion engine. The greenhouse gases such as $BSCO_2$ and $BSNO$ are also desired a decreasing. Therefore, $BSNO$ emission reduction observed with the use of alcohol fuel in this study is important. $BSCO_2$ emission rises a little with alcohol fuels. This increase is insignificant when considering total $BSCO_2$ emission of fuels in the time period from the fuel production up to their use. In order to use pure ethanol and methanol more efficiently in SI engine, increasing the compression ratio and the IT must be optimized for each engine speed range. Furthermore, it should be developed that fuel-injection system can work in accordance with alcohol fuels.

CHAPTER 3. RESULTS and DISCUSSIONS:

3.1. 1D Engine Modeling with Detailed Reaction Kinetics:

Typical 1-D engine simulation tools available nowadays offer a rather advanced description of the physical phenomena within engines' cylinders. The inclusion of chemical information in one-dimensional flow calculations offers the prediction of auto ignition or engine knock, and/or the formation of exhaust pollutants: NO_x, soot, HC, CO. It further facilitates calculation of the overall fuel consumption and thereby the CO₂ emission. DARS (Digital Analysis of Reaction Systems) has been built with the specific purpose of enabling detailed chemical analysis to engineering applications, with one particular focus on internal combustion engines. This tool handles gas phase chemistry, surface chemistry and particulate modelling via a suite of reactor models and reaction mechanisms. DARS includes homogeneous models (theoretical and engine based), stochastic reactor models (SRM) for HCCI, DICI, SI engines, flame models (premixed or counter flow), a reaction mechanism database for various fuels and tools for mechanism development, reduction, and export. DARS also allows for combining detailed chemistry investigations with one-dimensional commercial engine simulation tools (GT-Power and Ricardo Wave and SRM-Suite). Recently the engine model was extended with a gas exchange model. For emission after treatment a catalyst model and a diesel particulate filter (DPF) model became available. The gas exchange model rounds off the SRM engine model. The stochastic reactor model assumes statistical homogeneity instead of full homogeneity as in a zero-dimensional reactor model. The model includes direct injection, valve flow and combustion using detailed chemistry. The one-dimensional catalyst model, briefly is based on earlier research in the field and uses a representative channel model to simulate the catalyst behavior. A transient one-dimensional thin film layer model is used to calculate the evolution of gas phase as well as surface sites. In the thin film layer either global gas-phase chemistry or detailed surface chemistry can be considered. The latter facilitates simulating site blocking and poisoning of the catalyst. The one-dimensional DPF model considers representative channel pairs to simulate the particulate filter behavior. Soot deposition inside and on top of the filter wall is modelled by the spherical unit collector concept. Deposited soot is oxidized by molecular oxygen (O₂) and

nitrogen dioxide (NO₂). In catalyzed particulate filters nitrogen dioxide can be created from nitrogen oxide through catalytic reaction paths. Among others, the model predicts the soot cake thickness, porosity and permeability, and the influence of the soot cake on back pressure and gas velocities. The DPF model further predicts the gas phase emissions for example NO₂. [58]

3.2. MODEL:

3.2.1. The stochastic reactor model for engine in-cylinder simulation:

The Stochastic reactor model (SRM) is a PDF (Probability Density Function) based model for simulation of reactive systems.

The strength of the SRM is that it provides means to include effects of inhomogeneties and turbulence. The idea behind the SRM is that the assumption of homogeneity within the combustion chamber is replaced by the one of statistical homogeneity, with physical quantities described by PDF distributions. This is realized by dividing the mass within the cylinder into an arbitrary number of virtual packages called particles. Each of these particles has a chemical composition, a temperature and a mass and is able to mix with other particles and exchange heat with the cylinder walls. Since the SRM is 1-dimensional, no information is provided on the position of the particles. [59]

3.2.2. The PDF and the MDF:

In a real engine or in a CFD model the chemical composition, temperature and mass, have distributions in space, but in the space dimensionless SRM the distributions of the particles variables can be described with probability density functions (PDFs), with one PDF for each variable. The PDF can be compared with the distributions from CFD calculations or from measurements in real engines.

In reality most PDFs have shapes that are skewed and with several peaks. During a calculation with the SRM the shape of the PDFs as well as their range of the variables changes with each time step. Since the models implemented in the present work all contain equal weighted particles, the mass density functions (MDF) are always equal to the PDFs. [59]

3.2.3. The SRM for DICI:

The SI-SRM is an extension of the HCCI-SRM, including the direct injection model. The model is intended to be computationally efficient and able to provide predictive information of engine performance and emissions. In direct injection engines, such as diesel engines (CI) the combustion process is strongly influenced by the mixing processes, if the chemical processes are much faster than the physical processes. Nevertheless, the actual initiation of the combustion and the formation of pollutants is a chemically decided phenomenon. The SRM offers, using a detailed kinetic model together with a reasonable mixing model, to predict chemistry flow interaction. It therefore predicts chemically slow processes such as auto-ignition or emission formation, such as soot, NO_x and CO formation. [58]

3.2.4. The Homogeneous Reactor Model (HRM):

The fastest way to calculate engine combustion with a solver for detailed chemistry would be to employ a homogenous reactor model. The model is based on the PFR (Plug flow Reactor) with the assumption that conditions within the cylinder are homogenous at all times. The model uses the Woschni-correlation for calculation of heat transfer.

The Chemkin-Pro employes homogeneous reactor model the numerical model is basically a set of zero-dimensional time dependent differential equations, solving the energy conservation and species balances. The matrix system of balance equations are solved using Newton's method and the time is resolved with higher order backward differential functions. The pressure is calculated as a function of the piston movement and of the pressure increase due to chemical reactions. The pressure is then calculated from the equation of state:

$$P = \rho RT / M \quad (3-1)$$

Since combustion in the engines modeled here, occur during the closed period, inflow and outflow calculations are omitted and a closed system assumed. The conservation equation for the chemical species is then given by:

$$dY_j/dt = M_j / \rho \sum_{k=1}^{N_r} V_j, k r k \quad (3-2)$$

And the energy conservation equation is given by:

$$m \sum_{j=1}^{N_s} U_j M_j / \rho \sum_{k=1}^{N_r} V_j, k r k h_g A_{wall} (T - T_{wall}) + P dv/dt + m C_v dt/dt = 0 \quad (3-3)$$

For both these balance equations, $V_{j,k}$ is the stoichiometric coefficient for species j in reaction k and r_k is the reaction rate of reaction k . Y_j , u_j and M_j are the mass fraction, specific internal energy and the mole mass respectively, of j . A_{wall} is the in-cylinder wall area and h_g is the heat transfer coefficient which is obtained with the Woschni correlation and from the engine geometry with an additional factor to account for the clearance volume. V , P , T , T_{wall} and t are cylinder pressure, instantaneous volume, in-cylinder temperature, cylinder wall temperature and time.

$$h_g = 3.26B^{-0.2}P^{0.8}T^{0.55}w^{0.8} \quad (3-4)$$

The instantaneous volume is calculated following the expression

$$V = V_c + \pi B^2/4(L_{cr} + R_{ct} - L_{cr}\cos(\theta) + \sqrt{L_{cr}^2 + R_{ct}^2 \sin(\theta)})^2 \quad (3-5)$$

The calculation approach is similar to that of an ideal constant volume process, with the exceptions that the volume is changed from one time-step to another, and that heat is transferred to and from the system through the cylinder wall.

The HRM is a fast and efficient tool that provides considerable useful information and trends in emissions and engine performance, but with limitations.

Since the HRM only contains one single volume, everything happens at once. This is evident in the pressure peak which for the

HRM is sharp. The result is that the maximum pressure, maximum pressure rate and maximum temperature are over predicted. From this follows that hydrocarbon and CO emissions are under predicted but that NOx emissions are over predicted. Further, the combustion duration cannot be determined although both the total amount of heat release and the ignition timing are predicted quite reasonable. To be able to get better predictions of emissions and engine performance, the SRM for engine simulations was developed. [59]

3.2.5. The catalyst model:

The transient 1D catalyst model is capable of modelling catalytic reaction paths, surface site blocking and reactant interdependence, external heat and mass transfer, gas phase chemistry, reaction-diffusion in the wash coat and heat conduction through the substrate. The catalyst model consists of a number of representative channels. Gas and surface properties are calculated as functions of axial distance for each channel. Heat is transported between the

representative channels by conduction in the substrate. Results from a single-channel model are presented in this article.

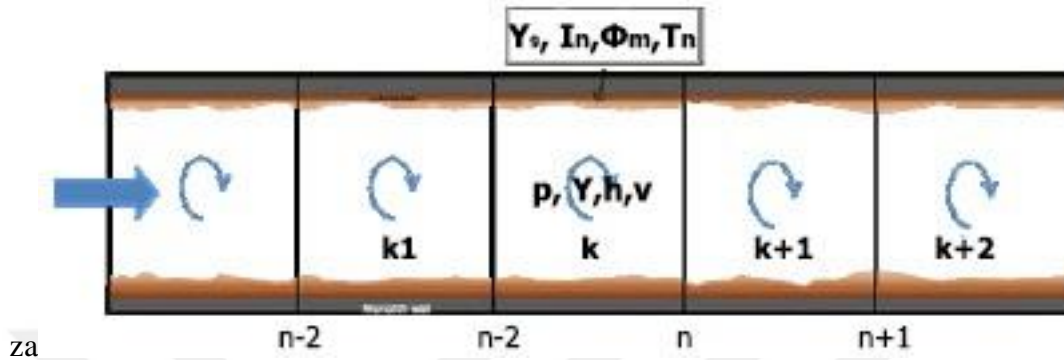


Figure 3.1. Illustration of the cell discretization in the catalytic channels. [59]

The channel model is built by discretization of the pipe into a finite number of sections of length. The conservation equations for gas flow, chemistry and surface properties are solved using an operator splitting technique, decoupling the continuity and momentum equation from the species and energy conservation equations. The species and energy conservation equations for gas and surface sites are calculated for each section and the continuity and momentum equations are solved over all sections. In each channel section the bulk gas is modelled as a 1-D perfectly stirred reactor (PSR). To account for external diffusion, the gas closes to and inside the wall is modelled as a separate zone, called the thin film layer. Mass and heat transfer between the zones is accounted for through heat and mass transfer coefficients, calculated from the properties of the gas flow. The conservation equations for gas species mass fractions, gas enthalpy, surface temperature, thin film layer gas species mass fractions and surface site fractions are solved in each zone for each time step. The Navier-Stokes equations for pressure and flow velocity are solved over all sections in a separate step. [58]

3.2.6. Diesel particulate filter model:

The DPF is a transient 1-D model capable of modelling soot deposition in the wall, soot oxidation, gas kinetics and catalytic surface reactions throughout the channels together with heat conduction through the DPF. The DPF is modelled by a number of representative pairs

of channels; each consisting of one inlet channel, a piece of substrate walls and one outlet channel. Gas properties and particulate mass accumulation and oxidation in the wall are calculated as functions of axial distance in each channel pair. Heat is transported between the representative channels by conduction in the substrate.

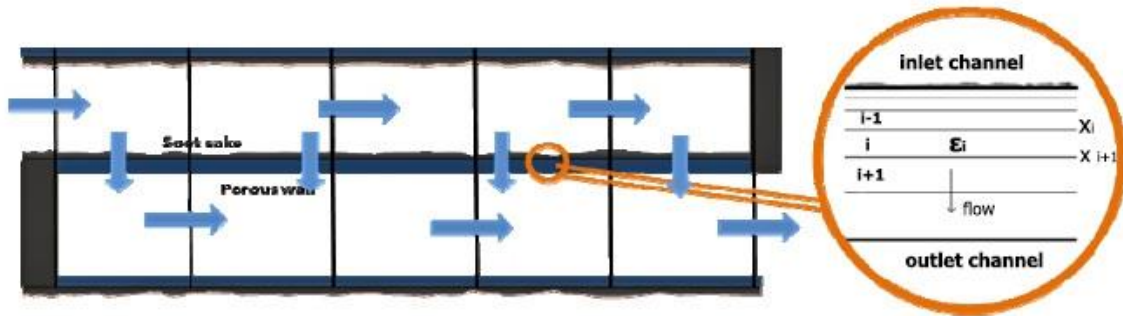


Figure 3.2. Illustration of the DPF model: representative channels and porous wall discretization

The Navier-Stokes equations for compressible flow, together with species and site conservation equations are the base for the channel model. An operator splitting method is applied to solve the governing equations. The pressure drop over the substrate wall is calculated by Darcy's law. Each channel section is modelled by a perfectly stirred reactor (PSR). The conservation equations for gas species mass fractions, gas specific enthalpy, and particulate matter deposit, oxidation and soot cake growth are solved at each time step at constant pressure. [58]

3.3. Chemkin-Pro vs SRM-Suite:

Detailed mechanisms which has been set for high carbon fuels commonly behold high number of elements and chemical reactions. It's possible to achieve solution in very short period of time for time independent, study-state, 1-D combustion analysis of detailed mechanism for high-carbon fuels.

During the recent year's lots of computer engineers have attempted to develop a software packages which can analyses 1-dimensional combustion to simulate IC engines correctly.

One of the software's that we used in this study is Chemkin-Pro which aim of its develop is to determining the accuracy of chemical mechanisms with analysis of ignition delay. Beside that its capable of doing analysis based on various reactor types one of these reactors is a 1-D IC engine reactor. As the Chemkin-Pro software is capable of simulating engine combustion 1-D reactor, it is possible to be combined with multi zone models and CFD simulation to achieve much detailed numerical outcomes.

In this study an SI engine was analyzed under two various chemical mechanisms under same operating condition using Chemkin-Pro and SRM-Suite software package results of both chemical mechanisms developed for the same fuel were tested according their proximity to the experimental data.

In addition, CPU times of codes and chemical mechanisms were tested as performance criterion.

To achieve the performance of the codes precisely, detailed and reduced chemical kinetic mechanisms were used for both chemical mechanisms.

In this study we compared computational outcomes to experimental results in terms of, pressure heat release rate, CO, CO₂ and O₂.

Experimental studies were obtained form (see source 60)

Engine parameters are given in details in Table (3.1)

Table.3.1. Engine parameters in details.[60]

| Parameter | Value | Unit |
|---------------------------|----------|---------|
| Cylinder diameter | 86 | mm |
| Stroke | 86 | mm |
| Length of connecting rod | 143.5 | mm |
| Compression ratio | 14.4 | |
| Engine RPM | 1200 | rev/min |
| Intake valve diameter | 32 | mm |
| Number of cylinders | 4 | |
| Intake valve opening time | 340 BTDC | CAD |
| Intake valve closing time | 108 BTDC | CAD |
| Exhust valve opening time | 120 BTDC | CAD |
| Exhust valve closing time | 332 | CAD |

In order to capture SI conditions experimentally the piston head was raised to adjust the geometrical compression ratio to 12.84 and inlet temperature to the cylinder increased to 250C°.

Experimental steps were performed under intake manifold pressure of 1bar and lambda valve of 3 for the air-fuel mixture in pre chamber.

Engine speed kept constant at 1200 rpm to obtain stable combustion. Fuel type which used in alcohol-gasoline blend in the engine was E100.

These studies go under two categories:

- i. Reduced chemical kinetic mechanisms which were used in both codes.
- ii. Detailed chemical mechanisms which were used in both codes.

3.4. Wiebe Function:

Zero-dimensional models are the most commonly used tools for parametric studies associated with SI engine development. The governing equations are ordinary differential equations since there is only one independent variable. Zero-dimensional SI models can contain multiple zones, for example, a high temperature core and one or more wall zones and within each zone, it is possible to consider burned and unburned gas. However, as systematic spatial trends often have little influence, the simplest approach is for a single zone containing spatially undifferentiated burned and unburned gas with a possible allowance for the influence of wall layers on heat transfer processes.

Within this type of zero-dimensional model, combustion progress can be described by a Wiebe function fitted as far as possible to the accumulated heat release derived from the measured cylinder pressure. The Wiebe method can describe the engine operating conditions for which it has been tuned and is often accurate enough to be used for semi-predictive modeling if care is taken when analyzing the results. There are two problems with using the standard Wiebe function for combustion progress. Firstly, the parameters that appear in the function vary with operating conditions. Secondly a standard Wiebe function can only be made to adopt a limited range of combustion progress shapes and if there are large differences between the burn rate at different times it can be difficult to obtain an accurate match between

any Wiebe shape and the real combustion progress variable through all stages of combustion. In SI, there are often large differences in effective burn rate between the main combustion period and late combustion. These differences arise because there is a greater spread of auto ignition times in the cooler (late-igniting) regions, where temperature gradients are high, compared to hotter (early-igniting) regions where temperatures are relatively uniform. [61]

3.4.1. Fuel burning and heat release rate correlations:

The Wiebe function can be expressed as follows:

$$X_b = 1 - \exp(-a(\Theta - \Theta_0)/\Delta\Theta)^{m+1} \quad (3-6)$$

where x_b is the mass fraction burned, h is the crank angle, h_0 , which fixes the timing, is the crank angle at the start of combustion, a and D_h are adjustable constants that determine the combustion duration, and m is an adjustable parameter that fixes the shape of the combustion progress curve. The constant, a , essentially duplicates the role of the burn duration, D_h . If a , and D_h are selected independently, there is a redundant parameter and the physical meaning of D_h is undefined. However it is useful to retain a because, if it is fixed judiciously, it allows D_h to be given a clear and simple meaning. Thus, for example, substituting specific burn fractions (0.1 and 0.9) and the associated crank angles into Eq. (1) and applying some algebra show that if

$$a = a_{10-90} = \left(\{\ln(1/(1-0.9))\}^{1/m+1} - \{\ln(1/(1-0.1))\}^{1/m+1} \right) \quad (3-7)$$

then $\Delta h = \Delta h_{1-9}$, where Δh_{1-9} is the 10–90% burn time. This definition of a in the modeling is used because it leads to a fixed, clear and simple interpretation of $\Delta\Theta$. For SI simulation, the simplest method of fixing the timing is to set $\Theta_0 = \Theta_{\text{spark}}$. However, a better fit to the measured pressures may be obtained by treating h_0 as an adjustable parameter and allowing it to drift slightly from Θ_{spark} . For curve fitting purposes it is often easier to set the timing by dealing with the 50% burn time rather than the ignition time because the 50% time occurs fairly close to the peak pressure and it is easy to use a measured value of the peak pressure timing as a first approximation to initiate a curve fitting process. Algebra based on Eq. (1) shows that the relationship between the ignition time, Θ_0 and the 50% burn time, Θ_{50} , is

$$\Theta_0 = \Theta_{50} - \Delta\Theta_{10-90} (\ln(2)/a_{10-90})^{1/(m+1)} \quad (3-8)$$

As noted in the introduction, single-zone models, with standard Wiebe function combustion tend to over predict the peak pressure because of the difficulty of representing the slower combustion that occurs adjacent to the walls. The slower combustion is commonly modeled with a multi-zone approach (usually 2 or 3 zones) but it is found that wall effects could be accommodated, without introducing a separate wall zone, by using a double-Wiebe function combustion model in which a fraction of the fuel (representing the wall region) burns at a reduced rate. The double-Wiebe function can be defined as:

$$X_b = (1 - \alpha_{wall}) \{ 1 - \exp(-a(\theta - \theta_0)/\Delta\theta)^{m+1} \} + \alpha_{wall} \{ 1 - \exp(-a(\theta - \theta_0)/K_{wall}\Delta\theta)^{m+1} \} \quad (3-9)$$

where α_{wall} is the fraction of the mixture that burns in the slow combustion region and K_{wall} is the ratio of the slow burn duration to the standard burn duration. The differences produced by the double-Wiebe function approach are illustrated in Figure 3.3

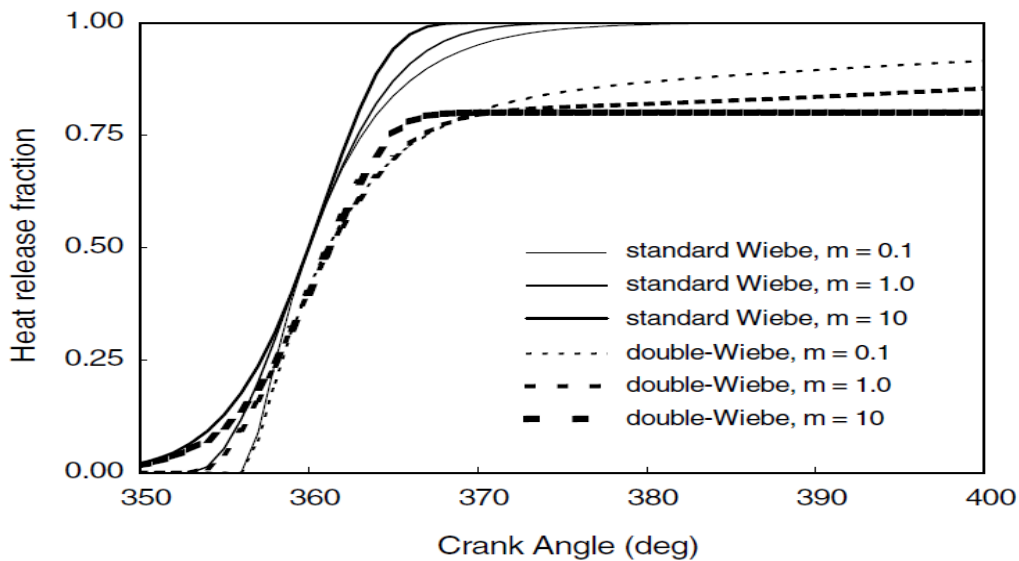


Figure 3.3. Wiebe functions with different m values. [61]

which shows Wiebe functions with different m values between 0.1 and 10 for a burn duration (10–90%) of 10 crank angle degrees and 50% heat release at TDC. The curves span virtually the full range of combustion rates that can be obtained by changing m and show that options here are quite limited. The dotted lines show the curves that can be obtained with a double-Wiebe function with $K_{wall} = 10$ and $a = 0.25$. A much more significant and extended late combustion period can now easily be represented. However, with large m values, the combustion is very slow to start and the slow burning mixture remains unburned during the

interval shown. Another possibility for representing slow combustion with a Wiebe function is to extend the burn duration. However it is not possible, even with low m values and therefore sharp combustion onset, to extend the duration of the late burn without also either extending the early burn an unrealistic amount or unrealistically retarding the 50% burn time. The extended early burn is illustrated in Figure 3.4., which shows how combustion progress varies as the burn duration is increased for a low m value of 0.1 and a fixed 50% burn time. [61]

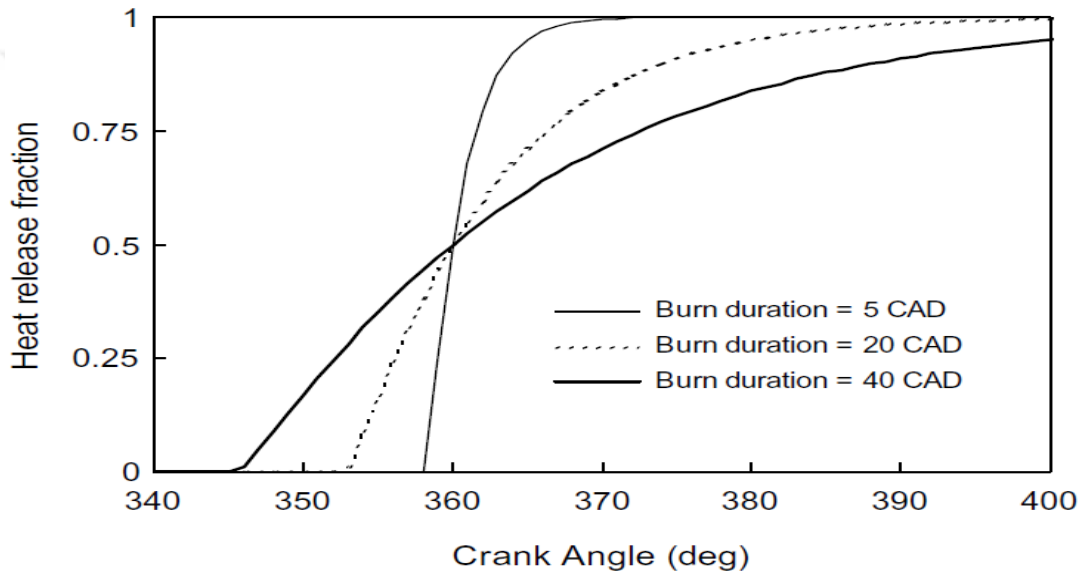


Figure 3.4. Wiebe functions of different duration, $m = 0.1$ [61]

3.4.2. Combustion Chemistry:

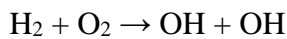
There are two kinds:

i. Thermal: This is because in an exothermic reaction if the energy cannot escape, the reaction rate increases fast due to concentration of energy.

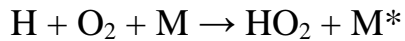
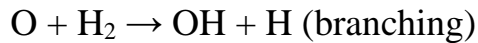
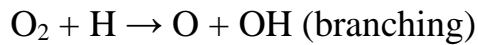
ii. Chain-branching: In this case, there are chain branching reactions and the number of carriers grows exponentially.

The mechanism is very complex. Yet there are these steps, which explain explosion.

Initiation:



Propagation: $\text{H}_2 + \text{OH} \rightarrow \text{H} + \text{H}_2\text{O}$



The explosions depend on temperature and pressure. This is explained in the figure below

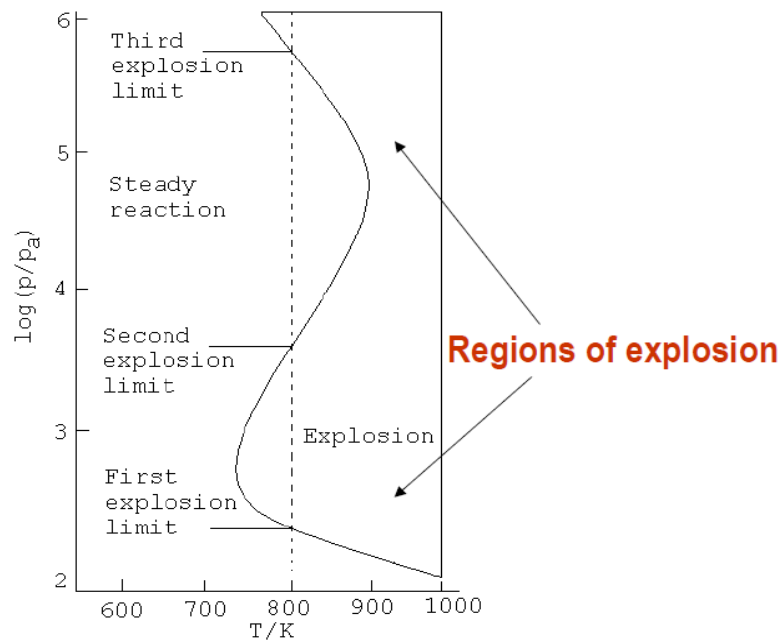


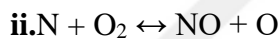
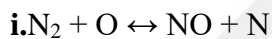
Figure 3.5. Combustion Process [62]

At low pressures the chain carriers can reach the walls and get lost. No explosion happens. As the pressure is increased along the dotted line shown, the radicals react before reaching the walls and the reaction suddenly becomes explosive. This is the first explosion limit. In the second explosion limit, the pressure of the products is high so that reactions of the type, $\text{O}_2 + \text{H} \rightarrow \cdot\text{HO}_2$ occur. These recombination reactions become efficient as the excess energy can be removed by three body collisions. Then the reaction goes smoothly. In the third explosion limit, thermal explosion occurs. In this limit, reaction such as $\text{HO}_2 \cdot + \text{H}_2 \rightarrow \text{H}_2\text{O}_2 + \text{H} \cdot$ dominates the elimination of $\text{HO}_2 \cdot$ by the walls.

As its clear the OH is a middle product in the combustion and if there isn't any OH in the reaction and the reaction will not continue and the pressure and temperature will not be available. [62]

3.4.2.1. Thermal NO_x formation

Thermal NO_x formation describes the process when nitrogen, N₂, in the combustion air reacts with oxygen, O₂, in the combustion air to produce NO_x. This process is best studied and understood. The formation requires very high temperatures and is exponentially dependent on the temperature. Because the process is very nonlinear, so called hot spots, local areas with higher temperature than the average temperature, can give very large effect on the amount of NO_x produced. The maximum rather than the average temperature is therefore very important and the process is very hard to model accurately because of this. Other important factors in thermal NO_x formation are the residence time, which describes how long time the combustion gas is having the high temperature. The turbulence and the amount of excess oxygen are two other important factors. The process is mainly governed by the following three equations, which together are called the Zeldovich mechanism, here written in the form of equilibrium reaction equations:

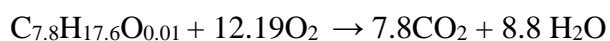
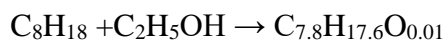


The strong triple bond in the N₂ molecule requires high temperature to break and equation i will therefore determine the rate of the thermal NO_x formation. This source of NO_x is usually dominating with temperatures over 1400 K (1100 C) and NO_x formation is usually modeled with these three equations. Thermal NO_x formation has its maximum for temperatures over 1900 K.

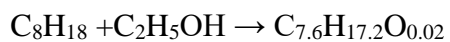
3.4. The Burning Reactions:

The burning reactions for alcohol gasoline blends are:

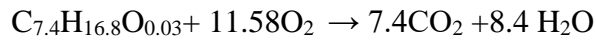
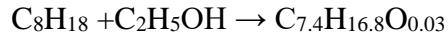
E₁: Gasoline %99 and Ethanol % 1



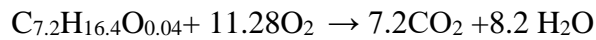
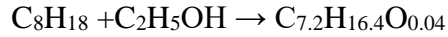
E₂: Gasoline %98 and Ethanol % 2



E₃: Gasoline %97 and Ethanol %3



E₄: Gasoline %96 and Ethanol %4



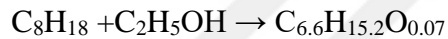
E₅: Gasoline %95 and Ethanol %5



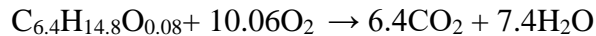
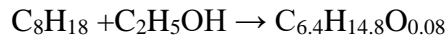
E₆: Gasoline %94 and Ethanol %6



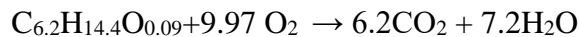
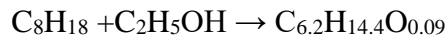
E₇: Gasoline %93 and Ethanol %7



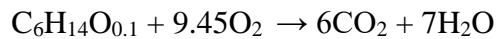
E₈: Gasoline %92 and Ethanol %8



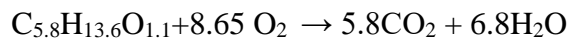
E₉: Gasoline %91 and Ethanol %9



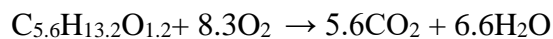
E₁₀: Gasoline %90 and Ethanol %10



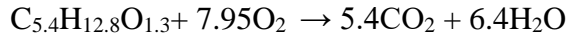
E₁₁: Gasoline %89 and Ethanol %11



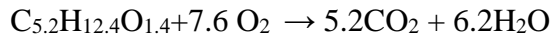
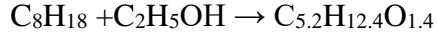
E₁₂: Gasoline %88 and Ethanol %12



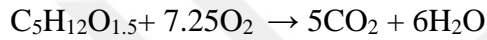
E₁₃: Gasoline %87 and Ethanol %13



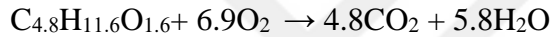
E₁₄: Gasoline %86 and Ethanol %14



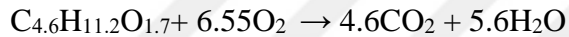
E₁₅: Gasoline %85 and Ethanol %15



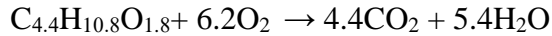
E₁₆: Gasoline %84 and Ethanol %16



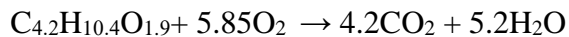
E₁₇: Gasoline %83 and Ethanol %17



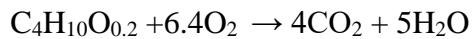
E₁₈: Gasoline %82 and Ethanol %18



E₁₉: Gasoline %81 and Ethanol %19



E₂₀: Gasoline %80 and Ethanol %20



3.5.1-D Combustion modeling:

Combustion modeling was done using SRM-Suite and Chemkin-Pro, SI engine module. All of the analysis were done between the intake valve closing time and the exhaust valve opening time.

We use geometrical compression ratio as effective compression ratio for SRM-Suite. We take effective compression ratio as 12.84 for Chemkin-Pro to match experimental pressure curve. We take the ratio of the connection rod length to the crank radius as 1.66.

Operating parameters were chosen on 1200 rpm experimental data. We take the same valves for both chemical kinetical mechanisms and the analysis steps is 0.1 we take 450 k for inlet temperature in reduced mechanism and 530 K for detailed mechanism at intake valve closing. We take intake pressure 1.33bar according to experimental data. We modeled the heat transfer according the following equation:

$$Nu = a \times Re^b \times Pr^c \quad (3-10)$$

Based on former studies for an SI engine we take constant as $a=0.032$, $b=0.79$, $c=0$.

We take the cylinder tempt 420 K.

The Chemkin-Pro uses woschini equation for heat transfer:

$$W = c_1 \times s_p + c_2 \left(\frac{Vd \times Tr}{Pr \times Vr} \right) (P - P_m) \quad (3-11)$$

For an SI engine constant are $C_{11}=2.28$, $C_{12}=0.308$, $C_2=3.24$.

We setup and simulate SRM suite models between the time interval of intake valve closing and exhaust valve opening as well.

We take the parameters entered in Chemkin-Pro same with parameters in SRM-Suite simulation.

We used 110 stochastic particles to sample in-cylinder property and also we took weight factor as 13.

We took mean mixing time as 5.5 ms and we used localness mixing model(LMM).

LMM is particularly recommended for SI engine applications since it factors in localness into account.

3.6. Result:

For detailed chemistry mechanism total CPU time is 12407 s and for reduced chemistry mechanism its 2851s for SRM-Suite software. In Chemkin-Pro total CPU time for detailed Chemkin mechanism is 3050 s and for reduced mechanism is 355 s.

We tested computational outcomes based on pressure–crank angle change, heat release rate, temperature and mole fractions of C_2H_5OH , C_8H_{18} , CO , CO_2 , H_2O and OH .

We compared experimental outcomes to computational in terms of pressure heat release rate, temperature and fractions of CO , CO_2 , and O_2 .

The quantities that are unavailable experimentally like C_7H_{16} , C_8H_{18} , CO , CO were reported using computational values also variation of H_2O_2 and OH , that are intermediate species in combustion, were showed graphically computations.

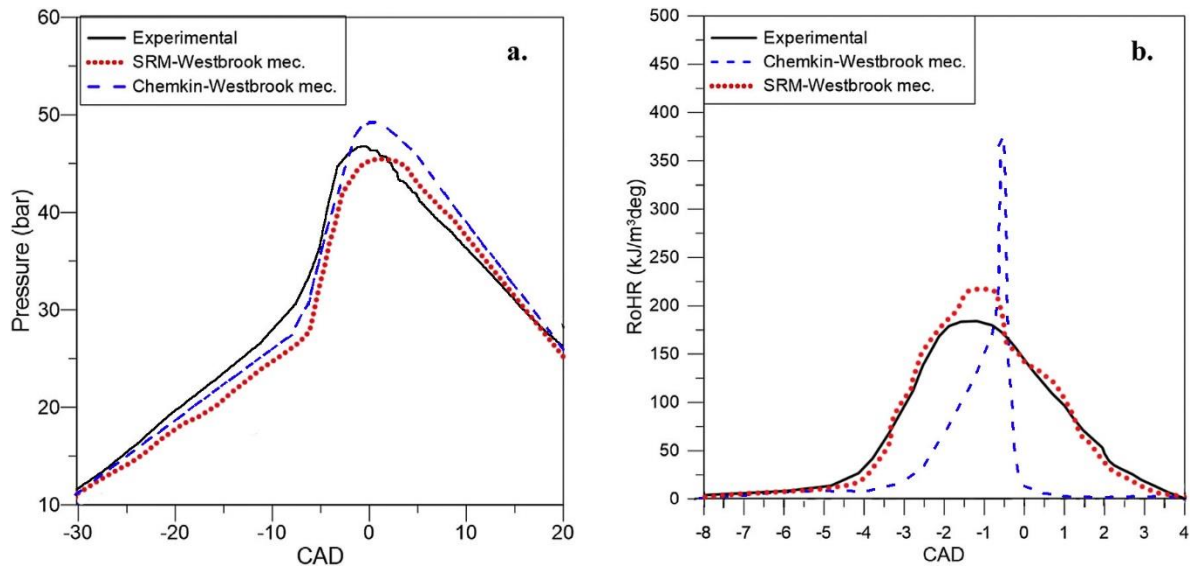


Figure. 3.6. (a) Pressure curves from experimental and modeling with detailed mechanism. (b) Experimental and modeling with detailed mechanism heat release rate curves.

In figure 3.6a it's obvious that in terms of peak pressure SRM-Suite is in much better agreement with experiments in pressure–crank angle curves than Chemkin-Pro.

It's obvious that pressure and temperature both increase at 0° of crank angle which shows TDC so the increasing of temperature and pressure near TDC is logical because it shows the combustion but there is an small increase in pressure just before TDC which means that an pre-combustion has occurred there which can result in knock in engine.

Figure3.6.b shows the experimental heat release rate vs crank angle and computational results of detailed kinetics using SRM and Chemkin –Pro.

As seen in the figures SRM-Suite results shows much better agreement in terms of trends and values than Chemkin-Pro when compared to experimental results.

It's clear in figure 3.7 a that the reduced mechanism outcomes show less proper results than detailed mechanism when compared to the experimental outcomes, SRM-Suite and Chemkin-Pro pressure–crank angle curve shows that combustion started later, but happened faster as compared to the experiment.

If we analyze Figure 3.7 b it shows delayed and faster combustion in computational analyses. Generally, in terms of pressure and heat release rate computational outcomes obtained with the detailed kinetic mechanism showed better agreement with experimental out comes.

In terms of heat release rate SRM-Suite out comes showed much better agreements than Chemkin–Pro.

In addition, software codes use the same fundamental flow and chemistry equations the main difference between two codes is the important contribution of stochastic to the solution. Chemkin-Pro assumes homogenous gas temperature throughout the entire combustion chamber and this causes sudden pressure raise and higher peak pressure values.

Combustion reactions happen faster than experimental actions due to the removal of many intermediate species and reactions in order to decrease the computational time significantly. This also results contribute to the sudden pressure rise and the deviation in heat release rate. Nevertheless, because of the contribution of the reduced mechanism to the solution time these deviations can be ignored.

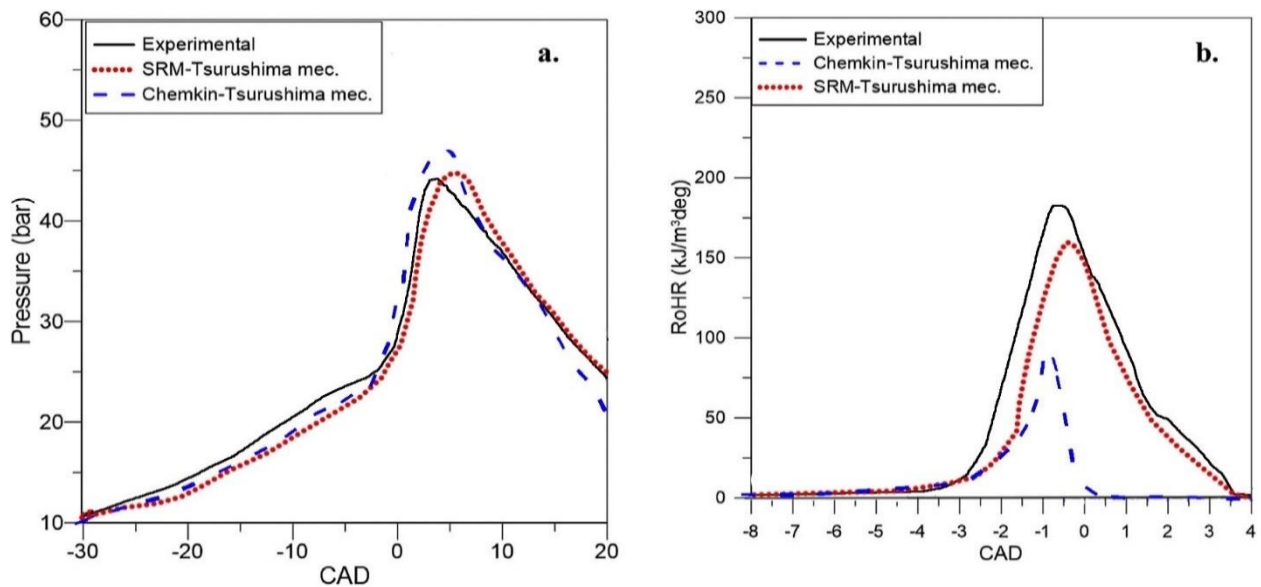


Figure. 3.7. (a) Pressure curves from experimental and modeling with reduced mechanism. (b) Experimental and modeling with reduced mechanism heat release rate curves.

Figure 3.8 shows computational temperature curves to see how the temperature rise during combustion. Maximum combustion temperature values were in between 1900K and 2000K.

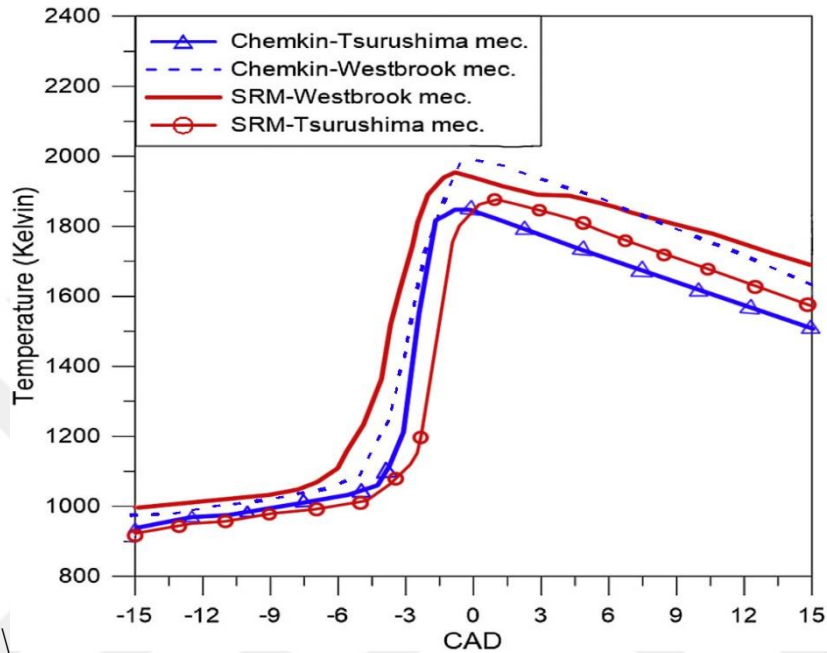


Figure. 3.8. Temperature curves.

As its clear the temperature increase at 0 ° of crank angle, which it shows the TDC as its clear in figure 3.8 the temperature starts to increase during the compression and at the combustion it reaches to peak and after combustion it decrease again all of the results are near to each other.

Figure3.9 shows fuel consumption for E100.In the reduced mechanism analyses (Tsurushima), fuel was consumed early and depleted gradually.

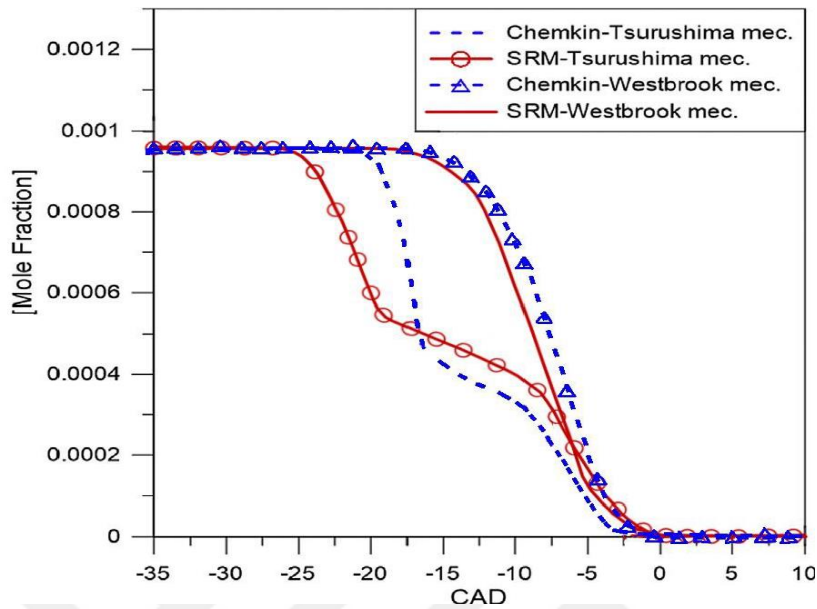


Fig. 3.9. Fuel consumption curves for E100 for different solvers and chemical mechanisms depending on CAD

Although the reason for early fuel consumption and depletion results of the reduced mechanism is obvious it's because of the absence of many intermediate reactions.

It worth to mention that all the computational analyses showed the same total amount of time (crank angle) for fuels to be consumed.

Figure 3.10 shows the change of CO and CO₂ as a function of crank angle. In general, the results showed similar trends except the ones using SRM-detailed chemistry. We cannot test the accuracy of the results by comparing to each other without valid experimental data, especially when we consider that SRM detailed chemistry results are in good agreement with experimental out comes in terms of the available data.

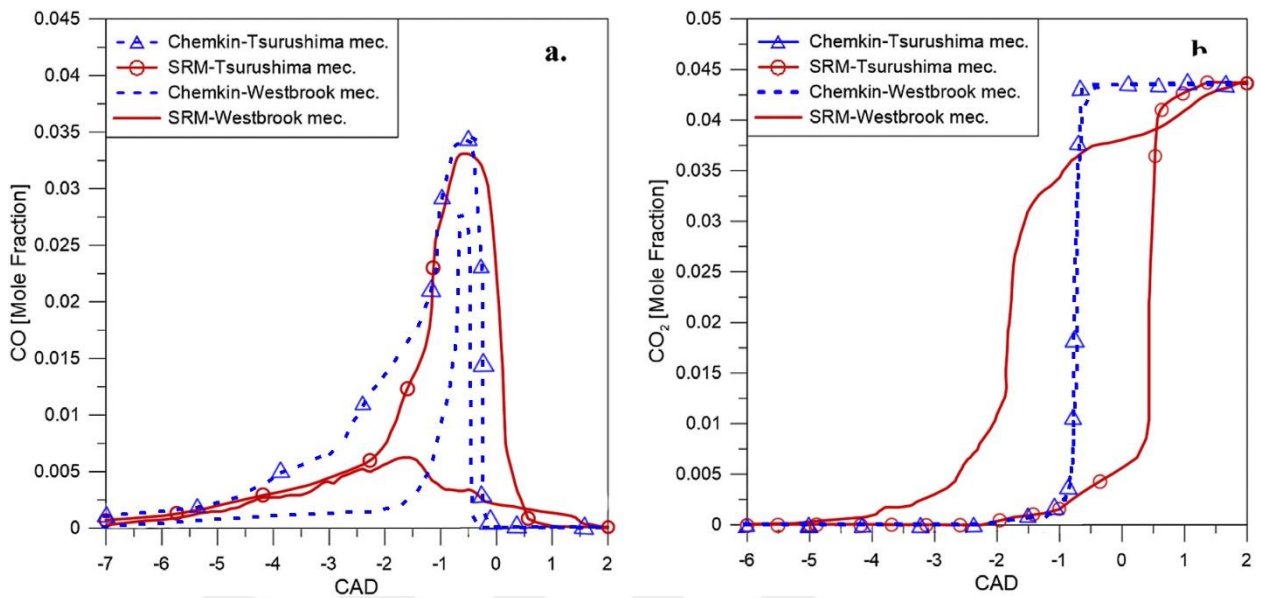


Figure.3.10. CO (a) and CO₂ (b) curves for different solvers and chemical mechanisms depending on CAD.

Figure 3.11 shows the change of OH and H₂O as a function of crank angle. When graphs are analyzed we find out that mole fraction of OH has changed for both codes and mechanisms SRM-detailed mechanism analysis showed earlier evaluation of OH with a lower peak value. In H₂O₂ trends there is lower fractions with the detailed mechanism than reduced mechanism. Mass fraction of H₂O₂ as a function crank angle was reported before, during and after combustion in an SI engine using an experimental data was in good agreement with SRM analysis using the mechanism of Tsurushima. Although the computational results for H₂O₂ couldn't be validated experimentally. It is interesting the deviation that SRM-detailed mechanism showed in terms of CO, CO₂ and OH cannot be seen in terms of H₂O₂. As seen in Figure 3.11 b, the formation of H₂O₂ starts earlier in the case of simulations with the reduced mechanism. But because the consumption time of H₂O₂ is almost the same for all analyses, this means the ignition delay times of the mechanisms overlap.

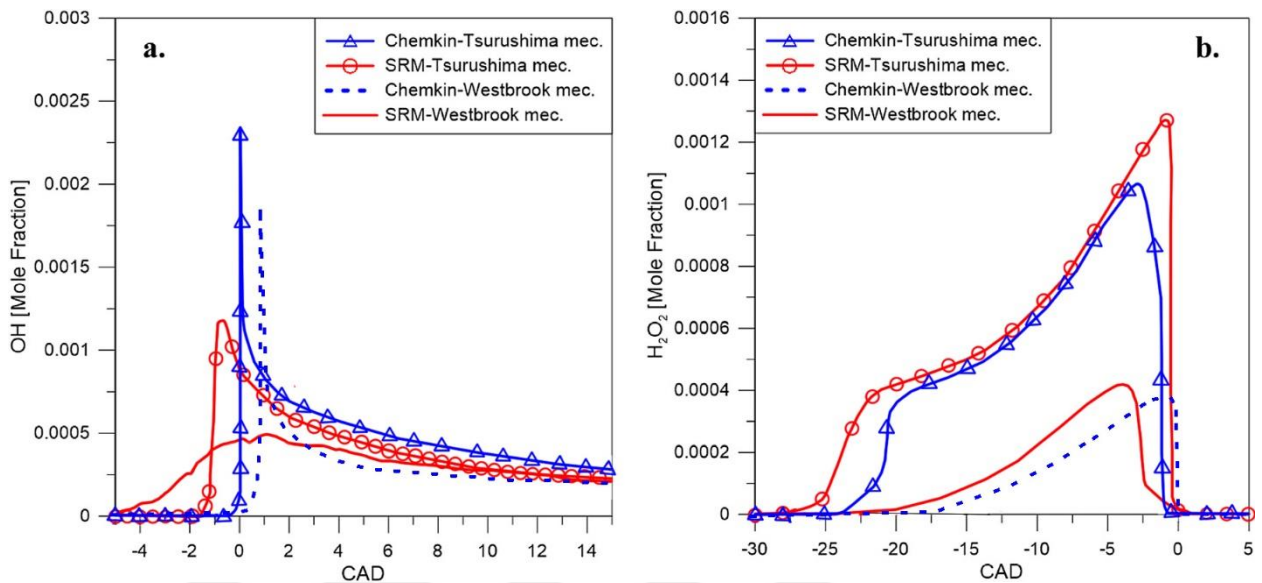


Figure.3.11. OH (a) and H₂O₂ (b) for different solvers and chemical mechanisms depending on CAD.

In Figure 3.12 experimental and four computational results of CO, CO₂ and O₂ emissions are shown. For CO emissions, Chemkin-Pro showed closer agreement with the experiment than SRM for both reduced and detailed mechanisms. In terms of CO₂ and O₂, all of the computational results showed good agreement with experimental results.

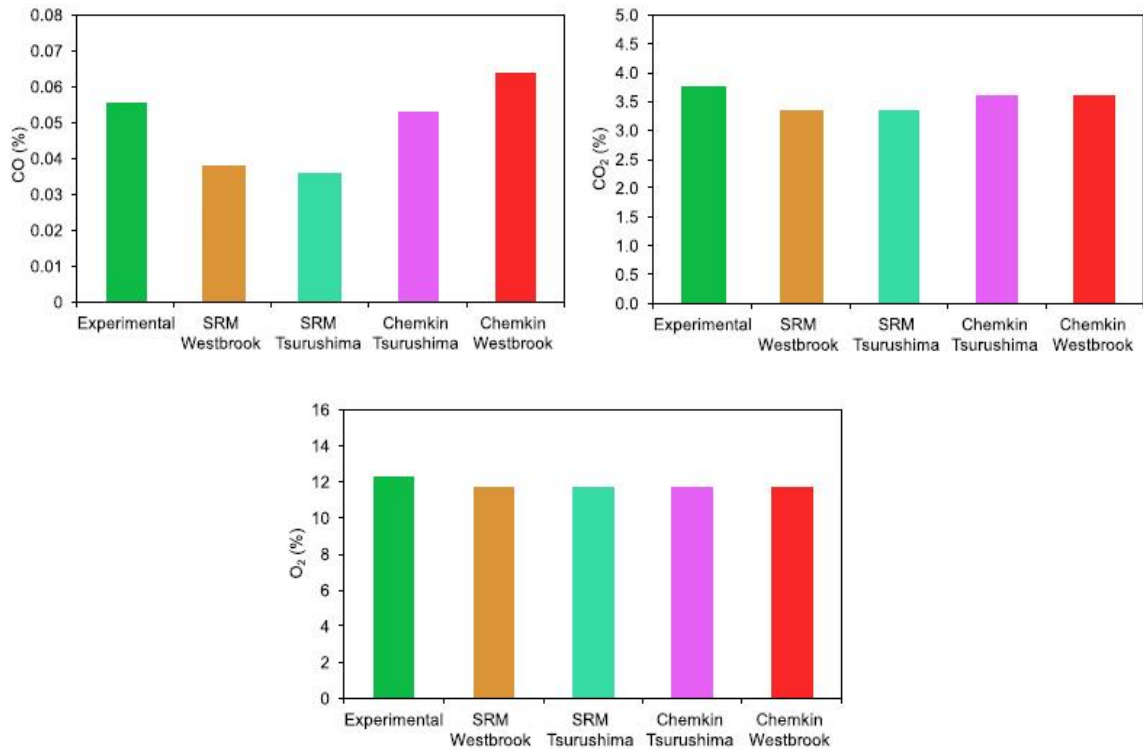


Figure.3 12. Experimental and computational values of CO, CO₂, and O₂.

In the second part of study various blends of gasoline-ethanol blends were investigated by employing GT-POWER software package.

In this cases numerical applications have been modeled at the same engine operating conditions proper and optimum cases were compared with respect to harmful exhausts emission results and in the ethanol cases engine operating leads to leaner due to ethanol chemical properties Figure 3.13 shows the variation of pressure with crank angle degree.

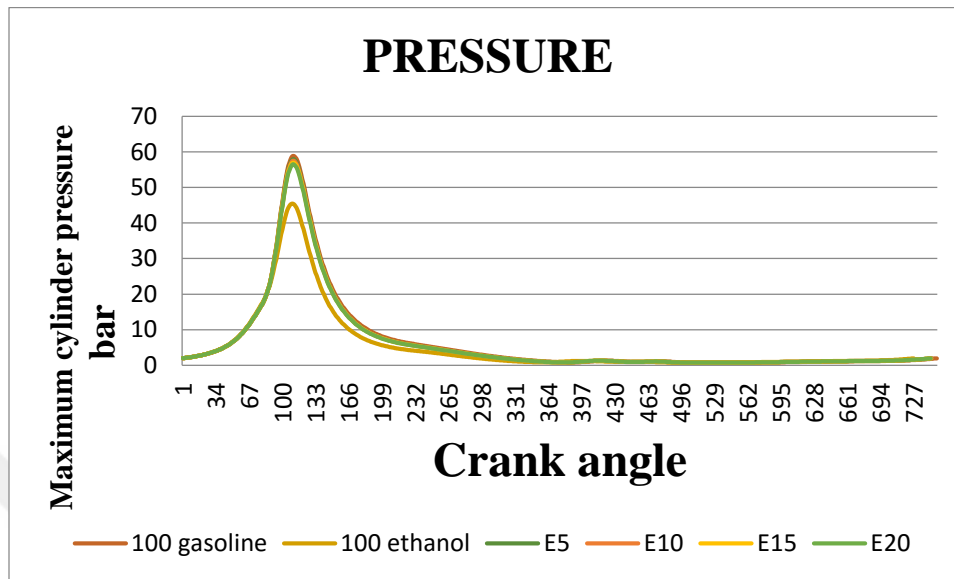


Figure 3.13 Variation of maximum cylinder pressure with ethanol concentration in the blend.

As its clear in figure 3.13 the highest pressure belongs to pure gasoline and least pressure belongs to pure ethanol and the various blends are in the interval between them the reason for this temperature distribution is that ethanol has higher latent heat of evaporation which results in worst fuel atomization and also pressure reduction. But this is right for low and medium engine loads at high engine loads because the in-cylinder temperature is high and it makes up the high heat of vaporization for ethanol and as the ethanol has higher flame speed it results in much efficient combustion and higher in-cylinder pressure. At the high load the positive effect of ethanol in blends is much more obvious because by adding ethanol to blend the blend will be stoichiometric and the in-cylinder pressure will increase.

As its clear in figure 3.14 the highest in-cylinder temperature belongs to pure gasoline and least in-cylinder temperature belongs to pure ethanol and the various blends are in the interval between them the reason is that because ethanol has higher heat of vaporization and lower heating value it results in lower in-cylinder temperature due to mentioned reasons by increase in ethanol amount the in-cylinder temperature will decrease even more but this is true for low engine loads, if engine work in medium or high loads and the concentration of ethanol in blend is not more than 20% the temperature of cylinder will increase because the ethanol has

the higher flame speed compared with gasoline and also because of oxygen content of gasoline it will result in much effective and complete burning.

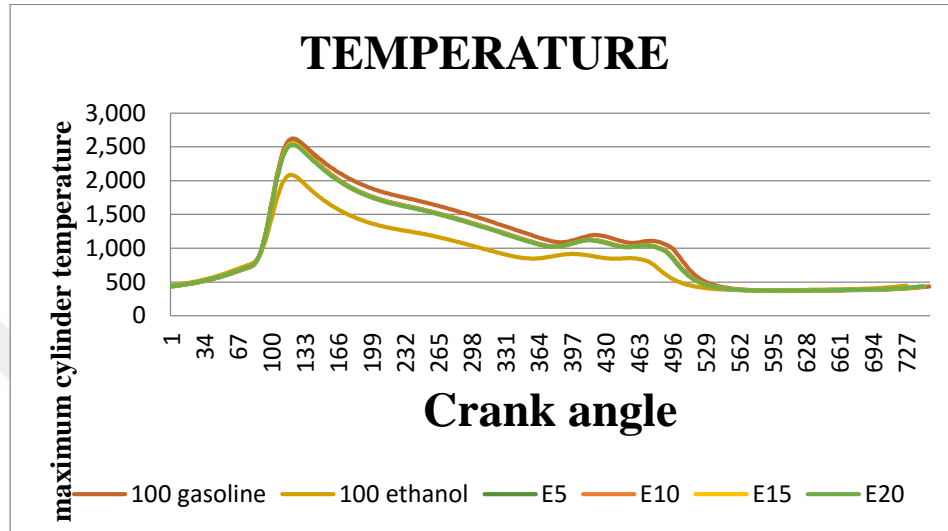


Figure 3.14. Variation of maximum cylinder temperature with ethanol concentration in the blend.

Ethanol addition reduces the heating value of gasoline ethanol blends; therefore, more fuel is needed (by mass) to obtain the same power when blended fuels are used instead of gasoline however as mentioned previously ethanol addition to gasoline makes the engine operation leaner and improves engine combustion and performance for this reasons shown in Figure 3.15 special fuel consumption measured at 0.07 when operating with gasoline ethanol blends are lower than those of gasoline fueled engine.

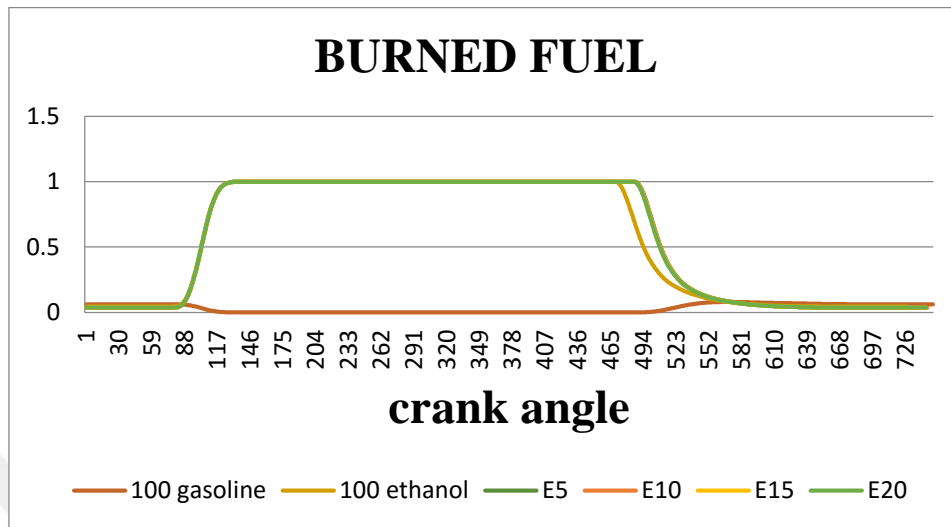


Figure 3.15 Variation of specific fuel consumption with ethanol concentration in the blend. Furthermore, carbon content of ethanol is lower than that of gasoline because of mentioned reasons, CO₂ concentration decrease with increasing ethanol concentration. Figure 3.16.

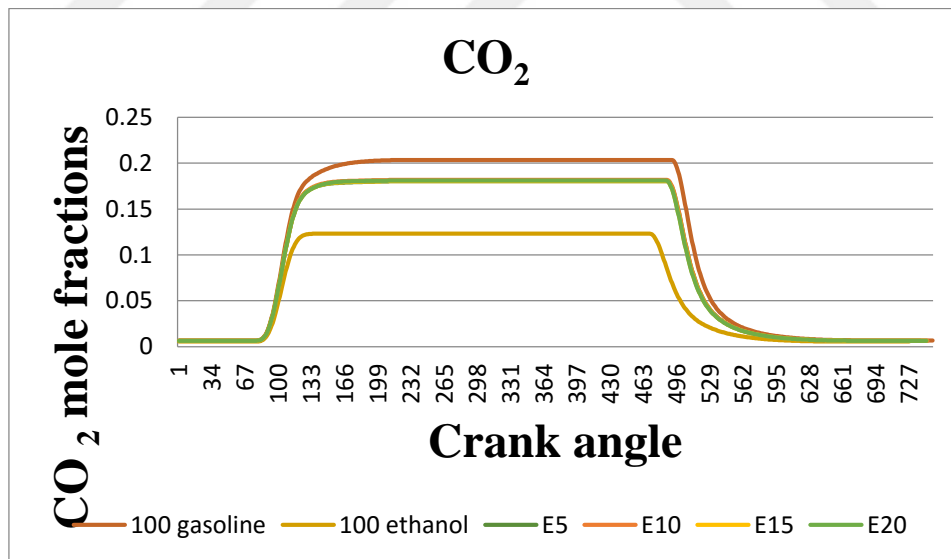


Figure 3.16 Variation of CO₂ mole fraction with ethanol concentration in the blend.

The NO emission results show real good agreement with literature review and experimental data as its clear in the figure 3.17 by increasing the ethanol concentration the NO emission

decrease because by increasing the ethanol concentration flame temperature decreases which this results in less NO emission.

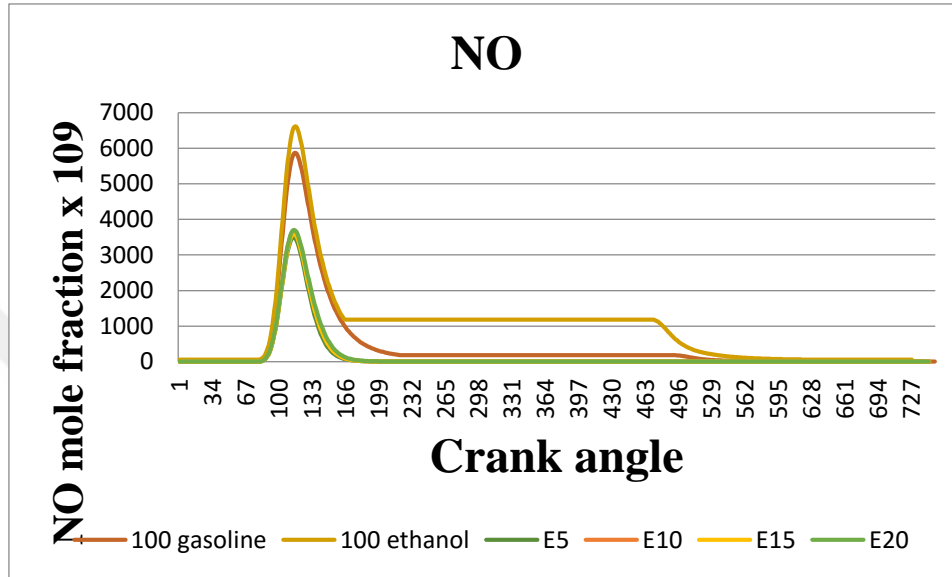


Figure 3.17 Variation of NO mole fraction with ethanol concentration in the blend.

CHAPTER 4 CONCLUSIONS

In this study, I have researched and optimized the effect of fuel ethanol in gasoline combustion engines from emission and performance point. At the first level, I surveyed the engine performance for pure gasoline fuel; then I used a mixture of ethanol and gasoline in which the amount of ethanol varies from 1% to 20 %. The engine RPM was chosen as 1200 and the engine parameters, when it works with 100% gasoline fuel, were compared to when ethanol-gasoline fuel were blended. From the performance and emission value points it was obvious that 8% ethanol-gasoline blend is the desirable amount. It is clear that from performance and emission point, there is a good agreement between the results and literature researches.

From performance and emission point it can be easily perceived that the gasoline-ethanol blend has advantages over pure gasoline. However, for obtaining the most decent value of gasoline-ethanol blend all of the engine parameters should be evaluated in an advanced optimization software in which the meantime factors in the gasoline-ethanol such as cost, engine performance and emission. If this conditions are met this study will be useful and practical.

In this study, all of the engine parameters were defined variable, at the same time, engine performance and emission values were optimized together.

If renewable sources are used to produce ethanol the cost of product will be high. Despite this, it is preferable to use gasoline-ethanol blend from performance and emission point under aforementioned conditions since passenger cars emissions have turned to be the main problem in air pollution and governments, therefore, pass strict rules about passenger cars, which result in emission every year.

From software point of view both, SRM and Chemkin-Pro have advantages and disadvantages over each other in results because: A significant advantage of the SRM-Suite software is that it uses stochastic particles and a probability density function (PDF) based approach which simplifies many aspects of CFD processes while keeping the predictive capability of 3-D CFD codes. On the other hand, Chemkin-Pro assumes bulk volume experimental results.

SRM-Suite includes modeling of piston crevice and blow-by, and such capabilities help prediction of better results as compared to Chemkin-Pro.

Although Chemkin-Pro showed less accurate results than SRM-Suite as compared to experimental data in terms of pressure and heat release rate, it still gave close approximations to the experiments in terms of exhaust emission. This once again shows Chemkin-Pro advantages of chemical kinetics mechanism development. Another advantage of Chemkin-Pro is faster analysis. Using the same computer, it takes 1min or less for Chemkin-Pro to complete an analysis while SRM-Suite requires 15-20 min for the same analysis.

In addition, if we go through results it's obvious that detailed mechanisms are more stable and closer to experiments in terms of inlet temperature and exhaust emissions but the detailed mechanism has its own disadvantage.

Disadvantage is that it increases the run time but it's not the same in both software .in fact the detailed mechanism increases the run time 10 times in Chemkin-Pro and 100 times in SRM-Suite.

REFERENCES

- [1] SHAFIEE , S ., TOPAL , E .,2008 , “When will fossil fuel reserves be diminished?”
Journal of Energy Policy”, Vol 37, pp. 181-189.
- [2] IEA World Energy Outlook 2008
- [3] IEA Key World Energy Statistics
- [4] BP Statistical review of world Energy, June 2014
- [5] BP Statistical review of world Energy, June 2014.
- [6].Anderson,J,E.,DiCicco,D,M.,Ginder,J,M.Kramer,U.Leone,T,G.Raney-Pablo,H,E.&
Wallington,T,J.(2012). High octane number ethanol–gasoline blends: quantifying the
potential benefits in the United States.*Fuel*,97,585-594. 10.1016/j.fuel.2012.03.017.
- [7] European Union emission inventory report 1990–2008 under the UNECE Convention
on Long-range Transboundary Air Pollution (LRTAP), EEA Technical Report No
7/2013
- [8] Pulkrabek,W,W.(1997). Engineering Fundamentals of the Internal Combustion Engine,
.Upper.Saddle,New Jersey:Prentice Hall
- [9].Aleiferis,P. & Behringer,M,K.(2015).Flame front analysis of ethanol, butanol, iso-
octane and gasoline in a spark-ignition engine using laser tomography and integral
length scale measurements. *Combustion and Flame*,162, 4533-4552.
doi:10.1016/j.combustflame.2015.09.008.doi:
- [10] Costagliola,M,A., Prati,M,V. Florio,S., Scorletti,P.,& Senatore,A.(2016).Performances
and emissions of a 4-stroke motorcycle fuelled with ethanol/gasoline blends,*Fuel*,183,
470-477,doi:10.1016/j.fuel.2016.06.105.
- [11] Chuepeng,S.(2016).Effects of heated ethanol on retrofit single-hole gasoline injector
performance. *Case Studies in Thermal Engineering*,8, 245-249.doi:
10.1016/j.csite.2016.08.003. 182-190.
- [12] Iodice,P. Senatore,A. Langella,G.& Amoresano, A.(2016).Effect of ethanol–gasoline
blends on CO and HC emissions in last generation SI engines within the cold-start
transient.,*Applied Energy*,179. 182-190. 10.1016/j.apenergy.2016.06.144.

- [13] Yılmaz,M.,Köten,H., & Gül,M,Z.(2012). Effects of the injection parameters and compression ratio on the emissions of a heavy-duty diesel engine *International Journal of Vehicle Design*, 59 ,147-162
- [14] Turner,D.,Cracknell,RF.,Natarajan, &V.Chen,X.(2006).Combustion performance of bio-ethanol at various blend ratios in a gasoline direct injection engine. *Fuel*,90,1999–2011.
- [15] Bielaczyc,P.,Szcotka,A,Woodburnv,J.(2011).The effect of various petrol–ethanol blends on exhaust emissions and fuel consumption of an unmodified light duty si vehicle .*SAE Technical Paper*,24,177-189.
- [16] Baec,O,H.,&Min,K. (2010).Spray and combustion characteristics of ethanol blended gasoline in a spray guided DISI engine under lean stratified operation. *SAE International Journal of Engines*;32,213–22.
- [17] Gravalos I, Moshou D, Gialamas T, Xyradakis P, Kateris D, Tsiropoulos Z. Performance and Emission Characteristics of Spark Ignition Engine Fuelled with Ethanol and Methanol Gasoline Blended Fuels. *Alternative Fuel* 2011.
- [18] Dwivedi G,Jain S,Sharma MP.Impact analysis of biodiesel on engine performance—A review.*Renewable and Sustainable Energy Reviews* 2011;15(9):4633–41.
- [19] Saleh HE.Effect of exhaust gas recirculation on diesel engine nitrogen oxide reduction operating with jojoba methyl ester.*Renewable Energy*2009;34(10):2178–86.
- [20] Sun J,Caton JA,Jacobs TJ.Oxides of nitrogen emissions from biodiesel-fueled diesel engines. *Progress in Energy and Combustion Science* 2010;36 (6):677–95.
- [21] Tschanz F, Amstutz A, Onder CH, Guzzella L. Feedback control of particulate matter and nitrogen oxide emissions in diesel engines. *Control Engineering Practice*, doi:10.1016/j.conengprac.2012.09.014, in press
- [22] Arbab MI,Masjuki HH,Varman M,Kalam MA,Imtenan S,Sajjad H.Fuel properties, engine performance and emission characteristic of common biodiesels as a renewable and sustainable source of fuel.*Renewable and Sustainable EnergyReviews* 2013;22:133–47.
- [23] Costa RC ,Sodré &JR.Hydrous.(2010).Ethanol vs. gasoline–ethanol blend:engine performance and emissions. *Fuel*;89,287–93.

- [24] Yunoki,S.&,Saito,M,A. (2009),Simple method to determine bioethanol content in gasoline using two-step extraction and liquid scintillation counting.*Bio resource Technology*,100,61–68.
- [25] Balat M, &Recent,H.(2009).Trends in global production and utilization of bioethanol fuel.*Applied Energy*;86,2273–82.
- [26] Rass,H,J.,&Christensen,R,M. (2008).Steam reforming of technical bioethanol for hydrogen production. *International Journal of Hydrogen Energy*;33,4547–54.
- [27] Okada,O.,Tabata,T.,Kokitsu,M.,Ohtsuka,H.,&Bellussi,G.(1997).Advanced catalyst for NOx reduction using hydrocarbons from lean-burning gas engine.*Applied Surface Science*,121,267–72.
- [28] Schifter,I.,Diaz,L.,Gómez,JP.,&Gonzalez,U.(2013).Combustion characterization in a single cylinder engine with mid-level hydrated ethanol–gasoline blended fuels. *Fuel*,103,292–8.
- [29] Magnusson,R.,Nilsson,C.,&Andersson,B.(2002).Emissions of aldehydes and ketones from a two-stroke engine using ethanol and ethanol-blended gasoline as fuel. *Environmental Science and Technology*,36,1656–64.
- [30] Leong,S,T., Muttamara, & S.,Laortanakul,P.(2002).Applicability of gasoline containing ethanol as Thailand's alternative fuel to curb toxic VOC pollutants from automobile emission.*Atmospheric Environment*,36,3495–503.
- [31] Gümüş,M., & Atmaca,M., DaSilva,M,G., (2010) . Energy and Exergy Analyses Applied to a CI Engine Fueled with Diesel and Natural Gas. *Energy Sources, Part A: Recovery, Utilization, and Environmental Effects*.35,1017-1027
- [32] Flavin,C.,Sawin,J,L.,Mastny,L.,Aeck,M.,Hunt,S.,Mac,E,A.,Stair,P.,Podesta,J., Cohen,A.,Hendricks,B.,(2006).American energy: the renewable path to energy security.Worl-watch Institute & the Center for American Progress, Washington, DC.
- [33] Al-Baghdadi.M.,(2008).Measurement and prediction study of the effect of ethanol blending on the performance and pollutants emission of a four-stroke spark ignition engine.*Proceedings of the Institution of Mechanical Engineers,Journal of Automobile Engineering*;222,859–73.

- [34] Szulczyk,K,R.,&McCarl,B,A.,(2010),Cornforth G.Market penetration of ethanol. Renewable and Sustainable *Energy Reviews*.14,394–403.
- [35] Maurya,RK,&Agarwal AK. (2011),Experimental study of combustion and emission characteristics of ethanol fueled port injected homogeneous charge compression ignition combustion engine. *Applied Energy*;88,1169–80.
- [36] Celik MB.(2008)., Experimental determination of suitable ethanol–gasoline blend rate at high compression ratio for gasoline engine.*Applied Thermal Engineering*,28,396–404.
- [37] Zhuang,Y.&,HongG.(2013).Primary investigation to leveraging effect of using ethanol fuel on reducing gasoline fuel consumption.*Fuel*,105,425–31.
- [38] Eyidogan,M.,Ozsezen,A,N.,Canakci,M,&Turkcan,A.(2010).Impact of alcohol–gasoline fuel blends on the performance and combustion characteristics of an SI engine. *Fuel*,89,2713–20.
- [39] Çelik,M,B.,Özdalyan,B.,&Alkan,F. (2011).The use of pure methanol as fuel at high compression ratio in a single cylinder gasoline engine. *Fuel*;90,1591–8.
- [40] Koç,M.,Sekmen,Y.,Topgöl,T.,&Yücesu,H,S.(2009).The effects of ethanol–unleaded gasoline blends on engine performance and exhaust emissions in a spark- ignition engine. *Renewable Energy*;34,2101–6.
- [41] Velliangiri M,Krishnan A.An experimental investigation of performance and emission in ethanol fueled direct injection internal combustion engines with zirconia coating.*Journal of Energy Technologies and Policy* 2012;2(2):42–53.
- [42] Ramesh Kumar C, Nagarajan G .Performance and emission characteristics of a low heat rejection spark ignited engine fueled with E20 .*Journal of Mechanical Science and Technology* 2012;26(4):1241–50
- [43] Anderson E.,Cyr J.,Cordon ,D,Steciak J, Beyerlein,S,and Budwig,R,Compression ratio and catalyst aging effects on aqueous ethanol ignition:Part 1.Compression Ratio Effects on Aqueous Ethanol Ignition;2009
- [44] Yanowitz,J, Knoll,K,Kemper,J,Luecke,J,Mc Cormick RL .The impact of adaption on flex-fuel vehicle emissions when fueled with E40. *Environmental Science and Technology* 2013;47(6):2990–7

- [45] Zhai,H.,Frey,H,C.,Rouphail,N,M.,Goncalves,G,A.,Farias,T,L.,Comparison of flexible fuel vehicle and life-cycle fuel consumption and emissions of selected pollutants and green house gases for ethanol 85 versus gasoline. Journal of the Air and Waste Management Association 2009;59:8.
- [46] Farkade,H,s., Pathre,A,P.,(2012).Experimental investigation of methanol, ethanol and butanol blends with gasoline on SI engine.International Journal of Emerging Technology and Advanced Engineering,2,2250-2459
- [47] Moxey,B., Cairns,A.,& Zhao, H.(2014), A Study of Turbulent Flame Development with Ethanol Fuels in an Optical Spark Ignition Engine. SAE Technical Paper,1,2622-2635, doi:10.4271/2014-01-2622.
- [48] Aleiferis,P,G.& Behringer,M,K.(2015). Flame front analysis of ethanol, butanol, iso octane and gasoline in a spark-ignition engine using laser tomography and integral length scale measurements. 162, 4533-4552.doi: 10.1016/j.combustflame.2015.09.008
- [49] Huang,Y., Huang,S., Huang,R., Hong,G.(2015). Spray and evaporation characteristics of ethanol and gasoline direct injection in non-evaporating, transition and flash-boiling conditions, Energy Conversion and Management,108,68-77, 10.1016/ doi: j.enconman.2015.10.081.
- [50] Liu,H. Wang,Z.Long,Y., Xiang,S,Z.Wang,J,X.,Fatouraie,M.(2015) Comparative study on alcohol-gasoline and gasoline-alcohol Dual-Fuel Spark Ignition (DFSI) combustion for engine particle number (PN) reduction,159, 250-258,10.1016/j.fuel.2015.06.059
- [51] Freudenberger,R.,(2009).Alcohol Fuel : A Guide to Making and Using as a Renewable Fuel
- [52] Najafi, G., Ghobadian, B., Yusaf,& T.,Mamat,R.(2015),Optimization of performance and exhaust emission parameters of a SI (spark ignition) engine with gasoline–ethanol blended fuels using response surface methodology, Energy,1815-1829, doi:10.1016/ j.energy.2015.07.004.
- [53] Najafi, G. Ghobadian,B. Moosavian,T. Yusaf,R.& Azmi,W,H. *performance and exhaust emissions of a SI engine with gasoline–ethanol blended fuels.*(2016),95,186-203,doi:10.1016/j.applthermaleng.2015.11.009

- [54] Iliev,S. A Comparison of ethanol and methanol blending with gasoline using a 1-D engine.(2015),100, 1013-1022, 10.1016/doi: j.proeng.2015.01.461.
- [55] Thangavel,v., Momula,y., Gosala,D,B.,& Asvathanarayanan,R.,(2016). Experimental studies on simultaneous injection of ethanol–gasoline and n-butanol–gasoline in the intake port of a four stroke SI engine, *Renewable Energy*, 91, 347-360, doi:10.1016/j.renene.01.074.
- [56] Hsieh, W.,Chen,R,H., Wu,T,I.Lin,T,H.(2002).Engine performance and pollutant emission of an SI engine using ethanol–gasoline blended fuels,36,403 410, doi: 10.1016/S1352-2310(01)00508-8
- [57] Wang,X.,Chen,Z., Ni,J.,Liu,S.,& Zhou,H.(2015) The effects of hydrous ethanol gasoline on combustion and emission characteristics of a port injection gasoline engine. *Case Studies in Thermal Engineering*,6, 147-154. doi:10.1016/j.csite.2015.09.007
- [58] Fröjd,K., Perlman,C., (2013). Tunér,A.,& Mauss,F. 1D engine modeling with detailed reaction kinetics. 17, 223-70
- [59] Martin,T.(2008),*Stochastic Models for Engine Simulation* ,Sweden ,Lund University.
- [60] Demir,U., Yilmaz,N., Coskun,G &Soyhan,H,S.,(2014). Evaluation of zero dimensional Codes in.simulating IC engines using primary reference fuel.*Applied Thermal Engineering*,76,18-24.
- [61] Yasar , H., Soyhan,H,S., Walmsley,H., Head,B., & Sorousbay,C.,(2007). Double Wiebe function: An approach for single-zone HCCI engine modeling.*Applied Thermal Engineering*,28, 1284–1290.
- [62] Glumac,N,G.(2015), *Combustion*,UK,Elsevier.

CURRICULUM VITAE:

Personal details

Name: Ramin Saadat Pour

Date Place of Birth: 02 September 1986, Tabriz, Iran

Nationality: Iranian

Marital Status: Single

Telephone: +98-41-33810798

GSM: +90-5531113294

E-mail: raminsaadatpour@yahoo.com, saadatpourramin@gmail.com

Educational Background

2016: MSc, Department of Mechanical Engineering,
Marmara University, Istanbul, TURKEY

2010: BSc, Department of Mechanical Engineering,
Tabriz University, Tabriz, IRAN.

Research Activity:

Fluid dynamics, production of any kind of mechanical part, computer programs, automotive.

Ongoing Researches:

Modeling of IC engines.